Doctorate Program in Molecular Oncology and Endocrinology
Doctorate School in Molecular Medicine

XXIV cycle - 2008–2011
Coordinator: Prof. Massimo Santoro

“Regulation of hepatic lipogenesis by the transcription complex Prep1-Pbx1”

Serena Cabaro

University of Naples Federico II
Dipartimento di Biologia e Patologia Cellulare e Molecolare
“L. Califano”

Administrative Location

Dipartimento di Biologia e Patologia Cellulare e Molecolare “L. Califano”
Università degli Studi di Napoli Federico II

Partner Institutions

Italian Institutions
Università degli Studi di Napoli “Federico II”, Naples, Italy
Istituto di Endocrinologia ed Oncologia Sperimentale “G. Salvatore”, CNR, Naples, Italy
Seconda Università di Napoli, Naples, Italy
Università degli Studi di Napoli “Parthenope”, Naples, Italy
Università degli Studi del Sannio, Benevento, Italy
Università degli Studi di Genova, Genova, Italy
Università degli Studi di Padova, Padova, Italy
Università degli Studi “Magna Graecia”, Catanzaro, Italy
Università degli Studi di Udine, Udine, Italy

Foreign Institutions
Université Libre de Bruxelles, Bruxelles, Belgium
Universidade Federal de Sao Paulo, Brazil
University of Turku, Turku, Finland
Université Paris Sud XI, Paris, France
University of Madras, Chennai, India
University Pavol Jozef Šafàrik, Kosice, Slovakia
Universidad Autonoma de Madrid, Centro de Investigaciones Oncologicas (CNIO), Spain
Johns Hopkins School of Medicine, Baltimore, MD, USA
Johns Hopkins Krieger School of Arts and Sciences, Baltimore, MD, USA
National Institutes of Health, Bethesda, MD, USA
Ohio State University, Columbus, OH, USA
Albert Einstein College of Medicine of Yeshiwa University, N.Y., USA

Supporting Institutions
Dipartimento di Biologia e Patologia Cellulare e Molecolare “L. Califano”, Università degli Studi di Napoli “Federico II”, Naples, Italy
Istituto di Endocrinologia ed Oncologia Sperimentale “G. Salvatore”, CNR, Naples, Italy
Istituto Superiore di Oncologia, Italy

Italian Faculty

Salvatore Maria Aloj
Francesco Saverio Ambesi
Impiombato
Francesco Beguinot
Maria Teresa Berlingieri
Bernadette Biondi
Francesca Carlomagno
Gabriella Castoria
Maria Domenica Castellone
Angela Celetti
Lorenzo Chiariotti
Vincenzo Ciminale
Annamaria Cirafici
Annamaria Colao
Sabino De Placido
Gabriella De Vita
Monica Fedele
Pietro Formisano
Alfredo Fusco
Domenico Grieco
Michele Grieco
Maddalena Illario
Massimo Imbriaco
Paolo Laccetti
Antonio Leonardi
Paolo Emidio Macchia
Barbara Majello
Rosa Marina Melillo
Claudia Miele
Nunzia Montuori
Roberto Pacelli
Giuseppe Palumbo
Silvio Parodi
Nicola Perrotti
Maria Giovanna Pierantoni
Rosario Pivonello
Giuseppe Portella
Giorgio Punzo
Maria Fiammetta Romano
Antonio Rosato
Giuliana Salvatore
Massimo Santoro
Giampaolo Tortora
Donatella Tramontano
Giancarlo Troncone
Giancarlo Vecchio
Giuseppe Viglietto
Mario Vitale

“Regulation of hepatic lipogenesis by the transcription complex Prep1-Pbx1”

TABLE OF CONTENTS

LIST OF PUBLICATIONS.....4

LIST OF ABBREVIATIONS.....5

ABSTRACT.....7

1. BACKGROUND……...8

1.1 Diabetes…….8

1.2 Insulin-Resistance…….8

1.3 Insulin signaling in the liver……10

1.3.1 Insulin signaling pathway……...10

1.3.2 Insulin controls hepatic glucose and lipid metabolism……...11

1.4 Hepatic lipogenesis ……13

1.4.1 Regulation of hepatic lipogenesis..…….15

1.4.2 Lipogenesis and genes…….20

1.5 TALE proteins…….22

1.5.1 Pbx1 protein……23

1.5.2 Prep1 protein……...25

1.5.3 Prep1 and insulin-resistance……26

1.6 Tyrosine and lipid phosphatases…….28

2. AIMS OF THE STUDY……..30

3. MATERIALS AND METHODS……...31

3.1 Materials……..31

3.2 Generation of Prep1 hypomorphic mice…….31

3.3 Quantitative assay of serum triglycerides…..……..31

3.4 Cell culture procedures and transfection…….31

3.5 Oil Red O staining……...32

3.6 Western blot analysis……..32

3.7 Real-Time RT-PCR analysis……...33

3.8 Chromatin immunoprecipitation (ChIP) and Re-ChIP assay……..33
3.9 Statistical procedure……34

4. RESULTS……35
4.1 Hepatic lipid metabolism in *Prep1*-deficient mice…….35
4.2 Prep1 effect on the AMPK-mediated lipogensis regulation in mouse liver…37
4.3 Prep1 regulates triglyceride synthesis in HepG2 cells……..……..39
4.4 SHP1 and SHIP2 mediate the effect of Prep1 on triglyceride synthesis…….41
4.5 Prep1 regulation of SHIP2 gene transcription…….44

5. DISCUSSION……..48

6. CONCLUSIONS…….52

7. ACKNOWLEDGEMENTS……53

8. REFERENCES……55

LIST OF PUBLICATIONS

This dissertation is based upon the following publications:

Oriente F, Iovino S, **Cabaro S**, Cassese A, Longobardi E, Miele C, Ungaro P, Formisano P, Blasi F and Beguinot F. *Prep1 controls insulin glucoregulatory function in liver by transcriptional targeting of SHP1 tyrosine phosphatase.* Diabetes. 2011 January; 60:138-147.

Iovino S, Oriente F, Botta G, **Cabaro S**, Iovane V, Paciello O, Viggiano D, Perruolo G, Formisano P and Beguinot F. *PED/PEA-15 induces autophagy and mediates TGF-beta1 effect on muscle cell differentiation.* Cell Death & Differentiation (Pending revision).

LIST OF ABBREVIATIONS

ACC: acetyl CoA carboxylase

AMPK: AMP-activated protein kinase

CAMKKβ/CAMK2: Ca^{2+}/calmodulin-dependent protein kinase kinase-β

CAP/cbl: Cbl associated protein

ChoRE: carbohydrate responsive element

ChREBP: carbohydrate responsive element-binding protein

CoA: coenzyme A

DGAT: diacylglycerol acyltransferase

DM: diabetes mellitus

FA: fatty acid

FAS: fatty acid synthase

FFA: free fatty acid

GK: glucokinase

GPAT: glycerol 3-phosphate acyltransferase

GSK3: glycogen synthase kinase 3

HMG-CoA reductase: 3-hydroxy-3-methylglutaryl-CoA

IRS1-4: insulin receptor substrate 1-4

LKB1: liver kinase B1

L-PK: liver pyruvate kinase

MAP kinase: mitogen-activated protein kinase

NASH: Non Alcoholic Steotohepatitis

$p160^{MBP}$: p160 Myb-binding protein

Pbx1: pre-B cell leukemia transcription factor

PEPCK: phosphoenolpyruvate carboxykinase

PGC-1α: PPARγ co-activator 1

PH: pleckstrin homology

PI3-K: phosphatidylinositol 3-kinase

PKA: protein kinase A

PKB/Akt: protein kinase B

PKC: protein kinase C

PPARγ: peroxisome proliferator-activated receptor gamma

Prep1: Pbx regulating protein 1

PTEN: phosphatase and tensin homolog deleted on chromosome ten

PTP1B: protein tyrosine phosphatase 1B

PTPases: protein tyrosine phosphatases

SCD1: stearoyl CoA desaturase

SGK: glucocorticoid-induced protein kinase

SHC: Src homology 2 domain containing

SHIP2: SH2-containing inositol 5'-phosphatase 2

SHP1: SH-PTP1 Src homology domain tyrosine phosphatase

SKIP: kidney-enriched inositol phosphatase

SREBP: sterol regulatory element-binding protein

STRAD: STE-20 related adaptor protein

SYP: SH-PTP2 Src homology domain tyrosine phosphatase

T1D: type 1 Diabetes

T2D: type 2 Diabetes

TAG: triacylglycerol

TALE: three-amino acid loop extension

TG: triglyceride

UEF-3: urokinase enhancer factor-3

uPA: urokinase plasminogen activator

VLDL: very low-density lipoprotein

ABSTRACT

Prep1 is an homeodomain transcription factor belonging to the TALE proteins, including also Pbx1, which plays an essential role in hematopoiesis, organogenesis and development. Prep1 forms transcriptionally active complexes with Pbx1 and regulates the activity of several genes. The Prep1 null mutation leads to embryonic death at a very early stage. Therefore, Prep1 hypomorphic ($Prep1^{i/i}$) mice have been generated. Prep1 heterozygous ($Prep1^{i/+}$) mice, which express only 55-57% of protein, have a complex metabolic phenotype with at least two relevant features. One is the presence of smaller but otherwise normally structured islets with reduced fasting and post-loading plasma insulin levels. The second is increased insulin sensitivity in skeletal muscle and in liver which is accompanied by protection from streptozotocin-induced diabetes. In muscle, decreased Prep1 levels are followed by an increase of the PGC1alpha/Glut4-mediated glucose uptake. In liver, better insulin sensitivity is due to a reduced SHP1 tyrosine phosphatase expression followed by an increase of insulin signaling. Also, triglyceride levels are significantly reduced in the liver of $Prep1^{i/+}$ mice. However, the molecular mechanism by which Prep1 controls lipogenesis is unclear. In this study, we have focused our attention on the role of Prep1 on the regulation of the triglyceride synthesis.

To study the lipogenesis in the liver of the Prep1 heterozygous mice, we have examined the expression of the lipogenetic enzyme FAS (Fatty Acid Synthase) by real-time RT-PCR analysis. Hepatic expression of FAS is significantly decreased. Western Blot analysis have shown increased phosphorylation of PKCzeta, LKB1, AMPK and ACC, which may control FAS expression and triglycerides production in $Prep1^{i/+}$ mice liver. Protein and mRNA levels of the lipid phosphatase SHIP2, an inhibitor of PI3Kinase/PKCzeta signaling, are reduced by 40% in the liver of $Prep1^{i/+}$ mice. Consistent with these data, HepG2 (Human Hepatocarcinoma cell line) cells overexpressing Prep1 display increased triglyceride levels and FAS expression, while PKCzeta, LKB1, AMPK and ACC phosphorylation is strongly reduced. Moreover, SHIP2 levels are increased by 50%. Interestingly, overexpression of Pbx1 cDNA in HepG2 cells mimicked Prep1-induced triglyceride synthesis. At the opposite, $Prep1_{HR1}$ mutant, which is unable to bind Pbx1, fails to elicit these effects. ChIP and Re-ChIP experiments indicate that Prep1/Pbx1 complex can bind SHIP2 promoter region and regulate its expression.

These data suggest that Prep1/Pbx1 dimer regulates hepatic triglycerides production by increasing SHIP2 levels and thereby inhibiting the PKCzeta/AMPK signaling.

1. BACKGROUND

1.1 Diabetes

Diabetes mellitus (DM) includes a group of metabolic disorders that requires long-term medical attention both to limit the development of its devastating complications and to manage them when they do occur. Diabetes mellitus is a chronic metabolic syndrome caused by insulin deficiency and characterized by elevated glucose levels. The metabolic dysregulation and the chronic hyperglycemia associated with DM causes secondary pathophysiological damage in multiple organ system, such as eyes, kidneys, nerves, heart and blood vessels.

According to the classification recommended by the American Diabetes Association (2004), there are three main form of diabetes: type 1 diabetes (T1D), type 2 diabetes (T2D), and gestational diabetes mellitus.

Type 1 diabetes is characterized by beta cell destruction caused by an autoimmune process, usually leading to absolute insulin deficiency. Insulin injection is always necessary for survival because T1D patients lack endogenous insulin.

Type 2 diabetes is the most common form of diabetes mellitus and is characterized by insulin resistance in peripheral tissue, insulin secretory defect of the beta cell and excessive hepatic glucose production (Harrison 2009). People with T2D are not dependent on exogenous insulin, but may require the hormone for the control of glucose homeostasis if this is not achieved with diet alone or with oral hypoglycaemic agents. The etiology of type 2 diabetes mellitus is multifactorial and genetically based, but it also has strong behavioral components.

1.2 Insulin-Resistance

Insulin is the primary hormone involved in glucose homeostasis and in the stimulation of glucose transport. Secreted by pancreatic beta cells in response to increase of plasmatic glucose and amino acids levels after feeding, insulin promotes the synthesis and storage of carbohydrates, lipid, proteins and inhibits their degradation and release into the circulation.

Insulin-resistance is a common pathological state in which target tissue fail to respond properly to normal levels of circulating insulin. Pancreatic β-cells first compensate for peripheral insulin-resistance by increasing insulin secretion to maintain euglycaemia. Thereafter, impaired glucose tolerance can develop, leading to overt clinical type 2 diabetes. The coexistence of insulin-resistance and hyperinsulinaemia appears to contribute directly or indirectly to many other disorders, such as dyslipidaemia, hypertension, atherosclerosis and a pro-coagulant state (Samaras et al. 2006).

Insulin-resistance is determined by impaired sensitivity to insulin of its main target organs, i.e. adipose tissue, liver, and muscle. Insulin regulates glucose uptake and circulating free fatty acid (FFA) concentrations. In adipose tissue, insulin decreases lipolysis thereby reducing FFA efflux from adipocytes; in liver, insulin inhibits gluconeogenesis by reducing key enzyme activities, and in skeletal muscle insulin predominantly induces glucose uptake by stimulating the translocation of the GLUT4 glucose transporter to the plasma membrane. Insulin-resistance leads to increased circulating FFA concentrations and ectopic fat accumulation that impede insulin mediated glucose uptake in skeletal muscle and elevated glucose production in liver (Zeyda end Stulnig 2009) (Figure 1).

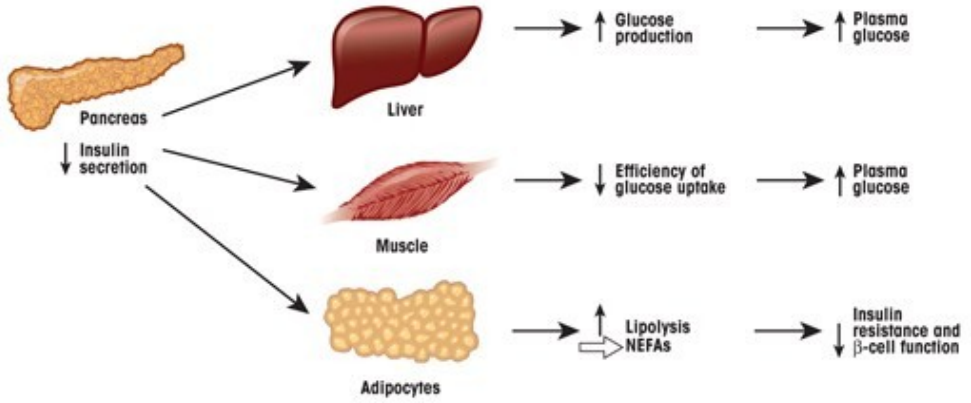

Figure 1: Model of the critical role of impaired insulin release in linking obesity with insulin-resistance and type 2 diabetes.
Impaired insulin secretion results in decreased insulin levels and decreased signaling, leading to increased food intake and weight gain, decreased inhibition of hepatic glucose production, reduced efficiency of glucose uptake in muscle, and increased lipolysis in the adipocyte, resulting in increased plasma NEFA levels. The increase in body weight and NEFAs contribute to insulin-resistance, and the increased NEFAs also suppress the β-cell's adaptive response to insulin-resistance. The increased glucose levels together with the elevated NEFA levels can synergize to further adversely affect β-cell health and insulin action, often referred to as 'glucolipotoxicity'.
Adapted from Kahn SE, Hull RL, Utzschneider KM. *Nature*. 2006;444(7121):840-846

In the liver, insulin is involved in a number of actions responsible for glucose control and lipid metabolism. In case of insulin-resistance, insulin levels are raised to overcome this resistance. The resulting effects depend on the metabolic pathway: a deficient insulin response for glucose metabolism leads to increased glucose production in the fasting state, while elevated insulin leads to activation of the lipid biosynthetic pathway, resulting in increased VLDL production and dyslipidemia. Given the central role played by the liver in glucose and lipid metabolism, any imbalance between the entry and the export of lipid derivatives results in steatosis. Steatosis and insulin-resistance have a

number of reciprocal relationships and can enhance each other. A number of arguments suggest that insulin-resistance leads to steatosis and that steatosis, or rather the presence of fatty acid (FA) derivates used for triglyceride (TG) synthesis, enhances insulin-resistance. In human, steatosis and insulin-resistance are clearly associated, and lead to an increased prevalence of diabetes and cardiovascular risk. A number of mechanisms might explain this association, some of which are extrahepatic, such as adipose tissue or diet, while some are intrahepatic.

1.3 Insulin signaling in the liver

Hepatocytes are one of three main types of insulin target cells (along with myocytes and adipocytes) that carry a large number of insulin receptors on their cell surfaces. Insulin signaling can only take place through insulin receptors (Chapeau 2005; Taniguchi et al. 2006).

1.3.1 Insulin signaling pathway

Insulin binding to its receptor induces complex signaling cascades. The insulin receptor is an heterotetrameric bifunctional transmembrane glycoprotein comprising two extracellular α subunits and two transmembrane β subunits linked by disulfide bonds. The β subunits possess tyrosine-kinase activity in their intracytoplasmic domain, which is activated after linkage with insulin and phosphorylated on specific tyrosine residues on the receptor itself. This phosphotyrosine signal is recognized by protein substrates of the receptor that become activated and transmit the insulin signal in the cell. Several intracellular substrates of the insulin receptor kinases have been identified. Four of these belong to the family of insulin-receptor substrate (IRS1-4) proteins (White 1998). In addition, phosphotyrosines of the insulin receptor β subunit can also be recognized by substrates from the SHC and CAP/cbl families. Two main pathways diverge from the receptor: one leads to activation of phosphatidylinositol 3-kinase (PI3-K), then PKB/Akt or atypical PKC, like PKC-ζ and λ and stimulates the metabolic activities such as increased glycogen synthesis, lipogensis and inhibition of gluconeogenesis; the other, called MAP kinase pathway, leads to activation of cell proliferation and differentiation (Figure 2). However, in most cases, a specific effect of insulin requires the participation of both the pathways in a complex interplay which could explain the pleiotropy and the specificity of the insulin signal (Cusi et al. 2000).

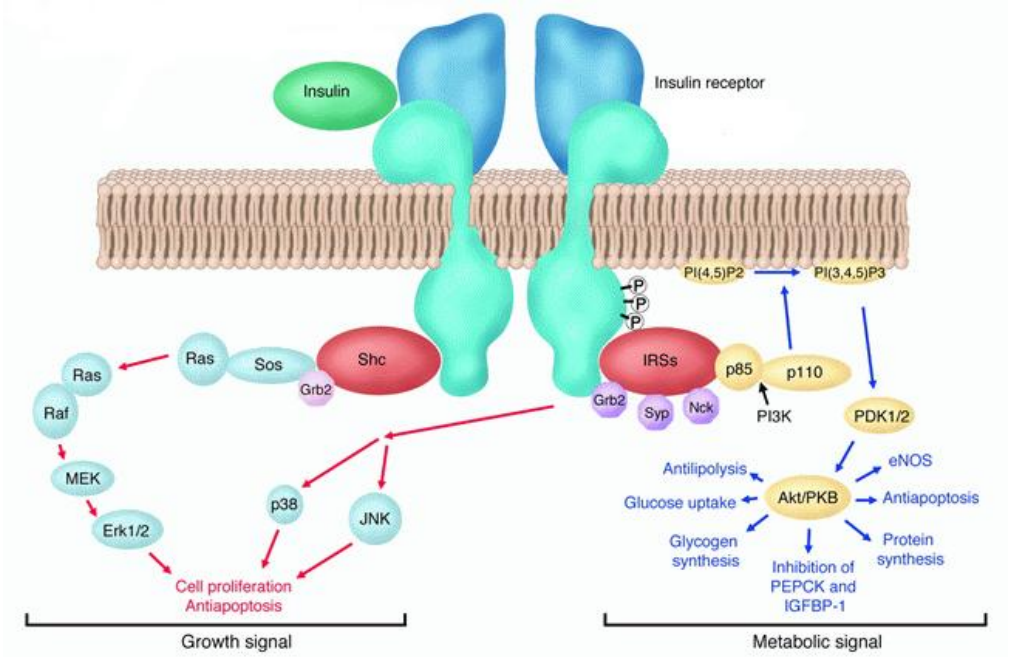

Figure 2: Insulin signaling.
Insulin binding to the extracellular domain of the insulin receptor elicits a conformational change, which in turn leads to receptor autophosphorylation (P) and tyrosine phosphorylation of intracellular protein substrates. Two main branching pathways are activated by insulin: **(a)** One is the MAPK signaling cascade, in which the Grb2/Sos pathway leads to activation of Ras signaling, affecting cell proliferation and apoptosis. In view of their mitogenic nature, these can be characterized as "growth signal" effects. **(b)** The other is the IRS pathway, which leads to activation of kinases dependent upon the heterodimeric (p85/p110) PI3K, such as Akt, also referred to as protein kinase B (PKB); Akt modulates enzyme activities that, besides affecting NO generation and apoptosis, control glucose, lipid, and protein metabolism. This PI3K-branching pathway is termed the "metabolic signal." PI(4, 5)P2, phosphoinositide 4,5 di-phosphate; PI(3, 4, 5)P3, phosphoinositide 3,4,5 tri-phosphate; PDK1 phosphoinositide–dependent kinase–1; MEK, MAPK kinase.

1.3.2 Insulin controls hepatic glucose and lipid metabolism

Insulin controls glucose metabolism in the liver suppressing hepatic glucose output by stimulating glycogen synthesis and inhibiting glycogenolysis and gluconeogenesis.
The regulation of gluconeogenesis in the liver is dependent on a number of key enzymes: pyruvate carboxylase, phosphoenolpyruvate carboxykinase (PEPCK), fructose-1,6-bisphosphatase, and glucose-6-phosphatase (Pilkis and Claus 1991). Insulin directly regulates the expression of these genes (Pilkis and Granner 1992), inhibiting the transcription of the gene encoding PEPCK or fructose-1,6-bisphosphatase and glucose-6-phosphatase and increasing transcription of glycolytic enzymes such as glucokinase and pyruvate kinase.

Insulin stimulates glycogen accumulation through a coordinated increase in glucose transport and glycogen synthesis. The GSK3, a serine/threonine kinase, phosphorylates glycogen synthase and inactivates it. As glycogen synthase is a rate-limiting enzyme in glycogen synthesis, inactivation of GSK3 by insulin removes the inhibitory effect of GSK3 on glycogen synthase and leads to increased glycogen synthesis (Avruch 1998; Virkamaki et al. 1999; Fang et al. 2000). When glycogen stores and energy requirements are fulfilled, glucose is diverted towards lipid synthesis, first by glycolysis, then by the initiation of the mitochondrial tricarboxylic cycle and, finally, by lipogenesis in the cytosol to produce fatty acids. This means that lipid metabolism is strongly related to glucose metabolism in hepatocyte and biosynthetic pathways leading to glycogen and TG synthesis activated by insulin (Figure 3).

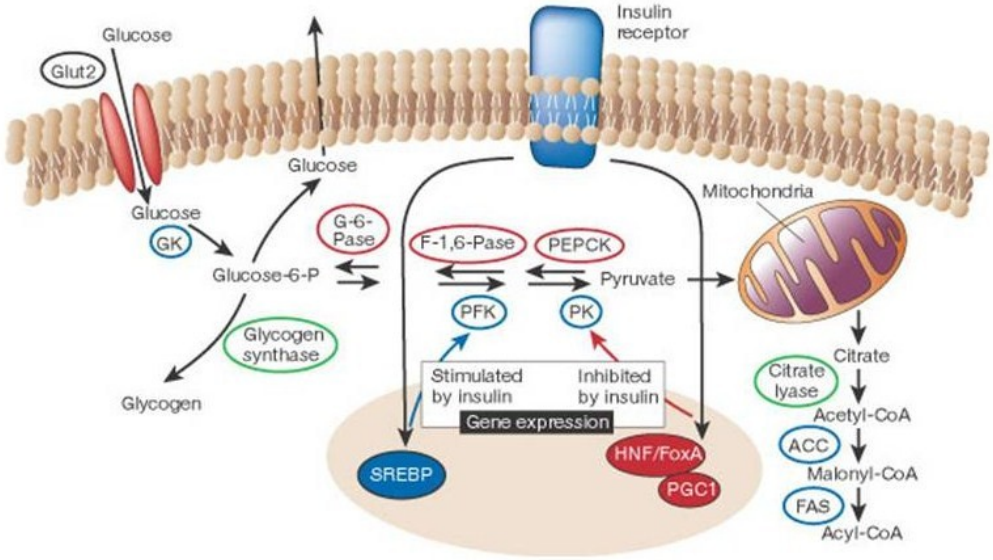

Figure 3: The regulation of glucose metabolism in the liver.
In the hepatocyte, insulin stimulates the utilization and storage of glucose as lipid and glycogen, while repressing glucose synthesis and release. This is accomplished through a coordinated regulation of enzyme synthesis and activity. Insulin stimulates the expression of genes encoding glycolytic and fatty-acid synthetic enzymes (in blue), while inhibiting the expression of those encoding gluconeogenic enzymes (in red). These effects are mediated by a series of transcription factors and co-factors, including sterol regulatory element-binding protein (SREBP)-1, hepatic nuclear factor (HNF)-4, the forkhead protein family (Fox) and PPARγ co-activator 1 (PGC1). The hormone also regulates the activities of some enzymes, such as glycogen synthase and citrate lyase (in green), through changes in phosphorylation state. GK, glucokinase; Glucose-6-P, glucose-6-phosphate; G-6-Pase, glucose-6-phosphatase; F-1,6-Pase, fructose-1,6-bisphosphatase; PEPCK, phosphoenolpyruvate carboxykinase; PFK, phosphofructokinase; PK, pyruvate kinase; ACC, acetyl-CoA carboxylase; FAS, fatty-acid synthase.

1.4 Hepatic lipogenesis

Storage of energy when food is available is determinant for survival. Quantitatively, the main form of energy storage is represented by lipids in adipose tissue. The origin of the stored lipids can be either the diet or *de novo* synthesis from carbohydrate through lipogenesis.

Triacylglycerol (TAG) is synthesized by esterification of glycerol-3-phosphate with fatty acid (FA). The two major tissues that synthesize FA and TAG at high level are the liver and adipose tissue and are also called lipogenic tissues. TAG synthesized in the liver is used for VLDL assembly to be secreted to the circulation, while TAG synthesized in adipose tissue is stored as the main energy storage form in mammals, and is hydrolyzed to release FA into circulation to be used by other tissues during periods of energy demand. Dysregulation of FA and TAG metabolism often contributes to metabolic diseases (Wong and Sul 2010).

Triglycerides are formed in response to fluxes of non-esterified fatty acids and glucose. Glucose provides *de novo* lipogenesis, via pyruvate citrate which generates acetyl-CoA for fatty acid synthesis.

Increased lipogenesis results from transcriptional activation of many genes econding glycolytic and lipogenic enzymes including glucokinase (GK), liver-pyruvate kinase (L-PK), acetyl CoA carboxylase (ACC), fatty acid synthase (FAS), stearoyl CoA desaturase (SCD1) which catalizes fatty acid elongation and desaturation steps, and finally mitochondrial glycerol3-phosphate acyltransferase (GPAT) and diacylglycerol acyltransferase (DGAT) for TG synthesis (Figure 4).

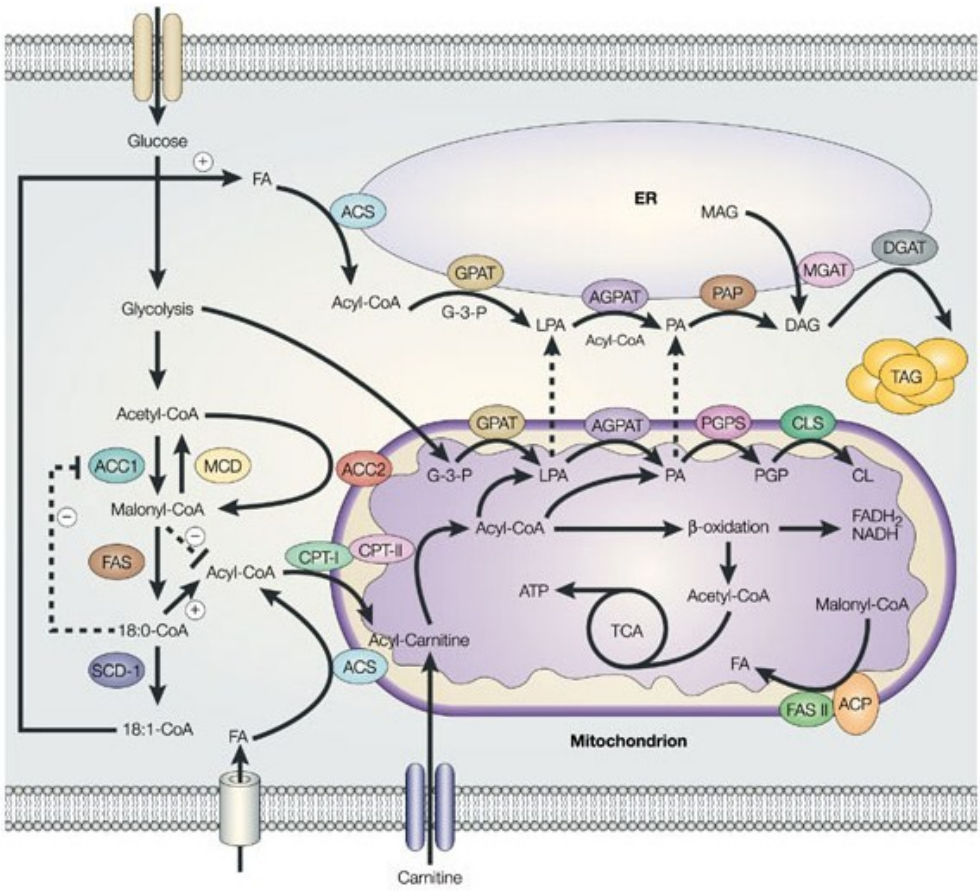

Figure 4: Interconnection of metabolic pathways involved in lipid synthesis in the endoplasmic reticulum and lipid oxidation in mitochondria of liver and skeletal muscle. Among the lipid metabolic enzymes, acetyl-CoA carboxylase (ACC), fatty-acid synthase (FAS) and carnitine palmitoyl transferase (CPT) are the three main enzymes that regulate the synthesis of malonyl-CoA, which is the principal inhibitor of fatty-acid entry into mitochondria for β-oxidation. Stearoyl-CoA desaturase-1 (SCD1) regulates lipid oxidation by converting stearic acid (18:0) to oleic acid (18:1). The saturated fatty acyl-CoAs are known to allosterically inhibit ACC1, whereas monounsaturated fatty acyl-CoAs are the preferred substrates for the lipid synthesis of triacylglycerol (TAG) in the endoplasmic reticulum (ER). Malonyl-CoA and stearic acid reciprocally regulate the entry of acyl-CoA into mitochondria by modulating the activity of CPTA. Lysophosphatidic acid (LPA) and phosphatidic acid (PA) are synthesized in the ER; they are also produced in mitochondria and transported to the ER where the terminal enzymes for TAG synthesis are located. Mitochondrial FAS (FAS II) and acyl-carrier protein (ACP) are involved in fatty-acid synthesis, but their role in lipid metabolism remains elusive. ACS, acyl-CoA synthase; AGPAT, acylglycerol-3-phosphate acyltransferase; CLS, cardiolipin (CL) synthase; DGAT, diacylglycerol (DAG) acyltransferase; GPAT, glycerol-3-phosphate (G-3-P) acyltransferase; MCD, malonyl-CoA decarboxylase; MGAT, monoacylglycerol (MAG) acyltransferase; PAP, phosphatidic-acid phosphohydrolase; PGPS, phosphatidylglycerophosphate (PGP) synthase; TAG, triacylglycerol; TCA, tricarboxylic-acid cycle.

Fatty acid synthesis is a cytoplasmatic process. All acetyl-CoA must be exported from the mitochondrial matrix via citrate (first step in Krebs cycle). In

the cytoplasm, citrate is split into acetyl-CoA and oxaloacetate. Then, acetyl-CoA is activated by ACC to malonyl-CoA, the immediate precursor for fatty acid synthesis. In mammals, two ACC isoforms exist, each with distinct tissue distribution and physiological roles: ACC1 is cytosolic and participates in *de novo* lipogenesis, while ACC2 is mitochondrial and is thought to be involved in the negative regulation of mitochondrial β-oxidation by modulating local malonyl-CoA levels (Postic and Girard 2008).

FAS is a single multifunctional polypeptide containing seven catalytic sites and is the key enzyme of fatty acid biosynthesis; it elongates a carbon chain starting from an acetyl-CoA primer with molecules of malonyl-CoA provided by ACC and requires the presence of NADPH and synthesizes Palmitic Acid (Foufelle et al. 1996). Palmitate is then released from the enzyme and can then undergo separate elongation and/or unsaturation to yield other fatty acid molecules.

To efficiently incorporate newly synthesized fatty acid into triglyceride, a fraction of synthesized fatty acids must undergo desaturation to monounsaturated fatty acids because the middle position of the glycerol backbone is optimally esterified with an unsaturated fatty acid. The enzyme stearoyl-CoA desaturase-1 (SCD-1) effects this desaturation and is essential to the efficient formation of triglyceride in the absence of adequate dietary unsaturated fatty acids. SCD1 catalyzes the synthesis of monounsaturated fatty acids, particulary oleate and palmitoleate, which are the major components of memebrane phospholipids, TGs, and cholesterol esters.

Accumulation of lipids has been linked to functional disturbances in various tissues and organs, often referred to as lipotoxicity (Unger 1995). Fatty liver is associated with hepatic insulin-resistance and β-cell lipotoxicity with impaired insulin secretion, both of which trigger diabetes. Thus, the mechanisms that regulate the uptake, *de novo* biosynthesis, and oxidative catabolism of lipids are very important.

1.4.1 Regulation of hepatic lipogenesis

All living organisms possess mechanisms for repeatedly reassessing the status of long-term energy stores and, when the need arises, making compensatory adjustments to adapt their metabolism to the nutritional environment. Mammals have developed a complex series of nutrient cues, relieved by hormones or impulses from the central nervous system, to regulate whole-body metabolism in response to acute deficiencies or to prolonged excess or shortage of nutrient supply. Hepatic metabolism plays a key role in the regulation of whole-body energy status since the liver is the major site for storage and release of carbohydrates and for fatty acid synthesis. Indeed, during the postprandial period, net glucose uptake permits the repletion of hepatic glycogen stores, the excess dietary carbohydrates being then converted into triglycerides to promote long-term energy storage. By contrast, in the

fasted state, a series of metabolic modifications induces net glucose output and lipid breakdown in the liver to maintain whole body homeostasis (Viollet et al. 2006).

AMP-activated protein kinase (AMPK) is a phylogenetically conserved serine/threonine protein kinase that has been proposed to function as a cellular energy sensor (Kahn et al. 2005) mediating the cellular adaptation to environmental or nutritional stress factors. It is activated when nutrient supply is limited, ATP generation is impaired, or cellular energy demand is increased (Kemp et al. 2003; Hardie et al. 2003). In the last few years, AMPK has come to be regarded as a point of conversion of regulatory signals monitoring systemic and cellular energy status. AMPK has a critical role in many metabolic processes, and, once activated, AMPK phosphorylates a number of proteins that determine increased glucose uptake and metabolism as well as fatty acid oxidation and, simultaneously, inhibition of hepatic lipogenesis, cholesterol synthesis, and glucose production (Hardie et al. 2004; Kahn et al. 2005; Hardie 2005) (Figure 5).

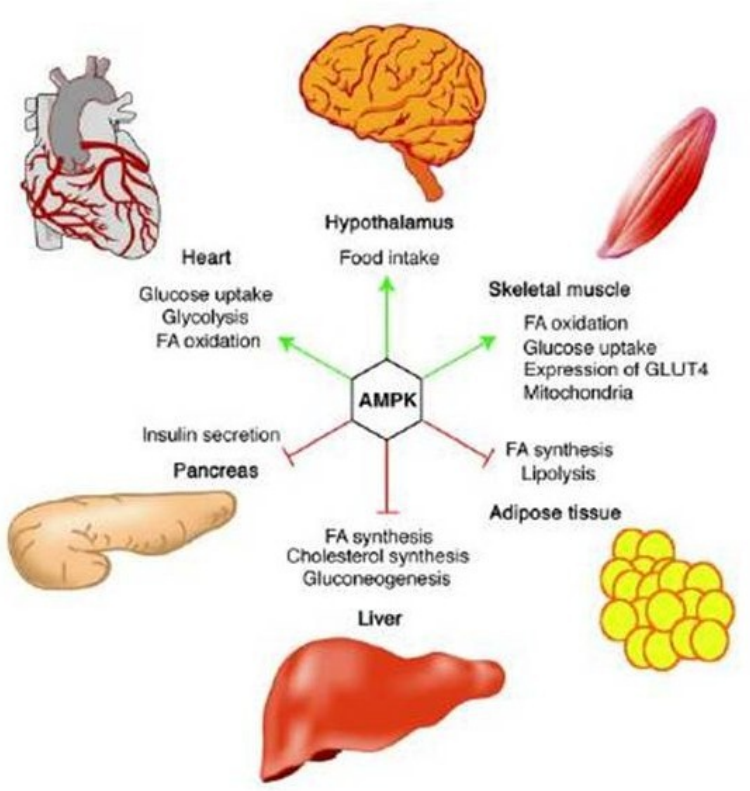

Figure 5: Role of AMPK in regulating energy balance at the whole-body level.
Green arrows indicate positive effects, and red lines with bars indicate negative effects. In the hypothalamus, activation of AMPK in response to low glucose or leptin levels increases food intake; references for other effects of AMPK activation can be found in recent reviews. FA, fatty acid.

AMPK exists as a heterotrimeric complex consisting of a catalytic subunit α and two regulatory subunits β and γ (Hardie et al. 1998) and isoforms of all three subunits (α1, α2, β1, β2, γ1, γ2 and γ3) have been identified in mammals (Carling 2004). AMPK phosphorylates multiple targets in the liver in order to acutely switch on alternative catabolic pathways and switch off anabolic pathways (Table 1).

Target	Enzymatic properties	Phosphorylation site(s)	Biological effect(s)	References
ACC1	↓ Activity	Ser^{79}	↓ Lipogenesis	Munday *et al.* (1988)
ACC2	↓ Activity	Ser^{218}	↑ Oxidation	Winder *et al.* (1997)
eEF2Kinase	↑ Activity	Ser^{398}	↓ Protein synthesis	Horman *et al.* (2002) Browne *et al.* (2004)
GPAT	↓ Activity	?	↓ Triglyceride synthesis	Muoio *et al.* (1999)
HMG-CoA reductase	↓ Activity	Ser^{872}	↓ Cholesterol synthesis	Clarke & Hardie (1990)
MCD	↑ Activity	?	↓ Malonyl CoA	Assifi *et al.* (2005)
PFK-2/FBPase-2	Weak kinetic effects	Ser^{22}, Ser^{32}	?	Guigas *et al.* (2006)
mTOR	↓ Activity	Thr^{2446}	↓ Protein synthesis	Cheng *et al.* (2004)
TSC2	↑ Activity	Thr^{1227}, Ser^{1345}	↓ Protein synthesis	Inoki *et al.* (2003)

Table 1: Role Hepatic targets of AMPK.

ACC and 3-hydroxy-3-methylglutaryl-coenzyme A reductase (HMG-CoA reductase) were the first enzymes shown to be downstream targets for AMPK (Hardie et al. 2004). ACC and HMG-CoA reductase are, respectively, key enzymes in fatty acid and cholesterol synthesis, known as ATP-consuming biosynthetic pathways. ACC is an important rate-controlling enzyme for the synthesis of malonyl-CoA, which is both a critical precursor in the biosynthesis of fatty acids and a potent inhibitor of mitochondrial fatty acid oxidation. Inhibition of ACC by AMPK leads to a fall in malonyl-CoA content and a subsequent decrease in fatty acid synthesis and increase in mitochondrial fatty acid oxidation via the allosteric regulation of carnitine palmitoyltransferase-1 (CPT-1), which catalyses the entry of long-chain fatty acyl-CoA into mitochondria. Accordingly, insulin activates ACC to promote malonyl-CoA synthesis by inhibiting AMPK (Witters and Kemp 1992).

AMPK has been implicated in the control of hepatic glucose and lipid homeostasis by many additional effects both on genes and on short-term regulation of specific enzymes. In the short-term regulation, AMPK phosphorylates and inactivates ACC (acetyl-CoA carboxylase), thus inhibiting FA biosynthesis. At the same time, inactivation of ACC decreases malonyl CoA concentration, which in turn de-represses CPT1 (carnitine palmitoyl transferase 1) and activates FA oxidation (Hardie et al. 1998). In the long term, AMPK is thought to regulate hepatic lipogenic gene expression by inhibiting transcription factors (Ferre et al. 2003). Indeed, AMPK has been found to down-regulate SREBP-1c (sterol-regulatory-element-binding protein-1c) (Zhou et al. 2001) and inhibit ChREBP (carbohydrate responsive element-binding protein) (Kawaguchi et al. 2002). Thus, in the liver, AMPK coordinates the changes in the activity of enzymes of lipid metabolism and regulates the partitioning of fatty acid between oxidative and biosynthetic pathways.

Recent studies have shown that both Liver Kinase B1 (LKB1) and Ca^{2+}/calmodulin-dependent protein kinase kinase-β (CaMKKβ/CAMK2) play important roles in phosphorylating and activating AMPK. LKB1 (also known as STK11) is a 50 kDa serine/threonine kinase which contains both a kinase domain and a nuclear localization signal in its N-terminal region. Germline mutations of the LKB1 gene are responsible for the cancer-prone Peutz-Jeghers syndrome (Jenne et al. 1998; Boudeau et al. 2003). The majority of Peutz-Jeghers syndrome missense mutations are located in the region coding for the kinase domain and result in the abolition of the enzymatic activity, thus disrupting all functions attributed to LKB1. The C-terminal region of LKB1 contains several post-translational modifications. Five phosphorylation sites have been identified in human; two residues are autophosphorylation sites (Thr^{336} and Thr^{402}), and three others (Ser^{325}, Thr^{363}, and Ser^{428}) are phosphorylated by upstream kinases (Boudeau et al. 2003). LKB1-Ser^{428} phosphorylation is required for both its nuclear export of LKB1 into cytosols, in which it forms an active complex with STRAD and MO25 and consequent AMPK phosphorylation. Because various stimuli increased the phosphorylation of LKB1 at Ser^{428}, it is tempting to speculate that LKB1-Ser^{428} phosphorylation might be a common pathway required for AMPK activation (Figure 6). LKB1 localization depends on its kinase activity, import into the nucleus, and retention within cytoplasm. It has been reported that cytoplasmic localization of LKB1 is critical for its normal function (Tiainem et al. 2002; Nezu et al. 1999; Boudeau, Baas et al. 2003). Recently, LKB1 was demonstrated to phosphorylate and activate the catalytic α-subunit of AMPK at its T-loop residue Thr^{172} in a cell-free system (Woods et al. 2003; Hawley et al. 2003). The major AMPK kinase activity in liver seems to correspond to LKB1 since it has been shown that deletion of LKB1 in the liver results in a proportional decrease of AMPK phosphorylation at Thr^{172} rendering AMPK insensitive to stimuli which normally activate it (Shaw et al. 2005). Thus, LKB1 is a crucial regulator of AMPK activation in muscle and liver cells and its activity is of potential importance to understand glucose and lipid metabolism.

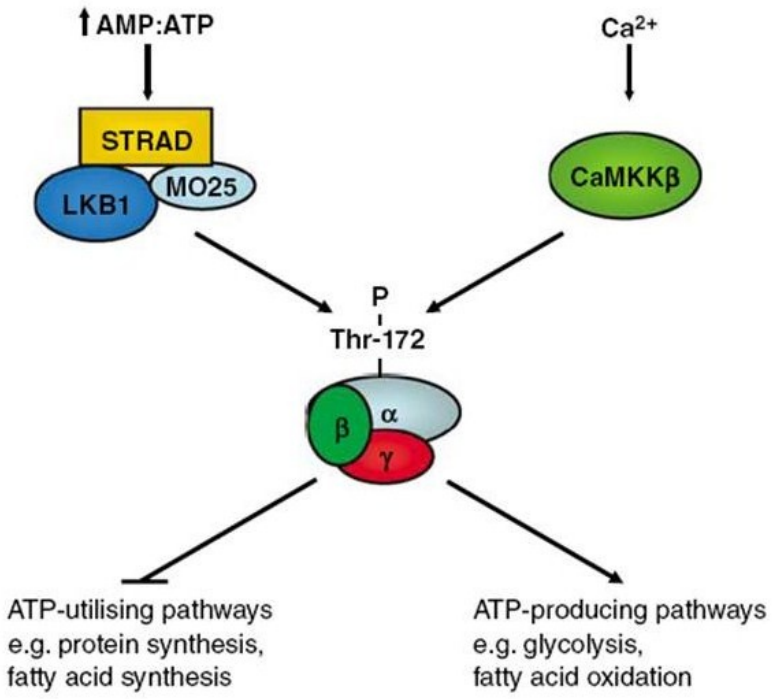

Figure 6: Role of AMPK in regulation of energy balance.
AMPK is activated by phosphorylation of threonine 172 (Thr-^{172}) within the catalytic a-subunit, catalysed by upstream AMPK kinases. Previous studies have identified LKB1 and CaMKKβ acting upstream of AMPK. LKB1, like AMPK forms a heterotrimeric complex, requiring binding of MO25 and STE-20 related adaptor protein (STRAD) for activity, and is involved in activation of AMPK in response to an increase in the AMP/ATP ratio. CaMKKβ is involved in the Ca^{2+}-dependent activation of AMPK. Following activation, AMPK phosphorylates a number of downstream targets with the overall effect of switching-off ATP consuming pathways, for example, protein synthesis and fatty acid synthesis, while switching-on ATP generating pathways, for example, glycolysis and fatty acid oxidation.

Together, LKB1 and AMPK control cell growth in response to environmental nutrient changes, which identifies new targets and drugs for cancer therapy, including several existing diabetes therapeutics that are known to potently activate AMPK.

Recent work has established a central role of atypical protein kinase Cζ (PKCζ), a protein kinase of the AGC family, as a key regulator in LKB1-dependent AMPK activation. Inhibition of PKCζ with pharmacological and genetic inhibitors effectively blocked AMPK activation caused by $ONOO^-$. This AMPK activation pathway was LKB1-dependent, involved LKB1 phosphorylation at Ser^{428} within the C-terminal part of LKB1, and led to the association of LKB1 with AMPK (Xie et al. 2006). PKCζ-dependent and LKB1-mediated AMPK activation might play important roles in regulating not only cellular energy metabolism but also signaling pathways that control cell growth, differentiation, and survival.

1.4.2 Lipogenesis and genes

The past few years have brought a deluge of new data about the mechanisms of regulation of lipogenesis by nutrient and hormones. Regulation of gene expression by nutrients is an important part of the mechanisms allowing mammals to adapt to their nutritional environment. This is especially true for enzymes involved in the storage of energy such as the lipogenic and glycolytic enzymes in the liver and adipose tissue. These enzymes are acutely regulated by post-translational and allosteric mechanisms but are mainly controlled on a long-term basis by a modulation of their transcription rate. It is clear that transcription factors and some other genes are attractive targets for pharmaceutical intervention of disorders such as hypertriglyceridemia and obesity.

It is now well accepted that the transcription factor Sterol Regulatory Element-Binding Protein-1c (SREBP-1c), itself stimulated by insulin, mediates the transcriptional effect of this hormone on the enzymes involved in fatty acid synthesis. SREBP family, originally identified as basic helix–loop–helix (bHLH) leucine zipper transcription factors, is involved in the regulation of genes participating in cholesterol biosynthesis and low-density lipoprotein receptor synthesis (Brown and Goldstein 1997; Brown and Goldstein 1999). The SREBP family consists of three isoforms: SREBP-1a, SREBP-1c, and SREBP-2. Each isoform has a different regulatory mechanism (Horton and Shimomura 1999; Shimano 2001; Shimano 2002; Ide et al. 2004). SREBP-1c activates transcription of genes involved in fatty acid and triglyceride synthesis, such as the genes encoding acetyl-CoA carboxylase, fatty acid synthase, Elovl-6, and stearoyl-CoA desaturase. These genes are regulated by SREBP-1c, depending on the nutritional conditions for triglyceride storage. Intake of energy molecules such as sugars, carbohydrates and saturated fatty acids activates SREBP-1c expression, which is eliminated under conditions of fasting and starvation. SREBP-1c activates insulin-mediated lipogenesis, whereas starvation signals such as glucagon, protein kinase A and AMP-activated protein kinase inhibit SREBP-1c. Thus, SREBP-1c plays a major role in the long-term control of glucose and lipid homeostasis by insulin, through the regulation of glycolytic and lipogenic gene expression.

With the exception of hepatic GK, which is exclusively induced by insulin (Magnuson et al. 1989), most of the glycolytic and lipogenic genes are also regulated by glucose (Girard et al. 1997; Towle et al. 1997; Vaulont et al. 2000). Another important protein that plays a critical role in the glucose-mediated induction of gene products involved in hepatic glycolysis and lipogenesis is the glucose-responsive transcription factor ChREBP (Carbohydrate response element-binding protein). Glucose affects the activity of ChREBP largely through post-translational mechanisms involving phosphorylation-dependent cellular localization (Sakiyama et al. 2008).

ChREBP is a large protein (864 amino acids and 94,600 Da) that contains

several domains including a nuclear localization signal (NLS) near the N-terminus, polyproline domains, a basic loop–helix–leucine-zipper (b/HLH/Zip), and a leucine-zipper-like (Zip-like) domain. Glucose activates ChREBP by regulating its entry from the cytosol into the nucleus (Dentin et al. 2005; Kawaguchi et al. 2001) thereby promoting its binding to carbohydrate responsive element (ChoRE) present in the promoter regions of glycolytic and lipogenic genes (Ishii et al. 2004). Moreover, ChREBP is also regulated by glucose at the transcriptional level (Dentin et al. 2004).
Together ChREBP and SREBP-1c provide a pair of transcription factors that functions in synergy through distinct binding response elements to coordinately regulate glucose metabolism and lipogenesis (Figure 7).

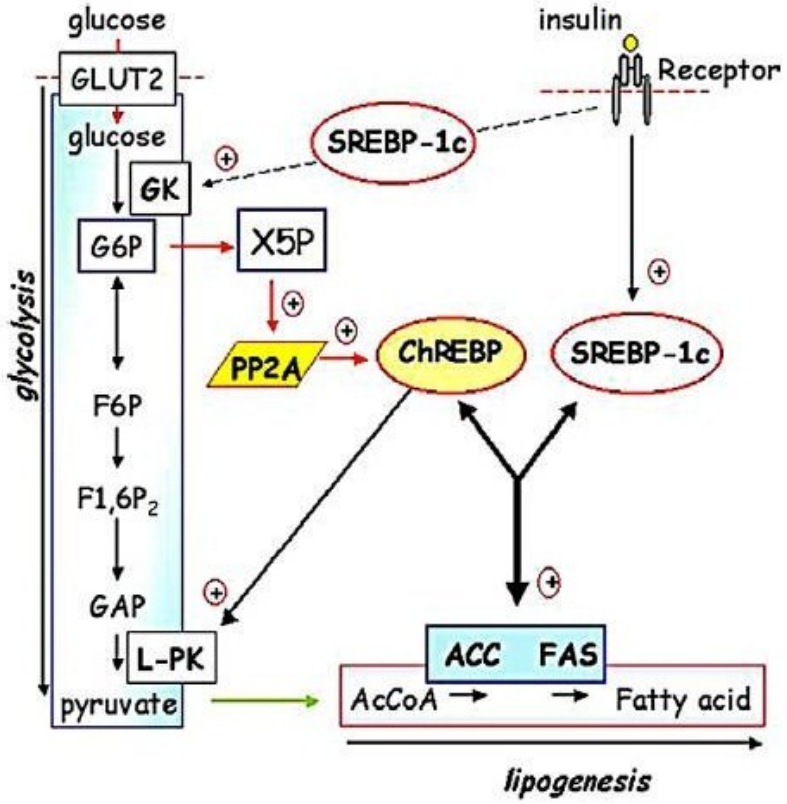

Figure 7: SREBP-1c and ChREBP act in synergy to regulate glycolytic and lipogenic gene expression.
The phosphorylation of glucose in glucose 6-phosphate, by hepatic glucokinase, is an essential step for glucose metabolism as well as for the induction of glycolytic and lipogenic genes. The recent identification of ChREBP has shed light on the possible mechanism whereby glucose affects gene transcription. The activity of ChREBP requires a mechanism of phosphorylation/dephosphorylation which is determined by the relative activity of protein phosphatase 2A (PP2A), regulated by X5P concentrations. SREBP-1c, which is induced by insulin, also plays an important role in mediating insulin signaling on lipogenic gene expression. These two transcription factors work synergistically to induce transcription of the lipogenic genes in the presence of glucose and insulin.

An important transcription factor in adipose tissue is the nuclear hormone receptor Peroxisome Proliferator-Activated Receptor gamma (PPARγ). This protein is part of the adipocyte differentiation program, inducing the differentiation of pre-adipocytes into mature fat cells. With respect to the liver, although PPARγ is normally only minimally expressed in hepatocytes, hepatic triglyceride accumulation is associated with a dramatic increase in PPARγ expression, suggesting that the protein may play a role in stimulating lipogenesis (Chao et al. 2000).
As discussed earlier, the state of insulin-resistance at the level of the liver may be associated with increased lipogenesis. Recently, several works suggest that the family of homeodomain-containing transcription factors named TALE (Three Aminoacid Loop Extension) is strongly related to diabetes and insulin-resistance (Kim et al. 2002; Oriente et al. 2008; Oriente et al. 2011).

1.5 TALE proteins

The three-amino acid loop extension (TALE) homeodomain proteins are recognized as transcription factors responsible for regulating growth and differentiation during vertebrate embryogenesis. The genes encoding these proteins are highly conserved and are present in the common ancestor of plants, fungi, and animals.
TALE proteins display a highly conserved DNA binding domain of approximately 60 amino acids called the homeodomain (Gehring et al. 1994). This region is composed of three alpha helices and a flexible N-terminal arm. The homeodomain interacts with the DNA through the third helix making base-specific contacts in the major groove of DNA and through the N-terminal arm which contacts the minor groove of DNA. Between the first and the second alpha helices of the homeodomain there is an extension of three amino acids, virtually represented by a proline (P) – tyrosine (Y) – proline (P) in position 24-26. This domain has been implicated in important protein–protein interactions that are required for fundamental aspects of development. The TALE homeodomain superclass is composed of two groups: the PBC and the MEIS families. The PBC subclass of the TALE homeodomain proteins, referring to the conserved PBC motif N-terminal to the TALE homeodomain (Burglin 1997; Burglin 1998), includes the vertebrate Pbx proteins, fly Extradenticle and worm Ceh-20. The MEIS class includes Homothorax (Hth) in flies and the Meis and Prep proteins in vertebrates (Figure 8) (Moens and Selleri 2006).

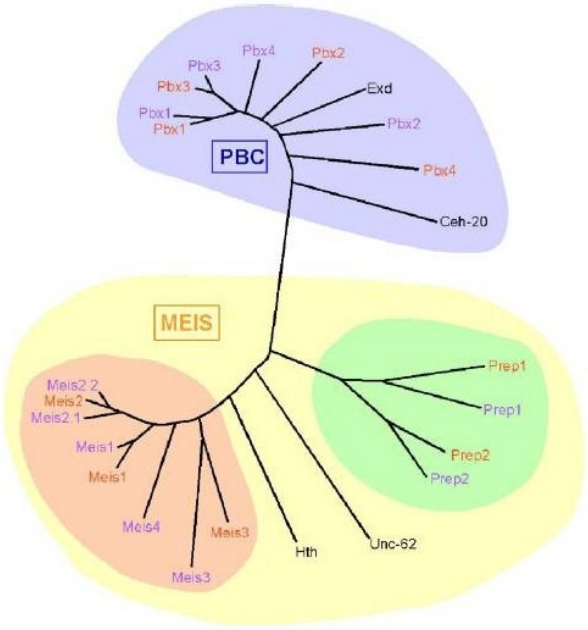

Figure 8: Phylogeny of Hox cofactors.
TALE homeodomain proteins are divided into two groups: the PBC family, including the vertebrate Pbx proteins, fly Extradenticle and worm Ceh-20, and the MEIS family, including vertebrate Meis and Prep, fly Homothorax (Hth) and worm Unc-62. Orange letters indicate mouse proteins, purple lettering indicates their zebrafish orthologs. Although in some cases the orthology assignments are not clear (as for *pbx2* and *pbx4*), genetic rescue experiments in zebrafish have suggested that the different *pbx* genes are functionally identical. Similar information is not yet available with regard to mammalian *Pbx* genes.

Cooperative function among TALE family members is critical for transcription regulation (Bischof et al. 1998; Chang et al. 1997; Knoepfler et al. 1997), and several members have been shown to function as essential contributors to Hox-mediated developmental programs (Chan et al. 1994; Mann and Chan 1996; Rauskolb and Wieschaus 1994).

1.5.1 Pbx1 protein

Pbx1 (pre-B cell leukemia transcription factor) protein is a small ubiquitous molecule which belongs to the PBC family. The proto-oncogene *PBX1* was identified as one of the loci affected in the t(1;19) translocation found in a quarter of all pediatric pre-B-cell acute lymphoblastic leukemias (Kamps et al. 1990; Nourse et al. 1990). This translocation results in expression of a fusion protein consisting of the activation domains of E2A and most of Pbx1, including its homeodomain.
In mice, the individual contribution of each member of PBC family seemed to be different because, whereas the *Pbx1* single mutant had a wide range of malformations, only minor or no phenotypes were obvious in *Pbx2* and *Pbx3* mutants suggesting an important role for Pbx1 in the embryonic development.

Pbx1 protein is characterized by the homeodomain region including the three aminoacid loop extension which interacts with the specific sequences of the HOX transcription factors or the Pancreatic and Duodenal homeobox-1 transcription factor (PDX-1). Near the amino terminal region there are two higly homologous regions named PBC- A and –B important for the protein-protein interaction (Figure 9) (Burglin 1997; Piper et al. 1999; Moens and Selleri 2006). The primary interaction between Pbx and HOX is via the three amino acid loop in the Pbx homeodomain, which binds a tryptophan-containing hexapeptide motif (N-Y/F-P/DW-M-K/R) N-terminal to the homeodomain in HOX proteins.

Genetic studies indicate the role of TALE homeodomain protein Pbx1 in the development and function of pancreatic islets, which contain the insulin secreting β-cells required for maintaining normal glucose homeostasis. Pbx1 is required in the developing pancreas for cell growth and differentiation and its relevance has been underlined by several studies involving knock-out mice. *Pbx1*$^{-/-}$ embryos exhibit pancreatic hypoplasia and marked defects in exocrine and endocrine cell differentiation before death at embryonic day (E) 15 or E16. Similarly, also PDX-1 is critical for pancreatic development. It is expressed in the foregut endoderm at E8.5, prior to the onset of bud formation and embryonic deletion of *PDX-1* results in pancreatic agenesis (Jonsson et al. 1994). Examination of *Pbx1*$^{+/-}$ mice showed that Pbx1 was required for pancreatic insulin secretion in mature islets, and that germline *Pbx1* inactivation led to inadequate levels of circulating insulin and impaired glucose tolerance, conditions known to presage the onset of overt type 2 diabetes. In these animals, the levels of PDX-1 are strongly reduced, indicating that Pbx1 is important for its expression and most probably assessing the molecular events responsible for the observed phenotype (Selleri et al. 2001; Brendolan et al. 2005; Kim et al. 2002). Analysis of transheterozygous *Pbx1*$^{+/-}$/*Pdx1*$^{+/-}$ mice revealed *in vivo* genetic interactions between Pbx1 and Pdx1 that are essential for postnatal pancreatic function and regulate islet structure and function. Consequently, simultaneous haploinsufficiency for *Pbx1* and *Pdx1* resulted in an oligogenic mouse model of age-dependent diabetes mellitus (Kim et al. 2002). Similarly, a Pbx interaction-defective Pdx1 transgene is unable to rescue normal glucose homeostasis in *Pdx1* null mice (Dutta et al. 2001).

The other class of TALE proteins, the MEIS transcription factors, interacts with PBC proteins, participating in ternary complexes with Hox proteins, or modulating PBC protein stability and subcellular localization.

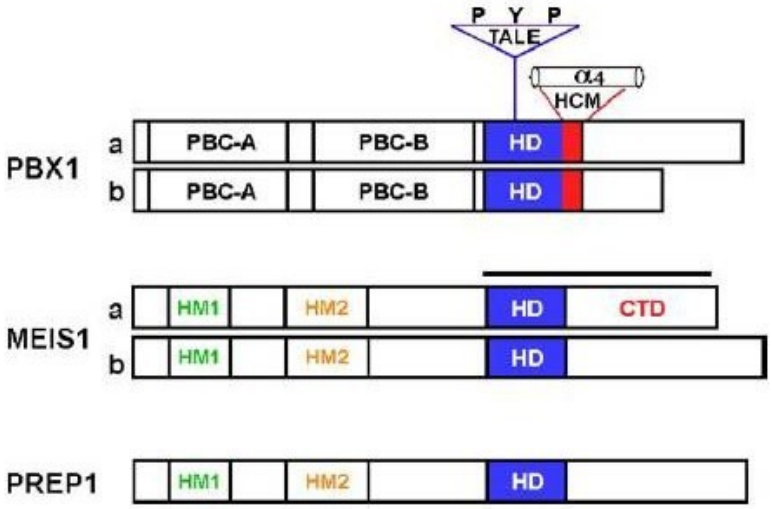

Figure 9: Structure of TALE homeodomain proteins.
Prototype members of PBC and MEIS classes are shown here. ‘‘a’’ and ‘‘b’’ refer to splice isoforms of Pbx and Meis proteins. All TALE homeodomain proteins contain a divergent homeodomain (HD) containing a 3 amino acid loop extension (TALE) between the first and second a-helices. The TALE motif virtually always bears a proline (P)– tyrosine (Y)– proline (P) in positions 24– 26 and contacts the hexapeptide motif of Hox proteins. Pbx proteins contain an additional DNA-contacting *a-helix* (a4; HCM) C-terminal to the canonical homeodomain. The PBC-A and PBC-B domains are conserved among Pbx, Exd and Ceh-20, and the PBC-A domain interacts with Meis/Prep proteins (Ryoo et al., 1999). Conversely, the HM1 and HM2 domains are conserved among Meis/Prep proteins and are required for interactions with Pbx proteins. Posterior *Hox* genes of the AbdB subclass are unusual in that they can interact directly with Meis proteins via a C-terminal region (CTD) of Meis including the homeodomain; this region is indicated by a black bar.

1.5.2 Prep1 protein

Prep1 (Pbx regulating protein 1) is a 64 kDa ubiquitary homeodomain transcription factor of the three aminoacid loop extension (TALE) superclass of proteins mapping on the chromosome 21q.22.3. The Prep1 homeodomain is structurally related to the PBC homeodomain class and contains an isoleucine residue in the third position of the conserved WF_N sequence in the homeodomain. Indeed, Prep1 forms DNA-independent dimeric complexes with the Pbx homeodomain transcription factor, enhancing target specificity and regulatory function (Berthelsen et al. 1998). Prep1 shares homology with MEIS proteins within the homeodomain and in two well-preserved amino terminal regions termed HR1 and HR2 (Homology Region) (HM in Figure 9). HR1 and HR2 bind the N-terminal region of Pbx1 (PBC-A) and are essential for Prep1-Pbx1 heterodimerization, which in turn is required for DNA binding (Berthelsen et al. 1998). Prep1 could be localized both in cytoplasm and in nucleus and the heterodimerization with Pbx1 appears to be essential to translocate Prep1 into the nucleus to bind DNA target. On the other hand,

Prep1 dimerization prevents nuclear export and the proteasomal degradation of Pbx1 prolonging its half-life (Berthelsen et al. 1999). Formation of dimeric complex drastically increases binding affinity of Prep1/Pbx1 to the DNA and also broadens the DNA target selectivity of Pbx1 to include sequences containing the TGACAG sequence (Berthelsen et al. 1998). Together Prep1 and Pbx1 form the UEF-3 (Urokinase Enhancer Factor-3) transcription factor, which is important in regulating the activity of the urokinase plasminogen activator (uPA) gene enhancer. The UEF3 DNA target site is a regulatory element in the promoters of several growth factor and protease genes, such as interleukin-3 (IL-3), stromelysin and urokinase plasminogen activator (uPA) (Berthelsen et al. 1996). Prep1 and Pbx1 can form ternary complexes with PDX-1 to regulate somatostatin gene transcription (Goudet et al. 1999).
The role of Prep1 has been in part clarified by the generation of mutant mice. Nevertheless, *Prep1* null embryos results in early lethality before gastrulation (E7.5) (Fernandez-Diaz et al. 2010), precluding a study of the Prep1 role in later developmental processes. An insertion of a retroviral vector in the first intron of the *Prep1* gene results in a hypomorphic mutation (*Prep1*$^{i/i}$) that exhibits variable penetrance and expressivity. *Prep1*$^{i/i}$ embryos die between E17.5 and P0 and present a profound alteration in the hematopoietic development with a deficient radioprotection activity of fetal liver (FL) progenitors and all colony-forming progenitors and profound anemia (Ferretti et al. 2006). However, a small percentage of the *Prep1*$^{i/i}$ embryos are born alive and subsequently live a normal length-life. The mice escaping embryonic lethality show T-cell development anomalies with a decreased number of circulating $CD4^+$ and $CD8^+$ T cells and increased apoptosis (Penkov et al. 2005). In addition, Prep1$^{i/i}$ feature an impairment of erythropoiesis and angiogenesis accompanied by liver hypoplasia, decreased hematocrit, anemia, and delayed erythroid differentiation together with a decrease in capillary formation (Ferretti et al. 2006). These mice show also alterations in eye development, in fact in most cases the size of the lens is strongly reduced, similar to the phenotype of *Pax6*-deficient mice. *Prep1* deficiency affects the expression of both TALE class partners *Pbx* and *Meis*, both required for embryonic hematopoiesis (Azcoidia et al 2005; Di Martino et al. 2001; Hisa et al. 2004).

1.5.3 Prep1 and insulin-resistance

In our laboratory we have recently evidenced an important role of Prep1 in pancreas development, glucose homeostasis and regulation of insulin-action in muscle and liver (Oriente et al. 2008; Oriente et al. 2011).
Prep1-hypomorphic mice show smaller pancreatic islet but normal architecture. However, these mice feature islet hypoplasia, accompanied by significantly reduced absolute insulin levels (both basal and postloading). The Prep1$^{i/i}$ phenotype includes also a strong reduction of pancreatic *Pbx1*

expression, emphasizing the idea that Prep1 hierarchically acts upstream in the network regulating pancreas development by controlling the levels of Pbx1. Moreover, these mice exhibit protection from streptozotocin-induced diabetes and enhanced insulin sensitivity with improved glucose uptake and insulin-dependent glucose disposal by skeletal muscle. This muscle phenotype does not depend on reduced expression of *Pbx1*, rather than on reduced levels of the recently identified novel Prep1 interactor p160 Myb-binding protein ($p160^{MBP}$), a molecule which is known to inhibit the PGC-1α-mediated glucose transport and competes with Pbx1 to bind Prep1. Consistent with $p160^{MBP}$ decrease, these mice show a muscle-selective increase in mRNA and protein levels of PGC-1α, accompanied by enhanced expression of the GLUT4 transporter and glucose uptake in muscle. These effects have been confirmed by transfecting *Prep1*, *Pbx1* and $p160^{MBP}$ cDNA in differentiating L6 skeletal muscle cells. Overexpression of Prep1 stabilizes $p160^{MBP}$, inducing $p160^{MBP}$ escape from proteasomal and reduces the levels of PGC-1α and GLUT4.

The mechanisms responsible for Prep1 action in liver differ from those in the skeletal muscle since Pbx1 and $p160^{MBP}$ are expressed at different levels. In fact, while there is a marked reduction of $p160^{MBP}$ in the skeletal muscle of the hypomorphic mice compared to the wild type animals, this difference has not detectable in the liver because in this organ the expression of $p160^{MBP}$ is very low. Thus, at variance with muscle, Prep1 major functional partner in liver appears to be Pbx1 rather than $p160^{MBP}$.

Prep1 deficiency in animal models improves insulin signaling in liver increasing hepatic glycogen content and decreasing glucose output and triglyceride levels. Analysis of the initial steps in insulin signaling in the *Prep1*-deficient mouse liver revealed increased tyrosine phosphorylation of both insulin receptor and the major IRSs present in these cells. These effects are paralleled by a significant reduction of expression of SYP and SHP1 tyrosine phosphatases. The functional relevance of Prep1 control of SHP1 versus SYP expression to hepatic sensitivity to insulin was assessed in further experiments in HepG2 liver cells stable transfected with *Prep1*. These cells feature a very significant reduction of insulin effect on glycogen accumulation. In particular, expression of SHP1 in cellular models negatively correlates with insulin signaling. However, antisense silencing of *SHP1* rescued insulin effect in these cells, thus establishing SHP1 as the functionally relevant target of Prep1 in the liver. The regulatory region of *SHP1* gene contains several Prep1 binding sites in the 4,000 base-pair region upstream *SHP1* transcription initiation site and one Prep1/Pbx1 binding site responding to the ectopic expression of Prep1 and Pbx1 in cotransfection experiments in vitro. In these assays, a fragment containing single Prep1/Pbx1 binding site displays a powerful enhancer function. Thus, Prep1-Pbx1 complex enhances *SHP1* gene transcription by acting on regulatory sequences upstream the ATG codon.

On the basis of the results, Prep1 might be considered as a new gene involved in the pathogenesis of type 2 diabetes and insulin-resistance.

1.6 Tyrosine and lipid phosphatases

Insulin signaling cascade may be attenuated by several enzymes, like for example the protein tyrosine phosphatases (PTPases), which catalyse the rapid dephosphorylation of the receptor and its substrates. Several PTPases, as the tyrosine phospatases PTP-1B, SYP and SHP1 and the lipid phosphatases SHIP2 and PTEN, are expressed in insulin-responsive cells and are up-regulated in states of insulin-resistance.

The Protein Tyrosine Phosphatese 1B (PTP1B) is a major regulator of insulin sensitivity and body fat content and deletion of its gene leads to increased insulin sensitivity and resistance to obesity induced by high fat feeding (Cheng et al. 2002; Johnson et al. 2002; Elchebly et al. 1999; Klaman et al. 2000).

SYP is a widely expressed PTP and its overexpression in a transgenic mouse model induces insulin-resistance (Maegawa et al.1999).

Another PTP recently linked to insulin signaling and glucose metabolism is SHP1. Mice expressing a catalytically defective SHP1 are markedly glucose tolerant and insulin sensitive compared to wild-type controls, as a result of enhanced insulin receptor signaling to IRS-PI3K-Akt in liver and muscle (Dubois et al. 2006).

Insulin pathway can be regulated by other phosphatases, the lipid phosphatases. Insulin activates the phosphoinositide 3-kinase (PI3K) which phosphorylates phosphatidylinositol 4,5 bisphosphate transiently generating phosphatidylinositol 3,4,5 trisphosphate at the plasma membrane (Czech 2003). Regulation of the PI3K pathway is critical for the prevention of insulin-resistance. PtdIns(3,4,5)P3 binds to the pleckstrin homology (PH) domain of the AGC family protein kinases, including protein kinaseB (PKB)/Akt, serum- and glucocorticoid-induced protein kinase (SGK) and protein kinase C (PKC), localizing and activating these kinases (Cantley 2002). Lipid phosphatases, src homology 2 domain containing inositol 5'-phosphatase 2 (SHIP2) and skeletal muscle and kidney-enriched inositol phosphatase (SKIP) hydrolyze PI(3,4,5)P3 to PI(3,4)P2 and phosphatase and tensin homolog deleted on chromosome ten (PTEN) hydrolyzes PI(3,4,5)P3 to PI(4,5)P2.

SH2-containing inositol 5'-phosphatase 2 (SHIP2) is a lipid phosphatase that contributes to the negative regulation of insulin signaling specifically via its 5'-phosphatase activity. A *SHIP2* knockout mouse has been recently reported, generated by deleting the first 18 exons of the *SHIP2* gene which encodes the SH2 domain and catalytic 5-phosphatase domain, leaving exons 19–28 intact (Sleeman et al., 2005). On a normal diet the serum triglycerides, non-esterified free fatty acids cholesterol and leptin levels are decreased in $SHIP2^{-/-}$ mice, although the basal metabolic rate is the same as wild type litter mate controls. Significantly, $SHIP2^{-/-}$ mice do not become obese on a high fat diet, showing an increased metabolic rate and inability to increase body fat, but no increase in serum lipids, insulin or glucose levels under obesity inducing conditions. In addition, polymorphisms in the human *SHIP2* gene are associated, at least in part, with the insulin resistance of type 2 diabetes.

SHIP2 appears to play an important role in the control of glucose and/or energy homeostasis by the regulation of the insulin action and emerges as a potential target for the treatment of obesity and insulin-resistance.
Another key negative regulator of the phosphatidylinositol 3-kinase/Akt pathway is the lipid phosphatases PTEN (Stambolic et al. 1998). Whole body *PTEN* knockout (KO) mice die at the early stages of embryonic development, which prevents study of the role of PTEN in the mammalian insulin signaling pathway in a whole animal model (Di Cristofano et al. 1998; Suzuki et al. 1998). Recent development of a liver-specific *PTEN* KO mouse exhibiting a phenotype of fatty liver and steatohepatitis due to increased lipogenesis and TG storage suggests a key role of this phosphatase in hepatic lipid and lipoprotein metabolism (Horie et al. 2004; Stiles et al. 2004).

2. AIMS OF THE STUDY

Insulin-resistance is a common feature present in a number of physiological and pathological conditions in humans and is commonly found in a large number of adults, in particular those with android obesity, metabolic syndrome or type 2 diabetes. Strong adverse relationships between adipose tissue, liver and muscle in these patients determine lipotoxicity, with deposition of triglycerides within the liver and muscles together with insulin-resistance.

Prep1 is an homeodomain transcription factor that, in combination with its major partners, Pbx proteins, regulates the overall size of the organism and individual organs as well as major developmental pathways. Data produced in our lab indicate that *Prep1* hypomorphic mice ($Prep1^{i/+}$) have a complex metabolic phenotype characterized by increased insulin sensitivity accompanied by protection from streptozotocin-induced diabetes and by the presence of smaller but normally structured islets with reduced fasting and post-loading plasma insulin levels. In muscle tissue, *Prep1* deficiency positively modulates the intracellular pool of GLUT4 by enhancing the transcription of PGC-1α gene. In the liver, the mechanism is independent on PGC-1α and the improvement of insulin signaling is characterized by a reduction of tyrosine phosphatases SHP1, whose transcription is mediated by the Prep1/Pbx1 complex and by an increase of insulin-stimulated insulin receptor and IRS1/2 tyrosine phosphorylation.

As mentioned before, $Prep1^{i/+}$ mice show decreased hepatic triglyceride levels (Oriente et al. 2011). Whether and how Prep1 affects lipid metabolism in liver is unknown at the present, thus the aim of my project has been to investigate the role of Prep1 on hepatic lipogenesis.

To achieve this aim I have studied the main genes involved in the regulation of lipid metabolism in the liver of Prep1 hypomorphic mice and focused my attention on the possibility that these genes could have been regulated by the transcription complex Prep1/Pbx1. Moreover, I have investigated whether the overexpression of Prep1 might increase triglyceride synthesis in HepG2 (hepatoma cells) and confirm the molecular mechanism by which Prep1 acts.

3. MATERIALS AND METHODS

3.1 Materials

Media, sera, antibiotics for cell culture and the lipofectamine reagent were from Invitrogen (Grand Island, NY). The Prep1, actin, Pbx1, SHP1, SHIP2, p-ACC, ACC, AMPK, LKB1, p-CAMK2, CAMK2, p-PKCζ, PKCζ, p-PKA, PKA antibodies were from Santa Cruz Biotechnology, Inc. (Santa Cruz, CA). The p-LKB1 and p-AMPK antibodies were from Cell Signaling Tecnology, Inc. Protein electrophoresis and Real Time PCR reagents were purchased from Bio-Rad (Hercules, CA), Western blotting and ECL reagents from Amersham Biosciences (Arlington Heights, IL). Oil Red O stain and all other chemicals were from Sigma (St. Louis, MO).

3.2 Generation of Prep1 hypomorphic mice

Prep1 targeted mice were generated by gene trapping by Lexikon Genetics, Inc. (The Woodlands, Texas) and have been previously described (Ferretti et al. 2006; Penkov et al. 2005; Fernandez-Diaz et al. 2010). In the experiments reported in this paper, heterozygous mice were backcrossed with wild-type (WT) C57BL/6 for 4 generations. All animal handling conformed to regulations of the Ethics Committee on Animal Use of H. S. Raffaele (IACUC permission number 207). Hepatic tissue samples were collected rapidly after mice were sacrificed by pentobarbitone overdose. Tissues were snap frozen in liquid nitrogen and stored at –80°C for subsequent western blotting and Real Time RT-PCR analysis.

3.3 Quantitative assay of serum triglycerides

The blood for serum biochemistry evaluation was collected with a intracardiac methods (IC), allowed to clot at room temperature and centrifuged for 10 min, then, the serum was separated for shipment. Quantitative analysis of serum triglycerides was performed with a ABX Pentra400 clinical chemistry analyser using the reagent ABX Pentra Triglycerides CP (ABX-Horiba, Montpellier, France) according to the manufacturer's instructions.

3.4 Cell culture procedures and transfection

HepG2 hepatoma cells and NMuLi mouse liver cells were cultured at 37°C in Dulbecco’ s modified Eagle’ s medium (DMEM) supplemented with 10% fetal bovine serum, 2% L-glutamine, 10,000 units/ml penicillin, 10,000 g/ml streptomycin. Transient transfection of *Prep1*, *Prep1*$_{HR1}$ and *Pbx1*

plasmid cDNAs or *SHIP2* (5'-GCTCTCTAGTTCCTGCTCCC-3') and *SHP1* (5'-GAGGTCTCGGTGAAACCACCTCACCATCCT-3') phosphorothioate antisense oligonucleotides or scrambled control oligonucleotides SHIP2 (5'-TCGCCACGTCGCTCATTGTT-3') and SHP1 (5'-GTAGAGTTCCGTGAG ACACCTCTCCACCAC-3') were performed by the Lipofectamine and Oligofectine reagent according to the manufacturer's instruction. For these studies, 60-80% confluent cells were washed twice with Optimem (Invitrogen) and incubated for 8h with 3-5 g of plasmid construct or with 250nM of oligonucleotides and 45-60 μl of lipofectamine reagent. In transient transfection, the medium was then replaced with DMEM with 10% fetal bovine serum and cells further incubated for 15 h before being assayed. In stably transfection individual G418-resistant clones were selected by the limiting dilution technique (G418 effective dose, 0.8 mg/ml).

3.5 Oil Red O staining

To measure cellular neutral lipid droplet accumulation, HepG2 cells were stained by the Oil Red O method. HepG2 cells were grown in a p60 plate and trasfected with *Prep1*, $Prep1_{HR1}$ and *Pbx1* plasmid cDNAs. After 48h cells were washed three times with iced PBS and fixed with 4% parafolmaldeide for 30 minutes. After fixation, cells were washed three times and stained with Oil Red O solution (working solution, 0.5g Oil Red O powder Sigma dissolved in 60% ethanol) for 15 min at room temperature. Cells were washed again with phosphate-buffered saline (PBS) to remove unbound staining. The HepG2 cells were examined under a light microscope, and the red oil droplets stained in the cells indicate TG accumulation.

3.6 Western blot analysis

Tissue samples were homogenized in a Polytron (Brinkman Instruments, N.Y.) in 20 ml T-PER reagent/gram of tissue according to manufacture (Pierce, IL). After centrifugation at 10,000 rpm for 5 minutes, supernatant was collected. Cells were solubilized in lysis buffer (50 mmol/l HEPES, pH 7.5, 150 mmol/l NaCl, 10 mmol/L EDTA, 10 mmol/l Na4P2O7, 2 mmol/L Na3VO4, 100 mmol/L NaF, 10% glycerol, 1% Triton X-100, 1 mmol/L PMSF, 10 mg/ml aprotinin) for 1 h at 4C and lysates were centrifuged at 5,000g for 20 min. Total homogenates were separated by SDS-PAGE and transferred on 0.45 m Immobilon-P membranes. Upon incubation with primary and secondary antibodies, immunoreactive bands were detected by ECL according to the manufacturer's instructions.

3.7 Real-Time RT-PCR analysis

Total cellular RNA was isolated from liver and HepG2 cells by using the RNeasy kit (QIAGEN Sciences, Germany), according to manufacturer's instructions. 1 μg of tissue or cell RNA was reverse-transcribed using Superscript III Reverse Transcriptase (Invitrogen, CA). PCR reactions were analyzed using SYBR Green mix (Bio-Rad, Hercules, CA). Reactions were performed using Platinum SYBR Green qPCR Super-UDG using an iCycler IQ multicolor Real Time PCR Detection System (Bio-rad, Hercules, CA). All reactions were performed in triplicate and β-actin was used as an internal standard. Primer sequences used were as follows:
mFAS F:5'-ACGACAGCAACCTCACGGCG-3', R:5' CTGCAGAGCCCGTG CCAGAC-3'; mACC F: 5'-CCTGGAGTGGCAGTGGTCTTCG-3', R: 5'-TCC TCCTCCCTCTGAGGCCTTG-3'; mSHIP2 F: 5'-TCAGATGTGGAGGACGA GAAG-3', R: 5'-TGCTGGAGTTGTGGGAGTC-3'; hPrep1 F: 5'-GGAGTGC CAACCATGTTAAGAAGAAGTCCC-3', R: 5'- GACACCGTGTGCTTCTC GCTCAAG-3'; hFAS F: 5'-GAGAGCCTCTTCTCCAGGGT-3', R: 5'-CTTCA GAGACTCCACCCAGC-3'; hACC F: 5'-TGTCAATCTTGAGGGCTAGG TC-3', R: 5'-TGAATCGAGAGTGCTGGTTC-3'; hSHIP2 F: 5'-ATCCTG GTTCACATCGAAGG-3', R: 5'-GCGGTAATCCAGATCCGTAA-3'.

3.8 Chromatin immunoprecipitation (ChIP) and Re-ChIP assay

The cross-linking solution, containing 1% formaldehyde, was added directly to cell culture media. The fixation proceeded for 10 min and was stopped by the addition of glycine to a final concentration of 125 mM. nMuLi cells were rinsed twice with cold phosphate buffered saline plus 1 mM phenylmethylsulfonyl fluoride and then scraped. Cells were collected by centrifugation at 800 X g for 5 min at 4 °C. Cells were swelled in cold cell lysis buffer containing 5 mM PIPES (pH 8.0), 85 mM KCl, 0.5% Nonidet P-40, 1 mM phenylmethylsulfonyl fluoride, and inhibitors mixture (Sigma) and incubated on ice for 10 min. Nuclei were precipitated by microcentrifugation at 2000Xg for 5 min at 4 °C, resuspended in nuclear lysis buffer containing 50 mM Tris-HCl (pH 8.0), 10 mM EDTA, 0.8% SDS, 1 mM phenylmethylsulfonyl fluoride and inhibitors mixture (Sigma), and then incubated on ice for 10 min. Samples were broken by sonication into chromatin fragments of an average length of 500/ 1000 bp and then microcentrifuged at 16,000 X g for 10 min at 4 °C. The sonicated cell supernatant was diluted 8-fold in chromatin immunoprecipitation (ChIP) dilution buffer containing 0.01% SDS, 1.1% Triton X-100, 1.2 mM EDTA, 16.7 mM Tris- HCl (pH 8.0), and 167 mM NaCl and precleared by adding salmon sperm and conjugating protein at equimolar concentration for 90 min at 4 °C. Precleared chromatin from 1X106 cells was incubated with 1 g of polyclonal antibody (anti-Prep1) or no antibody and rotated at 4 °C for 16 h. Rabbit IgG antibody (Upstate

Biotecnology/Millipore) was used as a non-specific antibody control. Immunoprecipitates were washed five times with radioimmune precipitation assay buffer containing 10 mM Tris-HCl (pH 8.0), 1 mM EDTA, 1% Triton X-100, 0.1% sodium deoxycholate, 0.1% SDS, 140 mM NaCl, and 1 mM phenylmethylsulfonyl fluoride, twice with LiCl buffer containing 0.25 M LiCl, 1% Nonidet P-40, 1% sodium deoxycholate, 1 mM EDTA, 10 mM Tris-HCl (pH 8.0), and then 3 times with TE (10 mM Tris-HCl (pH 8.0), 1 mM EDTA). Before the first wash, the supernatant from thereaction lacking primary antibody was saved as total input of chromatin and was processed with the eluted immunoprecipitates beginning at the cross-link reversal step. Immunoprecipitates were eluted by adding 1% SDS, 0.1 M NaHCO3, and reverse cross-linked by the addition of NaCl to a final concentration of 200 mM and by heating at 65 °C for at least 4 h. Recovered material was treated with proteinase K, extracted with phenol-chloroform-isoamyl alcohol (25:24:1), and precipitated. The pellets were resuspended in 30 l of TE and analyzed by PCR using specific primers for the analyzed regions. The input sample was resuspended in 30 l of TE and diluted 1:10 before PCR. For ReChIP assay, immunoprecipitates with the first antibody were eluted in 50 ml of DTT 10 mM, diluted 10-fold in ChIP Dilution Buffer supplemented with protease inhibitors, and immunoprecipitated with the second antibody (anti-Pbx1). Following immunoprecipitation, samples are processed as described above for ChIP assay and eluted DNA amplified by PCR with specific oligos: seq n°1 F: 5’-CACATTCCCTATTCCCATCA-3’, R: 5’-AGGCTAGAGGG TGCTTCTGC-3’; seq n°2 F: 5’-AGCTCTCTCCTTCCACCACA-3’, R: 5’-GA GGCAGAAGCAAATGGAAC-3’.

3.9 Statistical procedures

Data were analysed with the Statview software (Abacus-concepts) by one-factor analysis of variance. P values of less than 0.05 were considered statistically significant.

4. RESULTS

4.1 Hepatic lipid metabolism in Prep1-deficient mice

To study the role of Prep1 on hepatic lipogenesis, I first measured serum triglyceride (TG) content in Prep1$^{i/+}$ mice and in control littermates (wild type). As shown in figure 10A serum TG levels were reduced by 33% in Prep1$^{i/+}$ mice compared to the wild type mice. This result was consistent with our previous data showing a marked decrease of hepatic triglyceride content in the hypomorphic mice (Oriente et al. 2011).
To investigate in detail this issue, I focused my attention on the metabolic pathway that leads to the synthesis of triglycerides in the liver by measuring *FAS* mRNA levels. Consistent with the decrease of TG content, Prep1 hypomorphic mice showed a 62% reduction of *FAS* mRNA levels compared to control mice (Figure 10).

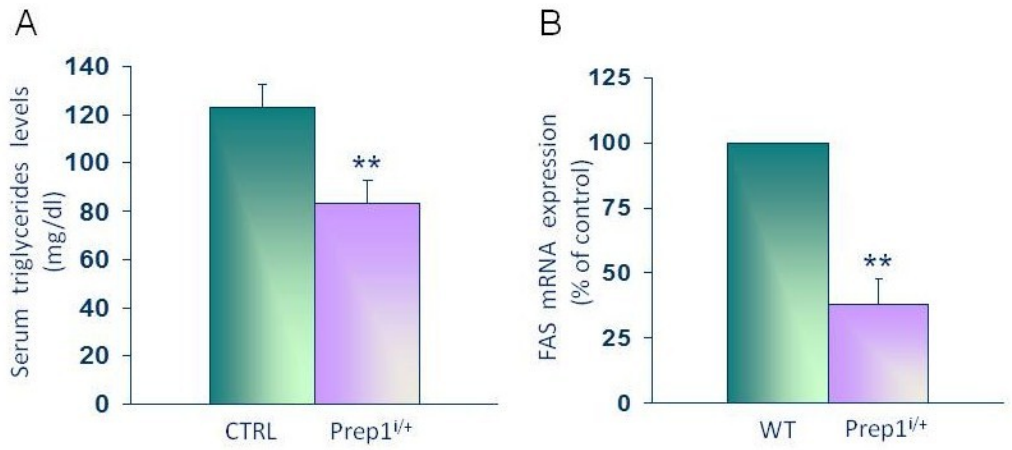

Figure 10: Serum triglyceride content and FAS mRNA levels in Prep1$^{i/+}$ mice.
A: Serum triglyceride content was measured using ABX Pentra400 clinical chemistry analyser as described in Materials and Methods. B: The abundance of *FAS* mRNA was determined by real-time RT-PCR analysis of total RNA isolated from the liver of hypomorphic and control mice, using *β-actin* as internal standard. Bar represents the mean ± SD of four independent experiments, in each of which reactions were performed in triplicate using the pooled total RNAs obtained from six mice per genotype. Asterisks denote statistically significant differences (**P < 0.01).

Next, I evaluated the phosphorylation and the expression of AMPK, one of the main molecules involved in regulation of hepatic lipogenesis. In parallel with the pattern of change FAS expression, Thr^{172}-phosphorylated AMPK (p-AMPK), was diminished in Prep1$^{i/+}$, while no differences were detected in AMPK protein levels. In addition, ratio of phospho-AMPK to total AMPK increased by 3-fold in Prep1 heterozygous mice (Figure 11).

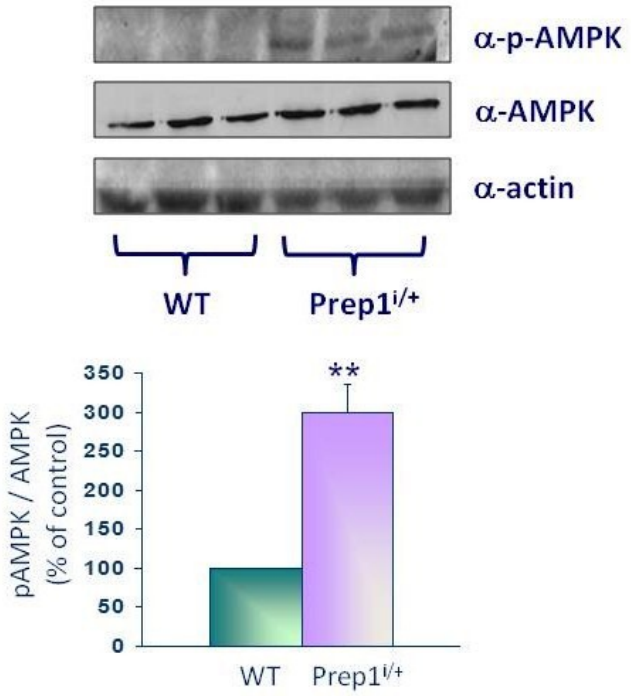

Figure 11: AMPK phosphorylation and expression in Prep1$^{i/+}$ mice.
Liver from Prep1 hypomorphic and control mice were dissected, solubilized, and protein samples analyzed by Western blot with p-AMPK and AMPK antibodies. Actin antibody was used for normalization. Blot were revealed by ECL and autoradiograph subjected to densitometric analysis. The autoradiograph shown on the top of the graphic is representative of four independent experiments. Asterisks denote statistically differences (**P < 0.01).

The increased AMPK threonine phosphorylation in Prep1$^{i/+}$ animals prompted me to explore the molecular status of ACC, the principal AMPK downstream kinase. Western blot analysis (Figure 12A) showed a significant increase in ACC-Ser^{79} phosphorylation in heterozygous mice. As for AMPK, the ratio of phosphorylated ACC to total ACC was elevated by 2.5-fold. Both ACC protein and mRNA levels did not change (Figure 12A, B).

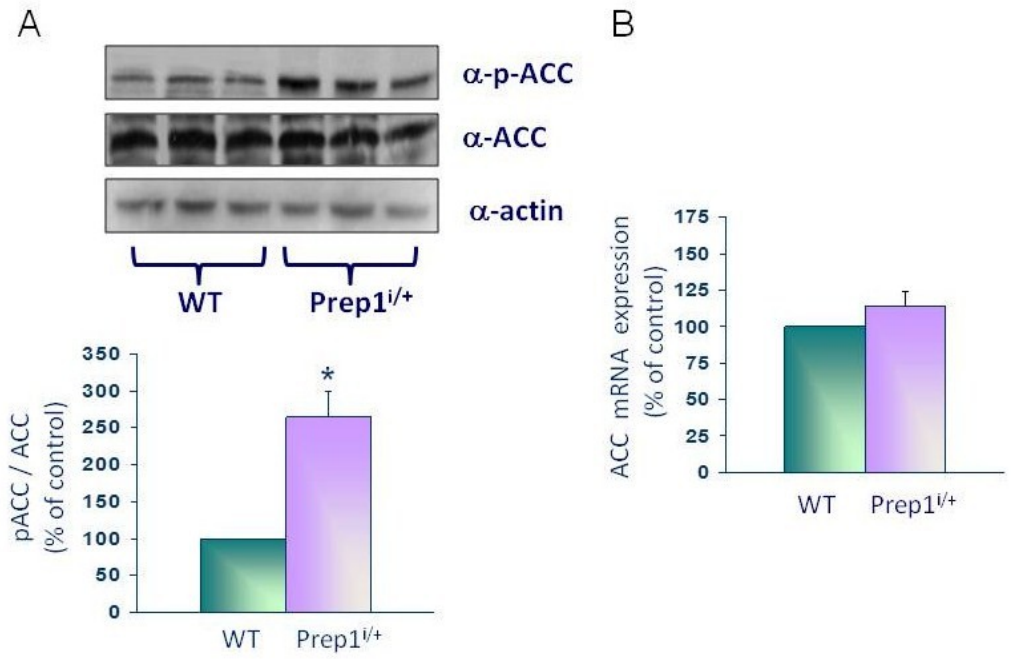

Figure 12: ACC phosphorylation and expression in Prep1$^{i/+}$ mice.
A: Tissues from Prep1 hypomorphic and control mice were dissected, solubilized, and protein samples analyzed by Western blot with p-ACC and ACC antibodies. Actin antibody was used for normalization. Blot were revealed by ECL and autoradiograph subjected to densitometric analysis. The autoradiograph shown on the top of the graphic is representative of three independent experiments. Asterisks denote statistically differences (*P < 0.05). B: The abundance of *ACC* mRNA was determined by real-time RT-PCR analysis of total RNA isolated from the liver of hypomorphic and control mice, using *β-actin* as internal standard. Bar represents the mean ± SD of three independent experiments, in each of which reactions were performed in triplicate using the pooled total RNAs obtained from six mice per genotype.

4.2 Prep1 effect on the AMPK-mediated lipogenesis regulation in mouse liver

To investigate the molecular mechanisms of AMPK activation, I studied the activation and the protein levels of several protein kinases involved in the regulation of hepatic lipogenesis. In particular, I measured the activation of two upstream molecules of AMPK signaling, the Liver Kinase B1 (LKB1) and the Calcium/calmodulin-dependent protein kinase type II (CAMK2). In parallel with AMPK and ACC, LKB1, but not CAMK2, phosphorylation, increased by 2.9-fold in Prep1$^{i/+}$ mice compaired to the wild type. No differences were detected in total levels of both the serine/threonine kinases (Figure 13A, B). These results demonstrated that the activation of AMPK in Prep1 hypomorphic mice may occur through the LKB1 pathway. Several authors have established a central role of atypical protein kinase Cζ (PKCζ) or protein kinase A (PKA) as key regulators in LKB1-dependent AMPK activation. As shown in figure 13C, PKCζ phosphorylation and ratio of

phosphorylated PKCζ to total PKCζ were significantly elevated in the heterozygous animals with no change of protein levels. In contrast, PKA featured no difference between WT and Prep1$^{i/+}$ mice (Figure 13D). These results suggest to me that the reduction of TG levels in the Prep1$^{i/+}$ could depend on a mechanism involving PKCζ, LKB1 and AMPK.

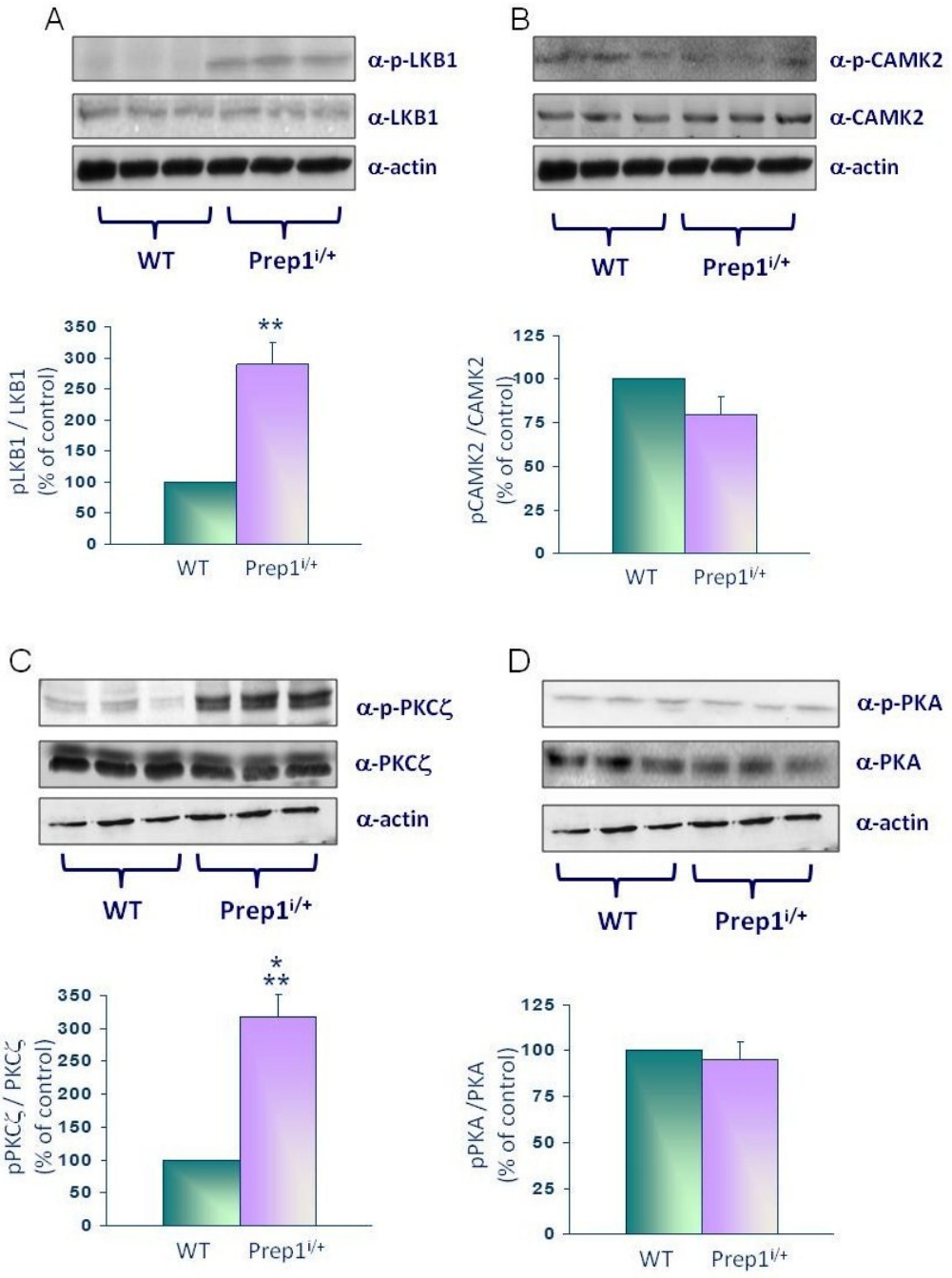

Figure 13: LKB1, CAMK2, PKCζ and PKA phosphorylation and expression in Prep1$^{i/+}$ mice.

Livers from Prep1 hypomorphic and control mice were dissected, solubilized, and protein samples analyzed by Western blot with p-LKB1 and LKB1 (A), p-CAMK2 and CAMK2 (B), p-PKCζ and PKCζ (C), p-PKA and PKA (D) antibodies. Actin antibodies were used for normalization. Blot were revealed by ECL and autoradiograph subjected to densitometric analysis. The autoradiograph shown on the top of the graphic is representative of four independent experiments. Asterisks denote statistically differences (**P < 0.01; ***P < 0.001).

4.3 Prep1 regulates triglyceride synthesis in HepG2 cells

To further examine Prep1 action on triglyceride synthesis and on regulation of AMPK-mediated pathway, I have transiently transfected a *Prep1* cDNA in the HepG2 hepatoma cells (Figure 14A) and triglycerides accumulation was analyzed by microscopy after staining of cells with Oil Red O. In Prep1 overexpressing cells, lipid droplets were clearly observed with light red cytoplasmic staining. In contrast, I barely noted visible lipid droplets in cells transfected with an empty vector (Figure 14B). Consistent with these data, also *FAS* mRNA levels were increased by 50% in Prep1 overexpressing cells (Figure 14C).

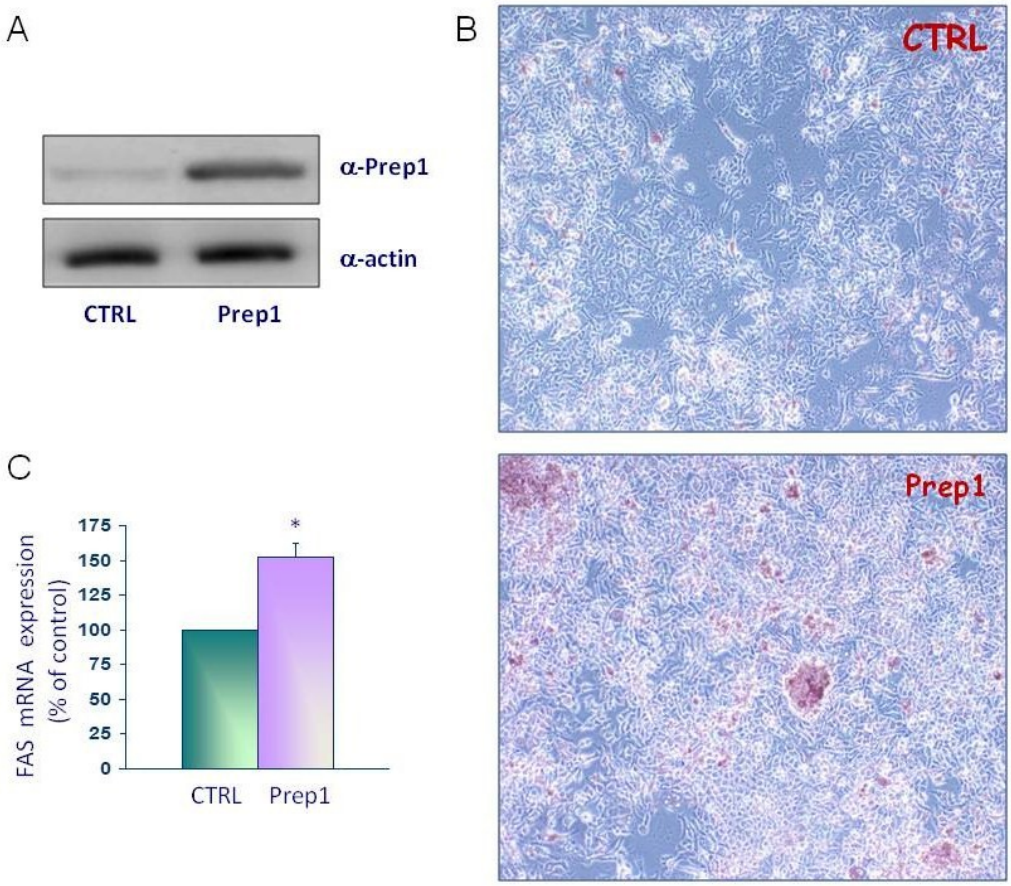

Figure 14: Effect of the overexpression of Prep1 on TG accumulation and on FAS expression in HepG2 cells.

A: HepG2 cells were transiently transfected with *Prep1* cDNA. Cells were then solubilized and lysates were analyzed by immunoblotting with Prep1 antibodies and autoradiography to verify the transfection. Actin antibodies were used for normalization. The autoradiograph shown is representative of different experiments. B: HepG2 cells were stained with Oil Red O as described in Material and Methods. The photograph shown is representative of five independent experiments. C: The levels of *FAS* mRNA in cells transfected with the *Prep1* cDNA was quantitated by real-time RT-PCR analysis, using β-actin as internal standard. Bars represent the mean ± SD of four independent experiments. Asterisks denote statistically significant differences (*P < 0.05).

Thus, I looked at the AMPK signaling. Prep1 transfection downregulated AMPK and ACC phosphorylation by 40 and 50%, respectively, without changing their protein levels (Figure 15A). Also *ACC* mRNA expression was not modulated by Prep1 (Figure 15B). In parallel, Prep1 overexpression caused a > 50% reduction of both LKB1 and PKCζ phosphorylation, confirming the data obtained in Prep1$^{i/+}$ mice (Figure 15A).

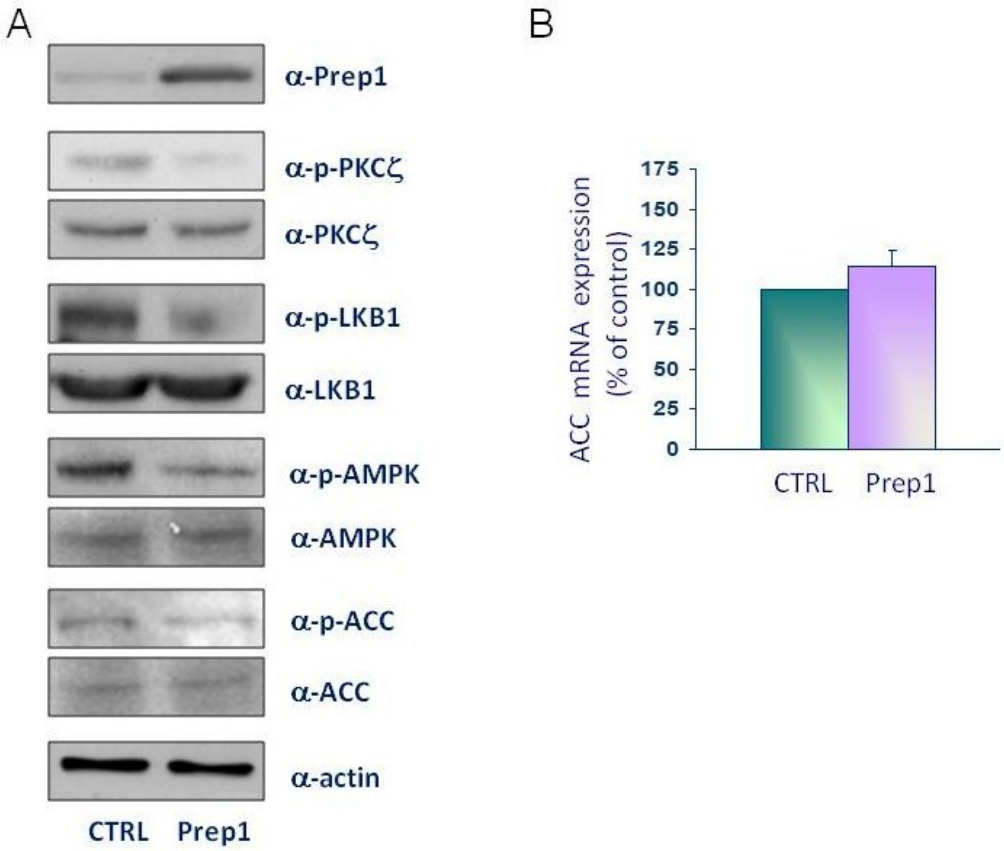

Figure 15: PKCζ, LKB1, AMPK and ACC phosphorylation and expression in HepG2 overexpressing Prep1.
A: HepG2 cells transiently overexpressing *Prep1* were lysed and analyzed by Western blot with p-PKCζ, PKCζ, p-LKB1, LKB1, p-AMPK, AMPK, p-ACC and ACC. Actin antibodies were used for normalization. The autoradiograph shown is representative of five independent experiments. B: The levels of *ACC* mRNA in cells transfected with the *Prep1* cDNA was

quantitated by real-time RT-PCR analysis, using β-actin as internal standard. Bars represent the mean ± SD of three independent experiments.

4.4 SHP1 and SHIP2 mediate the effect of Prep1 on triglyceride synthesis

Previously our work has demonstrated that in liver transcriptional activation of *SHP1* gene by Prep1 attenuates insulin signal transduction and reduces glucose storage. Given that PKCζ is a downstream substrate of the insulin receptor, I have transiently transfected a *Prep1* full-length cDNA in the HepG2 cells. Several clones were obtained and I chose the $HepG2_{Prep1c}$ clone overexressing Prep1 by 5-fold compared to wild type HepG2 cells and featuring a 3-fold increased expression of SHP1 (Oriente et al. 2011). Transient trasnsfection of the $HepG2_{Prep1c}$ cells with phosphorothioate antisense oligonucleotides specific for *SHP1* (SHP1-AS) silenced SHP1 expression by 50% (Figure 16A), but induced a modest increase of PKCζ, LKB1, AMPK and ACC phosphorylation and reduced *FAS* mRNA expression by 30% (Figure 16A, B).

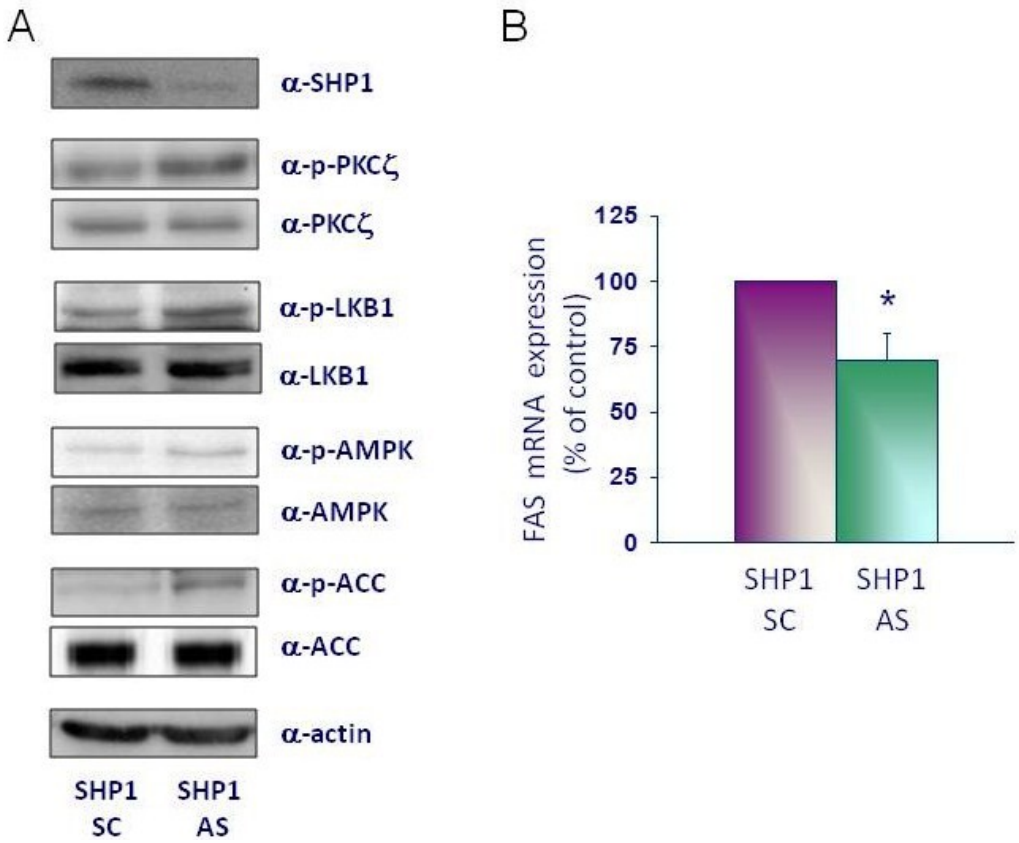

Figure 16: Effect of *SHP1* antisense oligonucleotides on lipogenesis regulation in HepG2 cells stable transfected with *Prep1*.

A: HepG2$_{Prep1c}$ cells were transfected with *SHP1* (SHP1-AS) specific phophorothioate antisense oligonucleotides. The lysates were also analyzed by Western blot with SHP1, p-PKCζ, PKCζ, p-LKB1, LKB1, p-AMPK, AMPK, p-ACC, ACC and actin. The autoradiographs shown are representative of four independent experiments. B: The levels of *FAS* mRNA in HepG2$_{Prep1c}$ transfected with the SHP1-AS were quantitated by real-time RT-PCR analysis, using β-actin as internal standard. Bars represent the mean ± SD of four independent experiments. Asterisks denote statistically significant differences (*P < 0.05).

Thus, I looked at the possible involvement of other phosphatases. Several authors have shown that the lipid phosphatase SHIP2 attenuates phosphatidylinositol 3,4,5-trisphosphate levels generated by PI3-kinase reducing the activation of the PI3K substrate PKCζ (Cantley et al. 2002). To study a possible regulation by Prep1, I have measured the levels of SHIP2 in the liver of the Prep1 heterozygous mice. As shown in figure 17A, SHIP2 was reduced by 40% and 50% in these mice compared to controls, respectively at the protein and the mRNA levels. In addition, Prep1 transfection in HepG2 cells induced a 2-fold increase of both SHIP2 protein and mRNA expression (Figure 17B).

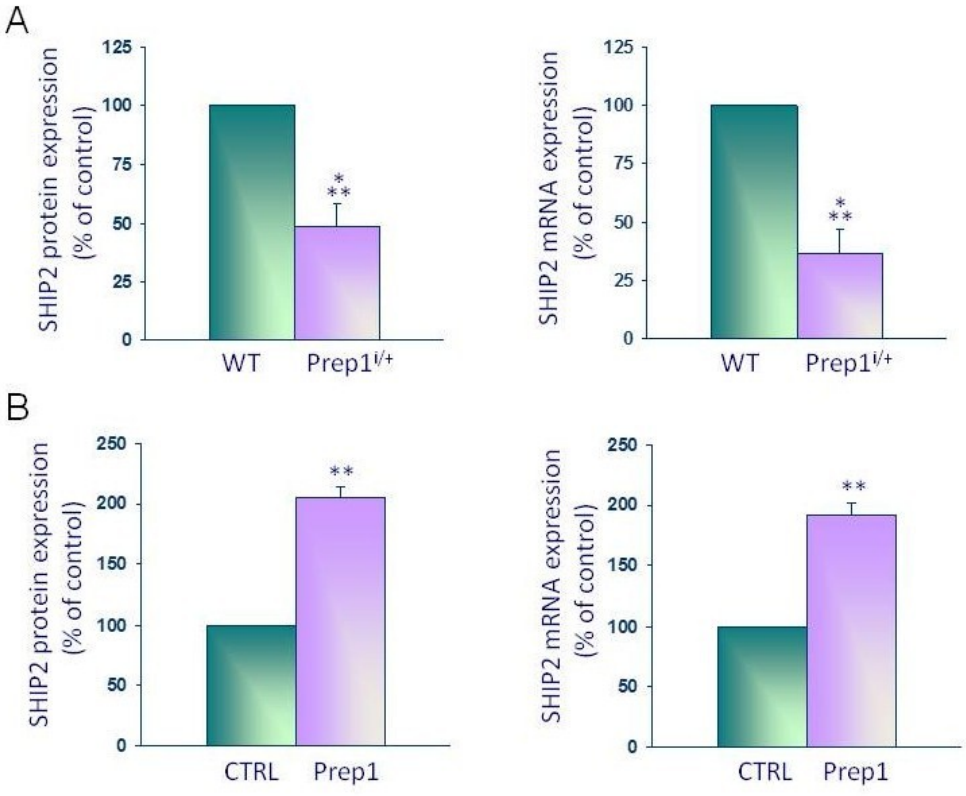

Figure 17: SHIP2 expression in Prep1$^{i/+}$ mice and in HepG2 overexpressing Prep1.
A: SHIP2 protein abundance was measured by Western blot on hepatic tissues from hypomorphic and control mice using specific antibodies. Actin antibodies were used for the normalization. Each bar represents the mean ± SD of duplicate determinations in ten mice per group. The abundance of *SHIP2* mRNA was determined by real-time RT-PCR analysis of total

RNA isolated from the liver of hypomorphic and control mice, using β-actin as internal standard. Bar represents the mean ± SD of four independent experiments, in each of which reactions were performed in triplicate using the pooled total RNAs obtained from six mice per genotype. B: Lysates from HepG2 cells overexpressing *Prep1* cDNA were blotted with SHIP2 antibodies, followed by ECL and densitrometry. Actin antibodies were used for normalization. Each bar represents the mean ± SD of duplicate determinations in four independent experiments. The levels of *SHIP2* mRNAs in cells transfected with *Prep1* cDNA was quantitated by real-time RT-PCR analysis, using β-actin as internal standard. Each bar represents the mean ± SD of duplicate determinations in four independent experiments. Asterisks denote statistically significant differences (**P < 0.01; ***P < 0.001).

To explore the significance of SHIP2 lipid phosphatase to Prep1 regulation of hepatic lipogenesis, I have transiently transfected the $HepG2_{Prep1c}$ clone with phosphorothioate antisense oligonucleotides specific for *SHIP2* (SHIP2-AS) reducing *SHIP2* levels by 75% (Figure 18A). Treatment with SHIP2-AS increased PKCζ and LKB1 phosphorylation by 6.4- and 5-fold respectively. Also the amount of phosphorylated AMPK and ACC were induced by 4.2- and 6-fold in presence of SHIP2-AS, while, at variance, no change in the amount of these proteins were observed (Figure 18A). Importantly, *FAS* mRNA expression was downregulated by 60% after depletion of SHIP2 (Figure 18B).

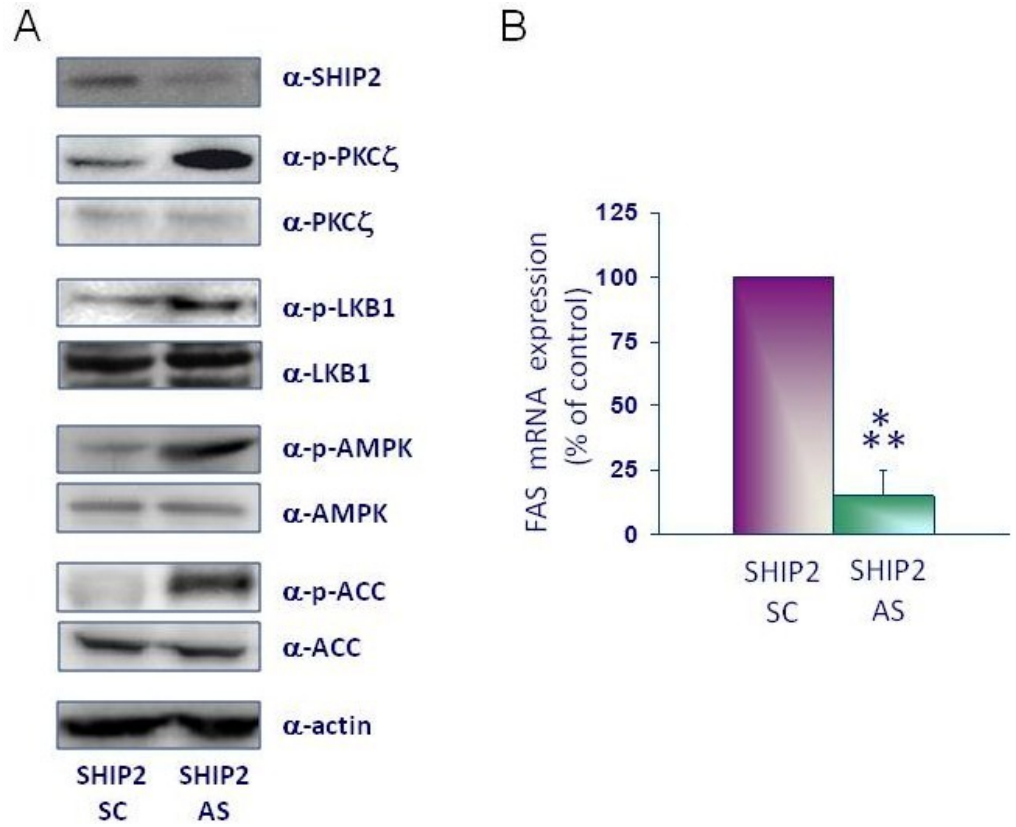

Figure 18: Effect of *SHIP2* antisense oligonucleotides on lipogenesis regulation in HepG2 cells stable transfected with *Prep1*.

A: HepG2$_{Prep1c}$ cells were transfected with *SHIP2* (SHIP2-AS) specific phophorothioate antisense oligonucleotides. For control, lysates were blotted with SHIP2 or actin antibodies. The lysates were also analyzed by Western blot with p-PKCζ, PKCζ, p-LKB1, LKB1, p-AMPK, AMPK, p-ACC and ACC. The autoradiographs shown are representative of four independent experiments. B: The levels of *FAS* mRNA in HepG2$_{Prep1c}$ transfected with the SHIP2-AS were quantitated by real-time RT-PCR analysis, using β-actin as internal standard. Bars represent the mean ± SD of four independent experiments. Asterisks denote statistically significant differences (***P < 0.001).

4.5 Prep1 regulation of SHIP2 gene transcription

Next, I examined the possibility that Prep1 could directly regulate *SHIP2* gene function. Bioinformatic analysis revealed the presence of two potential binding sites for Prep1 and Pbx1 in the 4,000 base pair region upstream the ATG codon of *SHIP2* gene. Thus, first I evaluated the role of Pbx1 on hepatic triglycerides synthesis. Previously our work has shown that Prep1 upregulated Pbx1 levels in HepG2 cells (Oriente et al. 2011). Interestingly, transfection of *Pbx1* significantly increased cellular lipid droplets compared with control. In contrast, the *Prep1$_{HR1}$* mutant cDNA, which is unable to bind Pbx1 (Diaz et al. 2007), had no effect on lipid accumulation (Figure 19A). Also *FAS* mRNA expression was induced by Pbx1 but not by Prep1HR1 mutant (Figure 19B). Consistent with these results, overexpression of *Pbx1* cDNA in HepG2 cells mimicked Prep1 effects on the phosphorylation of PKCζ, LKB1, AMPK and ACC. At opposite, Prep1$_{HR1}$ mutant failed to elicit these effects (Figure 19C). This indicates that the Prep1-Pbx1 dimer might control lipogenesis in liver cells.

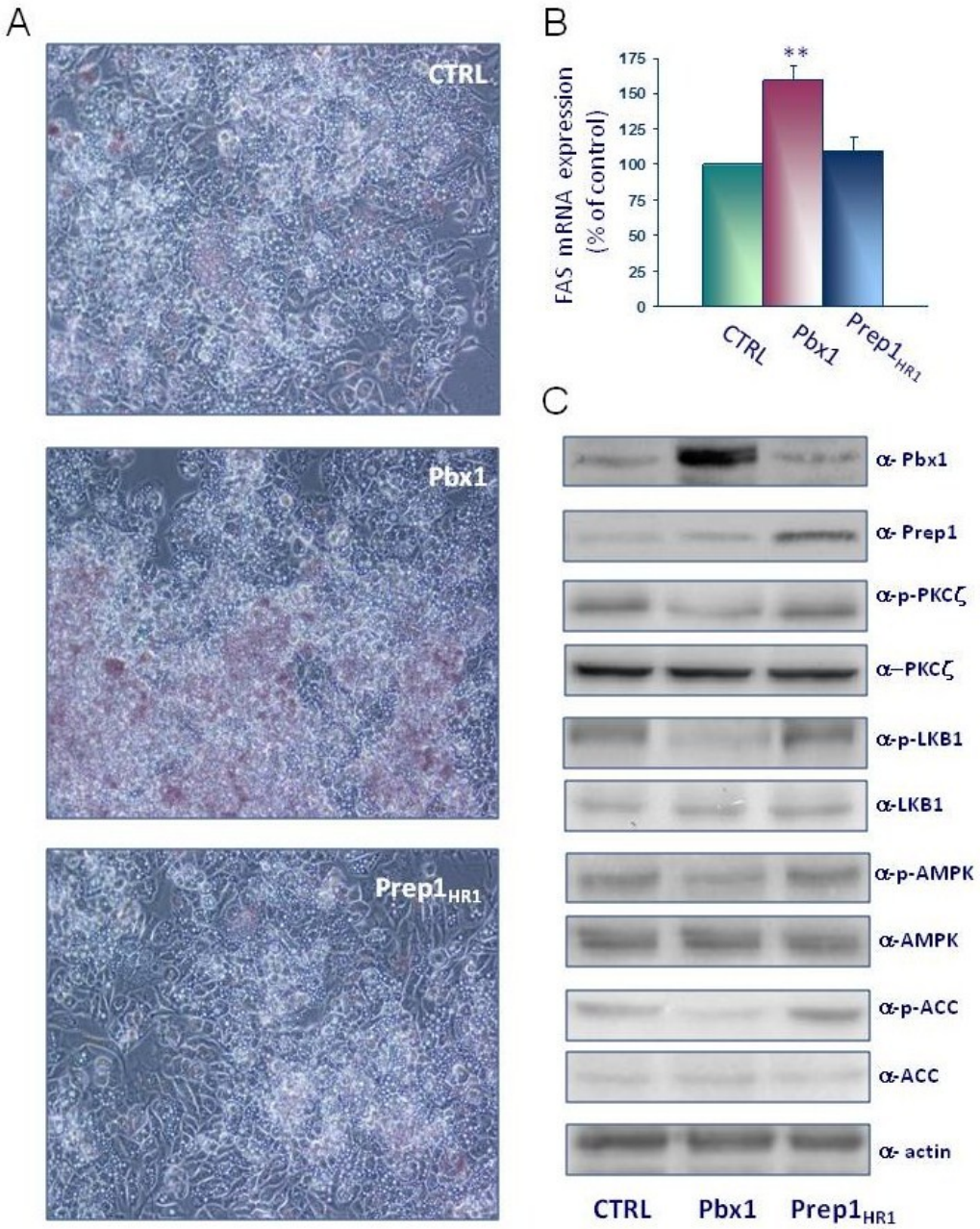

Figure 19: Effect of the overexpression of *Pbx1* and *Prep1*$_{HR1}$ on TG accumulation and on FAS expression in HepG2 cells.

A: HepG2 cells were transiently transfected with *Pbx1* and *Prep1*$_{HR1}$ cDNA. Cells were then stained with Oil Red O as described in Material and Methods. The photograph shown is representative of four independent experiments. B: The levels of *FAS* mRNA in cells transfected with the *Pbx1* and *Prep1*$_{HR1}$ cDNA was quantitated by real-time RT-PCR analysis, using β-actin as internal standard. Bars represent the mean ± SD of four independent experiments. Asterisks denote statistically significant differences (**P < 0.01). C: HepG2 cells transiently overexpressing *Pbx1* and *Prep1*$_{HR1}$ were lysed and analyzed by Western blot with p-PKCζ, PKCζ, p-LKB1, LKB1, p-AMPK, AMPK, p-ACC and ACC. Actin antibodies were

used for normalization. The autoradiograph shown is representative of four independent experiments.

Next, I measured the levels of SHIP2 in HepG2 cells transfected with *Pbx1* cDNA and *Prep1*$_{HR1}$ mutant. As shown in figure 20, Pbx1 transfection in HepG2 cells induced a 1.8-fold increase of both SHIP2 protein and mRNA expression, while I failed to observe a similar effect in presence of the Prep1$_{HR1}$ mutant.

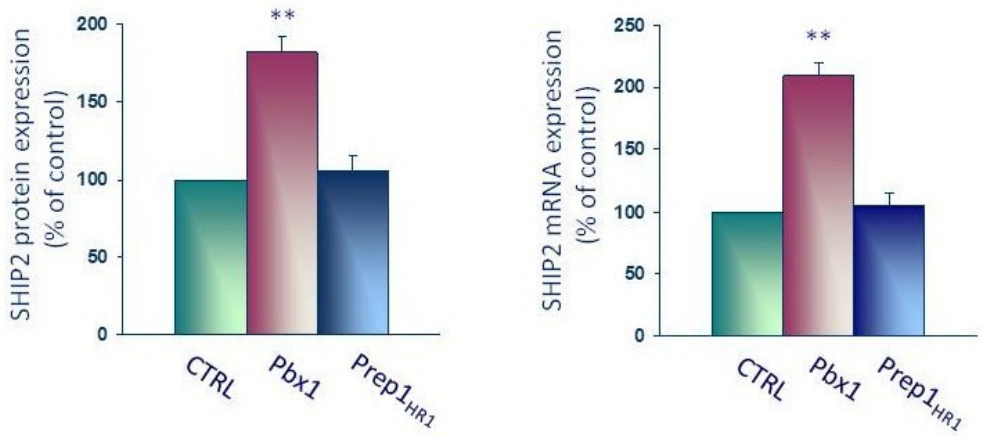

Figure 20: SHIP2 expression in HepG2 overexpressing *Pbx1* and *Prep1*$_{HR1}$.
Lysates from HepG2 cells overexpressing *Pbx1* and *Prep1*$_{HR1}$ mutant cDNAs were blotted with SHIP2 antibodies, followed by ECL and densitrometry. Actin antibodies were used for normalization. Each bar represents the mean ± SD of duplicate determinations in four independent experiments. The levels of *SHIP2* mRNAs in cells transfected with *Pbx1* and *Prep1*$_{HR1}$ mutant cDNAs was quantitated by real-time RT-PCR analysis, using β-actin as internal standard. Each bar represents the mean ± SD of duplicate determinations in four independent experiments. Asterisks denote statistically significant differences (**P < 0.01)

To validate the two regions putatively bound by Prep1 and Pbx1 complex in the 4,000 base pair region upstream the *SHIP2* transcription initiation site (Figure 21A; positions nucleotide [nt] -1,284 to -1,268 and nt -856 to -842), I performed chromatin imunoprecipitation (ChIP) and re-chromatin immunoprecipitation (re-ChIP) experiments in NMuli mouse liver cell line. By ChIP experiments the two sites bound Prep1 as shown in figure 21B, in addition Re-ChIP assays revealed that Pbx1 was simultaneously present at both positions (nt -1,284 to -1,268 and nt -856 to -842).

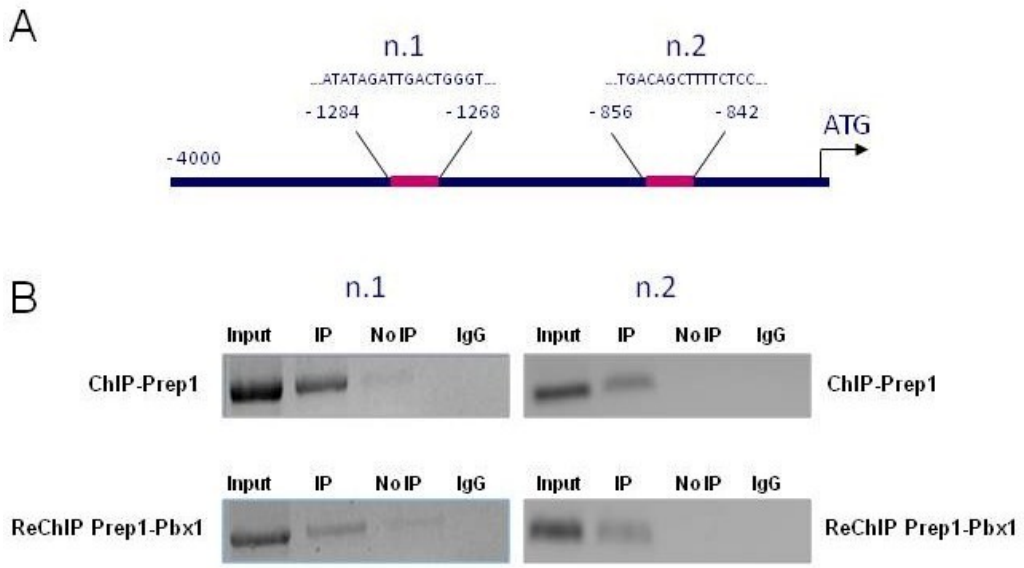

Figure 21: *Prep1/Pbx1* binding to the *SHIP2* DNA sequences.
A: Schematic representation of 5' sequences upstream the putative *SHIP2* transcription start site including the potential binding sites for Prep1 and Pbx1. B: Soluble chromatin was prepared from NMuLi mouse liver cells and immunoprecipitated with Prep1 antibodies. Total (input) and immunoprecipitated DNAs were amplified using primer pairs covering the indicating *SHIP2* fragments. Re-ChIP assay with Pbx1 antibodies was performed as described under Materials and Methods.

5. DISCUSSION

Insulin-resistance increases serum free fatty acid levels, which are taken up by the liver and drive triglyceride production and hepatic steatosis. In addition, insulin-resistance promotes *de novo* lipogenesis through upregulation of lipogenic transcription factors. Increased FAs might cause the accumulation of fat deposits in liver and impair hepatic metabolic functions.

Several studies have demonstrated the complex relationship between Non Alcoholic Steatohepatitis (NASH) and metabolic disorders such as central obesity, dyslipidemia and insulin-resistance in both humans and rodents (Samuel et al. 2004).

Previous studies have identified Prep1 as a physiologic regulator of insulin-mediated glucose metabolism both in skeletal muscle and in liver (Oriente et al. 2008; Oriente et al. 2011). In Prep1-deficient mice, muscle sensitivity to insulin action on glucose disposal is significantly increased, due to downregulation of an important Prep1 partner $p160^{MBP}$ and induction of the GLUT4 gene activator PGC-1α. In the liver, Prep1 silencing enhances insulin signaling, thereby increasing glucose storage and reducing glucose output. Indeed, Prep1 hypomorphic mice show increased hepatic glycogen content and decreased triglyceride levels. The potential significance of these findings to insulin-resistance and diabetes is further underlined by our experiments in the L6 skeletal muscle and HepG2 human hepatoma cell lines evidencing that overexpression of Prep1 induces resistance to insulin action. However, whether and how Prep1-induced insulin-resistance affects triglycerides synthesis in liver is still unknown but important to clarify.

In the present work, I show that in Prep1 hypomorphic mice serum level of triglycerides are strongly reduced, confirming our previous data about the reduction of hepatic TG content (Oriente et al. 2011). Thus, I focused my attention on the pathways inducing lipid synthesis. *De novo* lipogenesis plays a key role in hepatic lipid metabolism and is modulated by FAS, an enzyme that catalyzes the generation of palmitate from acetyl-CoA. In Prep1-deficient mice, FAS expression is significantly reduced, so I studied the activation of AMPK, which plays a key role in regulating carbohydrate and fat metabolism, serving as a metabolic master switch in response to alterations in cellular energy charge. In fact, AMPK turns off anabolic pathways and promotes catabolism by downregulating the activity of key enzymes of intermediary metabolism, such as ACC and FAS. Thus, AMPK cascades have emerged as novel targets for the treatment of obesity and fatty liver. My results show that the phosphorylation of AMPK is increased significantly in the liver of Prep1 hypomorphic mice, but no differences are observed in AMPK total protein levels. It is known that activation of AMPK stimulates fatty acid oxidation and is accompanied by suppression of ACC activity, the enzyme that catalyzes malonyl CoA synthesis. The phosphorylation of ACC leads to an inactivation of the enzyme that, in turn, inhibits the other lipogenic enzymes of the pathway. Increasing evidence suggests that AMPK regulates ACC trough a

short-term regulation in which AMPK phosphorylates and inactivates ACC inhibiting TG synthesis, or trough a long-term mechanism. In the long-term, AMPK regulates hepatic lipogenic gene expression by inhibiting transcription factors, such as SREBP-1c and ChREBP, that directly regulate ACC gene transcription. Analysis of ACC activation and expression in $Prep1^{i/+}$ mice revealed increased phosphorylation of the enzyme; but no change in ACC protein and mRNA expression suggesting that Prep1 controls ACC trough a short-term mechanism.

AMPK is physiologically activated by the phosphorylation of threonine 172 within the α subunit catalyzed by the kinase LKB1, the upstream kinase of AMPK. Neverthless, other proteins can activate AMPK, like for example CAMK2. Thus, I evaluated the role of these two kinases in $Prep1^{i/+}$ mice and my results indicate that LKB1, but not CAMK2, controls AMPK activity. In fact, $Prep1^{i/+}$ mice exhibit a very significant increase of LKB1 phosphorylation, while at variance, the phosphorylation of CAMK2 does not change. These results let me focus on the regulation of LKB1. This protein is phosphorylated at Ser^{428} by some kinases, such as PKCζ. In fact, phosphorylation of LKB1 at Ser^{428} induces nuclear export into the cytosol and its association with AMPK. Other kinases such as PKA are reported to phosphorylate LKB1-Ser^{428}. Interestingly, analysis of the two kinases in $Prep1^{i/+}$ mice reveals significant increased PKCζ phosphorylation, while PKA phosphorylation is unaffected in liver tissue from Prep1-deficient mice. These data demonstrate that, in Prep1-deficient mice, the PKCζ-mediated phosphorylation of LKB1 is important for the AMPK activation and inhibition of the TG synthesis.

To further address my hypothesis, I have transfected human hepatocarcinoma cell lines (HepG2 cells) with Prep1. At variance with the liver of Prep1-deficient mice, the overexpression of Prep1 significantly increases cellular lipid accumulation and FAS expression and induces a inhibition of ACC, AMPK, LKB1 and PKCζ phosphorylation.

Our previous work showed that regulation of the tyrosine phosphatase *SHP1* gene function represents a relevant mechanism for the Prep1 control on insulin signaling and action in hepatocyte. The activation of the insulin receptor leads to the tyrosine phosphorylation of the insulin receptor substrate (IRS) proteins, that activates phosphatidylinositol 3-kinase (PI3K) and induces activation of downstream signaling molecules such as Akt/protein kinase B (Akt/PKB) and atypical protein kinase C-ζ (PKCζ). To better understand the functional relevance of Prep1 control on SHP1 expression to hepatic lipogenesis, I stably transfected HepG2 cells with Prep1 and a specific antisense silencing *SHP1* was added to these cells. Depletion of SHP1 partially rescued lipogenesis inhibition, thus establishing SHP1 as possible target of Prep1 in the liver. Other tyrosine phosphatases, such as PTP1B, have received particular attention in negative regulating of insulin signal transduction and is associated with the development of insulin-resistance. Moreover, at least one genetic polymorphism of PTP1B is associated with several features of the insulin-resistance/metabolic syndrome (Di Paola et al. 2002). In my studies I have

excluded PTP1B because previously we have shown that its levels were unaffected both in liver tissue from Prep1-deficient mice and in cells overexpressing Prep1 (Oriente et al. 2011). However, given that SHP1 only partially contribute on Prep1-mediated TG synthesis, I supposed that other protein phosphatases might be involved in this mechanism. It is known that SH2-containing inositol 5′ phosphatase-2 (SHIP2) has been shown to have negative role on insulin signaling. Moreover, the molecular mechanism underlying insulin resistance in animal models of type 2 diabetes is involved, at least in part, at the step between PI 3-kinase and its downstream molecules, Akt and PKCζ. Thus, I hypothesized that there could be a possible involvement of SHIP2 in insulin-resistance and increased hepatic lipogensis. Interestingly, the levels of SHIP2 lipid phosphatases significantly decreases in Prep1 hypomorphic mouse liver while undergoes opposite changes in cultured liver cells transiently transfected with a *Prep1* cDNA. To specifically investigate the role of SHIP2, HepG2 cells stably overexpressing Prep1 were transfected with a phosphorothioate oligonucleotide antisense (SHIP2-AS) and a strongly inhibition of Prep1-mediated increase of TG synthesis was observed. Thus, regulation of the SHIP2 gene function seemed to represent a mechanism relevant to Prep1 control on hepatic lipid metabolism. SHIP2 downregulation in liver tissue from the Prep1-hypomorphic mice occurred both at the protein and at the mRNA levels, raising the possibility that Prep1 acts, at least in part, by regulating *SHIP2* gene expression. Understanding how Prep1 might regulate the expression of *SHIP2* gene is a critical point to better define the action of this transcription factor in modulating lipogenesis in liver. Thus, analyzing the 4,000 base-pair region upstream *SHIP2* transcription initiation site, I have identified that the regulatory region of *SHIP2* gene contains two Prep1/Pbx1 binding sites. The effects of Prep1 on gene regulation is tightly dependent on many interactors, which can recruit it in different transcription networks and modulate the target of its transcription activity. Thus, before studying the Prep1-mediated SHIP2 expression, I focused my attention on the role of Pbx1. In HepG2 cells Pbx1 mimics Prep1 action on cellular lipid accumulation, increasing FAS expression, ACC activity and inhibiting AMPK, LKB1, PKCζ-mediated lipogenesis regulation. The association of Prep1 with Pbx1 is important to increase triglycerides synthesis, because using a $Prep1_{HR1}$ mutant, this effect is lost. The $Prep1_{HR1}$ mutant mutant contains one point mutation in the domain HR1 which is fundamental for the interaction between Prep1 and Pbx1, resulting in an abolishment of the recruitment and function of the transcription complex.

Pbx proteins complexed with Prep1 exhibit strong affinity and specificity for different binding sites, the TGACAG sequence of the urokinase enhancer, the Pbx responsive sequence (PRS, TGATTGAT) and the b1-ARE R3 site (GTGATGGAT), a typical binding site restricted to a limit set of Hox proteins, including HOXB1 (Berthelsen et al. 1998). The DNA-target specificity of the Prep1/Pbx1 complex is restricted to the binding site sequence; my bioinformatic analysis of *SHIP2* regulatory region indicates that Prep1 or a

preassembled Prep1–Pbx complex can functionally interact with specific SHIP2 sequences, by forming a transcriptionally active complex. In addition, ChIP and Re-ChIP assays with Prep1 and Pbx1 antibodies show that both transcription factors bind the *SHIP2* regulatory region, suggesting that *SHIP2* gene is a target of the Prep1/Pbx1 complex. However, since Pbx1 increases the nuclear localization of Prep1 (Berthelsen et al. 1999; Jaw et al. 2000), it is also possible that the expression of Pbx1 causes the nuclear accumulation of Prep1, thereby enhancing its transcriptional effect on *SHIP2*.

Data obtained about the role of Prep1/Pbx1 complex on SHIP2 are very interesting given that the phenotype of Prep1-hypomorphic mice could be in part related to that of *SHIP2*-null mice. Deficiency of Prep1 and SHIP2 induce several perturbations of the wild-type phenotype. First, both *Prep1*-hypomorphic and *SHIP2*-null mice were smaller than wild-type littermates. Second, $SHIP2^{-/+}$ mice show insulin hypersensitivity with enhanced GLUT4 translocation to the cell surface in response to low dose insulin, a similar phenotype observed in the muscle of Prep1-hypomorphic mice. Moreover, an examination of serum chemistry shows that serum triglycerides are significantly lower in *Prep1*-hypomorphic and *SHIP2*-null mice. Thus, both animal models perform increased insulin sensitivity and reduced TG levels. The excessive accumulation of triglycerides and the formation of hepatic lipid droplets may cause liver steatosis and progress to NASH in the long term. Next experiment will try to clarify the role of Prep1 and SHIP2 on the pathogenesis of NASH.

In summary, the major finding of the present study is that Prep1-mediated SHIP2 expression induces an increase of TG synthesis by blocking PKCζ, LKB1, AMPK and ACC phosphorylation. Although the precise molecular mechanisms and signaling pathways regulated by Prep1 remain to be better clarified, suppression of this transcription factor may represent a beneficial strategy in the treatment of obesity and thereby prevent type 2 diabetes. Further focus on the pathways downstream of Prep1 may help to understand insulin-mediated alterations in metabolism and lipogenesis. Nevertheless, my data have been obtained in murine models, thus another point which I would like to study in the future is the clinical relevance of Prep1 in humans. We have preliminary data showing that first-degree relatives of type 2 diabetics (these individuals have an high risk of type 2 diabetes) overexpress Prep1 compared to control individuals with no family history of diabetes. In addition, in these first-degree relatives, Prep1 expression levels negatively correlate with insulin sensitivity. These subjects have a very high risk of diabetes and are known to be insulin-resistant, suggesting that Prep1 overexpression may provide an early contribution to diabetes progression in these individuals. However, whether Prep1 overexpression induces insulin-resistance in human and whether it is sufficient to impair glucose tolerance is still unknown and will be the subject of my future studies.

6. CONCLUSIONS

The liver is an insulin sensitive organ that plays a key role in the regulation of whole body energy homeostasis. Defective insulin signaling and development of insulin-resistance in the liver may have major consequences on energy balance and metabolism.

In the present work I have focused my attention on Prep1 action on hepatic lipid metabolism. I have described that Prep1 deficiency in animal models decreases triglyceride synthesis in liver enhancing PKCζ, LKB1, AMPK and ACC phosphorylation. These effects are paralleled by a significant reduction of expression of SHP1 tyrosine phosphatase and SHIP2 lipid phosphatase. In particular, cellular models evidence that SHIP2 is a main target of Prep1 in the control of hepatic lipogenesis. This evidence let me focus my research activity on the transcriptional regulation of *SHIP2* by the Prep1-Pbx1 complex. In this context, I have shown that Prep1-Pbx1 bind *SHIP2* gene on two regulatory sequences upstream the ATG codon.

In conclusion, these findings have contributed to underline the link between the TALE proteins, insulin-resistance and triglyceride synthesis and, in part, to clarify the role of tyrosine and lipid phosphatases on hepatic regulation of lipid metabolism.

7. ACKOLEDGEMENTS

…I wish to thank Professor Francesco Beguinot, for giving me the opportunity to work in his lab and for having been a precious guide during these years…

…I want to thank my supervisor, Professor Pietro Formisano. I appreciate all his contributions of time, ideas, and funding to make my PhD experience productive and stimulating…

…I am deeply indebted to Doctor Francesco Oriente, whose help, stimulating suggestions and encouragement helped me in all the time of research and writing of this thesis. The joy and enthusiasm he has for his research was contagious and motivational for me…

…Many thanks go in particular to Doctor Salvatore Iovino, it is a pleasure to collaborate with you…

I wish to thank my colleagues and friends for providing a stimulating and fun environment in which to learn and grow:
…Tonia, semplicemente per essere entrata nella mia vita nel momento in cui ne avevo più bisogno, grazie per la tua dolcezza e la tua presenza costante…
…Giuseppe, perché tra un sorriso ed un consiglio hai creduto in me da subito, accompagnandomi dal concorso alla consegna della tesi…
…Vittoria, amica più che collega, averti conosciuto è la cosa di cui farò più tesoro in questi anni…
…Federica, da te ho sempre da imparare, dall'informatica al calcio, parlare con te è uno stimolo a crescere…

In ordine sparso grazie a tutti coloro che, in modi e tempi diversi, hanno avuto un ruolo importante nelle mie giornate: Carmela, Francesca, Michele, Mimmo, Rossella, le mie "PhD colleghe" Antonella e Cecilia, le mie "bambine" e tutto il DiabLab, per le risate, i consigli, le discussioni, le domande e tutto ciò che ha reso possibile questo lavoro…

…Un grazie particolare va alle "amiche di sempre": Maria Teresa, la forza che hai trovato in questo periodo difficile ti rende unica, come unica e speciale è la tua presenza nella mia vita; Emanuela, grazie per la mano sempre tesa che mi hai fatto trovare nei momenti difficili e per le cose che hai condiviso con me dentro e fuori l'Università…

…grazie di cuore alla mia famiglia che mi ha insegnato a non mollare mai: ai miei genitori, se sono arrivata fin qui è solo merito vostro, e a mia sorella, perchè Morena è stato il regalo più bello che potessi farmi…

…e grazie a te, Luca, per il coraggio e la forza che mi hai spinto a trovare, per esserci sempre stato e per tutto ciò che mi stai regalando giorno dopo giorno. La tua dolcezza rende questo traguardo anche un po' tuo…

…finally, I would like to thank everybody who was important to the successful realization of this thesis, as well as expressing my apology that I could not mention personally one by one!

8. REFERENCES

Avruch J. Insulin signal transduction through protein kinase cascades. Mol Cell Biochem 1998; 182: 31–48.

Azcoitia V, Aracil M, Carlos-Martinez A and Torres M. The homeodomain protein Meis1 is essential for definitive hematopoiesis and vascular patterning in the mouse embryo. Dev Biol 2005; 280: 307–320.

Berthelsen J, Vandekerkhove J and Blasi F. Purification and characterization of UEF3, a novel factor involved in the regulation of the urokinase and other AP-1 controlled promoters. J Biol Chem 1996; 271: 3822-3830.

Berthelsen J, Zappavigna V, Mavillo F and Blasi F. Prep1, a novel functional partner of Pbx proteins. EMBO J 1998; 17: 1423-1433.

Berthelsen J, Kilstrup-Nielsen C, Blasi F, Mavillo F and Zappavigna V. The subcellular lacalization of PBX1 and EXD proteins depends on nuclear import and export signals and is modulated by association with PREP1 and HTH. Gen Dev 1999; 13: 946-953.

Bischof LJ, Kagawa N, Moskow JJ, Takahashi Y, Iwamatsu A, Buchberg AM and Waterman MR. Members of the meis1 and pbx homeodomain protein families cooperatively bind a cAMP-responsive sequence (CRS1) from bovine CYP17. J Biol Chem 1998; 273: 7941–7948.

Boudeau J, Baas AF, Deak M, Morrice NA, Kieloch A, Schutkowski M, Prescott AR, Clevers HC, Alessi DR. MO25alpha/beta interact with STRADalpha/beta enhancing their ability to bind, activate and localize LKB1 in the cytoplasm. EMBO J 2003; 22: 5102–5114.

Boudeau J, Deak M, Lawlor MA, Morrice NA, Alessi DR. Heat shock protein 90 and Cdc37 interact with LKB1 and regulate its stability, Biochem J 2003; 370: 849–857.

Boudeau J, Sapkota G and Alessi DR. LKB1, a protein kinase regulating cell proliferation and polarity. FEBS Lett 2003; 546: 159–165.

Brendolan A, Ferretti E, Salsi V, Moses K, Quaggiù S, Blasi F, Cleary ML and Selleri L. A Pbx1-dependent genetic and transcriptional network regulates spleen ontogeny. Development 2005; 132: 3113-3126.

Brown MS & Goldstein JL. The SREBP pathway: regulation of cholesterol metabolism by proteolysis of a membrane-bound transcription factor. Cell 1997; 89: 331–340.

Brown MS & Goldstein JL. A proteolytic pathway that controls the cholesterol content of membranes, cells, and blood. Proc Natl Acad Sci USA 96. 1999; 11041–11048.

Burglin TR. Analysis of TALE superclass homeobox genes (MEIS, PBC, KNOX, Iroquois, TGIF) reveals a novel domain conserved between plants and animals. Nucleic Acids Res 1997; 25: 4173– 4180.

Burglin TR. The PBC domain contains a MEINOX domain: coevolution of Hox and TALE homeobox genes? Dev Genes Evol 1998; 208: 113 – 116.

Cantley LC. The phosphoinositide 3-kinase pathway. Science 2002; 296(5573): 1655-1657.

Carling D. The AMP-activated protein kinase cascade-a unifying system for energy control. Trends Biochem Sci 2004; 29: 18–24.

Chan SK, Jaffe L, Capovilla M, Botas J and Mann RS. The DNA binding specificity of Ultrabithorax is modulated by cooperative interactions with extradenticle, another homeoprotein. Cell 1994; 78: 603–615.

Chang CP, Jacobs Y, Nakamura T, Jenkins NA, Copeland NG and Cleary ML. Meis proteins are major in vivo DNA binding partners for wild-type but not chimeric Pbx proteins. Mol Cell Biol 1997; 17: 5679–5687.

Chao L, Marcus-Samuels B, Mason MM, Moitra J, Vinson C, Arioglu E, Gavrilova O and Reitman ML. Adipose tissue is required for the antidiabetic, but not for the hypolipidemic, effect of thiazolidinediones. J. Clin. Invest. 2000; 106: 1221-1228.

Chapeau J. Insulin signaling: mechanisms altered in insulin resistance. Med Sci 2005; 21: 34-9.

Cheng A, Dube N, Gu F and Tremblay ML. Coordinated action of protein tyrosine phosphatases in insulin signal transduction. Eur J Biochem 2002; 269: 1050–1059.

Cusi K, Maezono K, Osman A, Pendergrass M, Patti ME, Pratipanawatr T, DeFronzo RA, Kahn CR and Mandarino LJ. Insulin resistance differentially affects the PI 3-kinase-and MAP kinase-mediated signaling in human muscle. J Clin Inv 2000; 105(3): 311-20.

Czech MP. Dynamics of phosphoinositides in membrane retrieval and insertion. Annu Rev Physiol 2003; 65: 791-815.

Dentin R et al. Hepatic glucokinase is required for the synergistic action of ChREBP and SREBP-1c on glycolytic and lipogenic gene expression. J. Biol. Chem. 2004; 279: 20314–20326.

Dentin R, Benhamed F, Pegorier JP, Foufelle F, Viollet B, Vaulont S, Girard J and Postic C. Polyunsaturated fatty acids suppress glycolytic and lipogenic genes through the inhibition of ChREBP nuclear protein translocation. J Clin Invest 2005; 115: 2843–2854.

Di Martino J, Selleri L, Traver D, Firpo M, Rhee J, Warnke R, O'Gorman S, Weissman IL and Cleary ML. The Hox cofactor and protoncogene Pbx1 is required for maintenance of definitive hematopoiesis in the fetal liver. Blood 2001; 98: 618–626.

Di Cristofano A, Pesce B, Cordon-Cardo C, Pandolfi PP. Pten is essential for embryonic development and tumour suppression. Nat Genet 1998; 19: 348-355.

Di Paola R, Frittitta L, Miscio G, Bozzali M, Baratta R, Centra M, Spampinato D, Santagati MG, Ercolino T, Cisternino C, Soccio T, Mastroianno S, Tassi V, Almgren P, Pizzuti A, Vigneri R and TrischittaV. A variation in 3' UTR of hPTP1B increases specific gene expression and associates with insulin resistance. Am J Hum Genet 2002; 70: 806–812.

Dubois MJ, Bergeron S, Kim HJ, Dombrowski L, Perreault M, Fournès B, Faure R, Olivier M, Beauchemin N, Shulman GI, Siminovitch KA, Kim JK, Marette A. The SHP-1 protein tyrosine phosphatase negatively modulates glucose homeostasis. Nat Med 2006; 12: 549-556.

Dutta S, Gannon M, Peers B, Wright C, Bonner-Weir S and Montminy M. PDX: PBX complexes are required for normal proliferation of pancreatic cells during development. Proc Natl Acad Sci USA 2001; 98: 1065–1070.

Elchebly M, Payette P, Michaliszyn E, Cromlish W, Collins S, Loy AL, Normandin D, Cheng A, Himms-Hagen J, Chan CC, Ramachandran C, Gresser MJ, Tremblay ML and Kennedy BP. Increased insulin sensitivity and obesity resistance in mice lacking the protein tyrosine phosphatase-1B gene. Science 1999; 283: 1544–1548.

Fang X, Yu SX, Lu Y, Bast CR, Woodgett JR and Mills GB. Phosphorylation and inactivation of glycogen synthase kinase 3 by protein kinase A. Proc Natl Acad Sci USA 2000; 97: 11960–11965.

Fernandez-Diaz LC, Laurent A, Girasoli S, Turco M, Longobardi E, Iotti G, Jenkins NA, Fiorenza MT, Copeland NG and Blasi F. The absence of Prep1 causes p53-dependent apoptosis of mouse pluripotent epiblast cells. Development 2010; 137(20): 3393-3403.

Ferre P, Azzout-Marniche D and Foufelle F. AMP-activated protein kinase and hepatic genes involved in glucose metabolism. Biochem Soc Trans 2003; 31: 220–223.

Ferretti E, Villaescusa JC, Di Rosa P, Fernandez-Diaz LC, Longobardi E, Mazzieri R, Miccio A, Micali N, Selleri L, Ferrari G and Blasi F. Hypomorphic mutation of the TALE gene Prep1 (pKnox1) causes a major reduction of Pbx and Meis proteins and a pleiotropic embryonic phenotype. Mol Cell Biol 2006; 26: 5650-5662.

Foufelle F, Girard J and Ferré P. Regulation of lipogenic enzyme expression by glucose in liver and adipose tissue: a review of the potential cellular and molecular mechanisms. Adv Enzyme Regul 1996; 36: 199-226.

Gehring WJ, Affolter M and Burglin T. Homeodomain proteins. Annu Rev Biochem 1994; 63: 487–526.

Girard J, Ferré P, Foufelle F. Mechanisms by which carbohydrates regulate expression of genes for glycolytic and lipogenic enzymes. Annu Rev Nutr 1997; 17: 325–352.

Goudet G, Delhalle S, Biemar F, Martial JA and Peers B. Functional and cooperative interactions between the homeodomain PDX1, Pbx, and Prep1 factors on the somatostatin promoter. J Biol Chem 1999; 274: 4067-4073.

Hardie DG, Carling D and Carlson M. The AMP-activated/SNF1 protein kinase subfamily: metabolic sensors of the eukaryotic cell. Annu Rev Biochem 1998; 67: 821–855.

Hardie DG, Scott JW, Pan DA, Hudson ER. Management of cellular energy by the AMP-activated protein kinase system. FEBS Lett 2003; 546:113–120.

Hardie DG. The AMP-activated protein kinase pathway – new players upstream and downstream. J Cell Sci 2004; 117: 5479–5487.

Hardie DG. New roles for the LKB1-AMPK pathway. Curr Opin Cell Biol 2005; 17: 167–173.

Harrison. Principi di Medicina Interna. Il Manuale 17/ed March 2009.

Hawley SA, Boudeau J, Reid JL, Mustard KJ, Udd L, Makela TP, Alessi DR, Hardie DG. Complexes between the LKB1 tumor suppressor, STRADalpha/beta and MO25alpha/beta are upstream kinases in the AMP-activated protein kinase cascade. J Biol 2003; 2(4): 28.

Hisa T, Spence SE, Rachel RA, Fujita M, Nakamura T, Ward JM, Devor-Henneman DE, Saiki Y, Kutsuna H, Tessarollo L, Jenkins NA and Copeland NG. Hematopoietic, angiogenic and eye defects in Meis1 mutant animals. EMBO J 2004; 23: 450–459.

Horie Y, Suzuki A, Kataoka E, Sasaki T, Hamada K, Sasaki J, et al. Hepatocyte-specific Pten deficiency results in steatohepatitis and hepatocellular carcinomas. J Clin Invest 2004; 113: 1774-1783.

Horton JD and Shimomura I. Sterol regulatory element-binding proteins: activators of cholesterol and fatty acid biosynthesis. Curr Opin Lipidol 1999; 10: 143–150.

Ide T, Shimano H, Yahagi N, Matsuzaka T, Nakakuki M, Yamamoto T, Nakagawa Y, Takahashi A, Suzuki H, Sone H, Toyoshima H, Fukamizu A and Yamada N. SREBPs suppress IRS-2-mediated insulin signalling in the liver. Nat Cell Biol 2004; 6: 351–357.

Ishii S, Iizuka K, Miller BC and Uyeda K. Carbohydrate response element binding protein directly promotes lipogenic enzyme gene transcription. Proc Natl Acad Sci USA 2004; 101: 15597–15602.

Jenne DE, Reimann H, Nezu J, Friedel W, Loff S, Jeschke R, Muller O, Back W, Zimmer M, Peutz–Jeghers syndrome is caused by mutations in a novel serine threonine kinase. Nat Genet 1998; 18: 38–43.

Johnson TO, Ermolieff J and Jirousek MR. Protein tyrosine phosphatase 1B inhibitors for diabetes. Nat Rev Drug Discov 2002; 1: 696–709.

Jonsson J, Carlsson L, Edlund T, Edlund H. Insulin-promoter-factor 1 is required for pancreas development in mice. Nature 1994; 371: 606–609.

Kahn BB, Alquier T, Carling D and Hardie DG. AMP-activated protein kinase: ancient energy gauge provides clues to modern understanding of metabolism. Cell Metab 2005; 1: 15–25.

Kamps MP, Murre C, Sun X-H and Baltimore D. A new homeobox gene contributes the DNA binding domain of the t(1;19) translocation protein in pre-B ALL. Cell 1990; 60: 547–555.

Kawaguchi T, Takenoshita M, Kabashima T and Uyeda K. Glucose and cAMP regulate the L-type pyruvate kinase gene by phosphorylation/dephosphorylation of the carbohydrate response element binding protein. Proc Natl Acad Sci USA 2001; 98: 13710–13715.

Kawaguchi T, Osatomi K, Yamashita H, Kabashima T and Uyeda K. Mechanism for fatty acid ‘sparing’ effect on glucose-induced transcription: regulation of carbohydrate responsive element-binding protein by AMP-activated protein kinase. J Biol Chem 2002; 277: 3829–3835.

Kemp BE, Stapleton D, Campbell DJ, Chen ZP, Murthy S, Walter M, Gupta A, Adams JJ, Katsis F, van DB, Jennings IG, Iseli T, Michell BJ, Witters LA. AMP-activated protein kinase, super metabolic regulator. Biochem Soc Trans 2003; 31: 162–168.

Kahn SE, Hull RL and Utzschneider KM. Mechanisms linking obesity to insulin resistance and type 2 diabetes. Nature 2006; 444(7121): 840-846.

Kim SK, Selleri L, Lee JS, Zhang AY, Gu X, Jacobs Y and Cleary ML. Pbx1 inactivation disrupts pancreas development and in Ipf1 deficient mice promotes diabetes mellitus. Nat Genet 2002; 30: 430-435.

Klaman LD, Boss O, Peroni OD, Kim JK, Martino JL, Zabolotny JM, Moghal N, Lubkin M, Kim YB, Sharpe AH, Stricker-Krongrad A, Shulman GI, Neel BG and Kahn BB. Increased energy expenditure, decreased adiposity, and tissue-specific sensitivity in protein-tyrosine phosphatase 1B-deficient mice. Mol Cell Biol 2000; 20: 5479–5489.

Knoepfler PS, Calvo KR, Chen H, Antonarakis SE and Kamps MP. Meis1 and pKnox1 bind DNA cooperatively with Pbx1 utilizing an interaction surface disrupted in oncoprotein E2a-Pbx1. Proc Natl Acad Sci USA 1997; 94: 14553–14558.

Maegawa H, Hasegawa M, Sugai S, Obata T, Ugi S, Morino K, Egawa K, Fujita T, Sakamoto T, Nishio Y, Kojima H, Haneda M, Yasuda H, Kikkawa R, Kashiwagi A. Expression of a dominant negative SHP-2 in transgenic mice induces insulin resistance. J Biol Chem 1999; 274: 30236–30243.

Magnuson MA, Andreone TL, Printz RL, Koch S, Granner DK. Rat glucokinase gene: structure and regulation by insulin. Proc Natl Acad Sci USA 1989; 13: 4838–4842.

Mann RS and Chan SK. Extra specificity from extradenticle: the partnership between HOX and PBX/EXD homeodomain proteins. Trends Genet 1996; 12: 258–262.

Moens CB, Selleri L. Hox cofactors in vertebrate development. Dev Biol 2006; 291: 193–206.

Nezu J, Oku A, Shimane M. Loss of cytoplasmic retention ability of mutant LKB1 found in Peutz-Jeghers syndrome patients. Biochem Biophys Res Commun 1999; 261: 750 –755.

Nourse J, Mellentin JD, Galili N, Wilkinson J, Starbridge E, Smith SD and Cleary ML. Chromosomal translocation t(1;19) results in synthesis of a homeobox fusion mRNA that codes for a potential chimeric transcription factor. Cell 1990; 60: 535–545.

Oriente F, Fernandez Diaz LC, Miele C, Iovino S, Mori S, Diaz VM, Troncone G, Cassese A, Formisano P, Blasi F and Beguinot F. Prep1 deficiency induces protection from diabetes and increased insulin sensitivity through a p160-mediated mechanism. Mol Cell Biol 2008; 28: 5634-5645.

Oriente F, Iovino S, Cabaro S, Cassese A, Longobardi E, Miele C, Ungaro P, Formisano P, Blasi F and Beguinot F. Prep1 controls insulin glucoregulatory function in liver by transcriptional targeting of SHP1 tyrosine phosphatase. Diabetes 2011; 60: 138-147.

Penkow D, Di Rosa P, Fernandez Diaz L, Basso V, Ferretti E, Grassi F, Mondino A and Blasi F. Involvment of Prep1 in the alpha beta T-cell receptor T-lymphocytic potential of hematopoietic precursor. Mol Cell Biol 2005; 25: 10768-10781.

Pilkis SJ and Claus TH. Hepatic gluconeogenesis/glycolysis: regulation and structure/function relationships of substrate cycle enzymes. Annu Rev Nutr 1991; 11: 465–515.

Pilkis SJ and Granner DK. Molecular physiology of the regulation of hepatic gluconeogenesis and glycolysis. Annu Rev Physiol 1992; 54: 885–909.

Piper DE, Batchelor AH, Chang CP, Cleary ML and Wolberg C. Structure of HoxB1-Pbx heterodimer bound to DNA: role of the exapaptide and a fourth homeodomain helix in complex formation. Cell 1999; 96: 587-597.

Postic C and Girard J. The role of the lipogenic pathway in the development of hepatic steatosis. Diabetes Metab 2008; 34: 643-648.

Rauskolb C and Wieschaus E. Coordinate regulation of downstream genes by extradenticle and the homeotic selector proteins. EMBO J 1994; 13: 3561–3569.

Sakiyama H, Wynn RM, Lee WR, Fukasawa M, Mizuguchi H, Gardner KH, Repa JJ and Uyeda K. Regulation of Nuclear Import/Export of Carbohydrate Response Element-binding Protein (ChREBP): Integration of an Alpha-helix of ChREBP with the 14-3-3 proteins and regulation by phosphorylation. The Journal of Biological Chemistry 2008; 283(36): 24899–24908.

Samaras K, McElduff A, Twigg SM, Proietto J, Prins JB, Welborn TA, Zimmet P, Chisholm DJ and Campbell LV. Insulin levels in insulin resistance: phantom of the metabolic opera. Med J Aust 2006; 185(3): 159-61.

Samuel VT, Liu ZX, Qu X, Elder BD, Bilz S, Befroy D, Romanelli AJ, Shulman GI. Mechanism of hepatic insulin resistance in non-alcoholic fatty liver disease. Journal of Biological Chemistry 2004; 279: 32345–32353.

Sanyal AJ. Mechanisms of disease: pathogenesis of nonalcoholic fatty liver disease. Nat Clin Pract Gastroenterol Hepatol 2005; 2: 46–53.

Scheen AJ and Luyckx FH. Obesity and liver disease. Best Pract Res Clin Endocrinol Metab 2002; 16: 703–716.

Selleri L, Depew MJ, Jacobs Y, Chanda SK, Tsang KY, Cheah KS, Rubenstein JL, O'Gorman S and Cleary M. Requirement for Pbx1 in skeletal patterning and programming chondrocyte proliferation and differentiation. Development 2001; 128: 3543-3557.

Shaw RJ, Lamia KA, Vasquez D, Koo SH, Bardeesy N, Depinho RA, Montminy M and Cantley LC. The kinase LKB1 mediates glucose homeostasis in liver and therapeutic effects of metformin. Science 2005; 310: 1642–1646.

Shimano H. Sterol regulatory element-binding proteins (SREBPs): transcriptional regulators of lipid synthetic genes. Prog Lipid Res 2001; 40: 439–452.

Shimano H. Sterol regulatory element-binding protein family as global regulators of lipid synthetic genes in energy metabolism. Vitam Horm 2002; 65: 167–194.

Sleeman MW, Wortley KE, Lai KM, Gowen LC, Kinter J, Kline WO, Garcia K, Stitt TN, Yancopoulos GD, Wiegand SJ and Glass DJ. Absence of the lipid phosphatase SHIP2 confers resistance to dietary obesity. Nat Med 2005; 11(2): 199-205.

Stambolic V, Suzuki A, de la Pompa JL, Brothers GM, Mirtsos C, Sasaki T, Ruland J, Penninger JM, Siderovski DP and Mak TW. 1998; Cell 95: 29–39.

Stiles B, Wang Y, Stahl A, Bassilian S, Lee WP, Kim YJ, Sherwin R, Devaskar S, Lesche R, Magnuson MA and Wu H. Liver-specific deletion of negative regulator Pten results in fatty liver and insulin hypersensitivity. Proc Natl Acad Sci USA 2004; 101: 2082-2087.

Suzuki A, de la Pompa JL, Stambolic V, Elia AJ, Sasaki T, del Barco Barrantes I, Ho A, Wakeham A, Itie A, Khoo W, Fukumoto A and Mak TW. High cancer susceptibility and embryonic lethality associated with mutation of the PTEN tumor suppressor gene in mice. Curr Biol 1998; 8: 1169- 1178.

Taniguchi CM, Emanuelli B, Kahn CR. Critical nodes in signaling pathways: insights into insulin action. Nat Rev Mol Cell Biol 2006; 7: 85-96.

Tiainen M, Vaahtomeri K, Ylikorkala A, Makela TP. Growth arrest by the LKB1 tumor suppressor: induction of p21(WAF1/CIP1). Hum Mol Genet 2002; 11: 1497–1504.

Towle HC, Kaytor EN, Shih HM. Regulation of the expression of lipogenic enzyme genes by carbohydrate. Annu Rev Nutr 1997; 17: 405–433.

Unger RH. Lipotoxicity in the pathogenesis of obesity-dependent NIDDM. Genetic and clinical implications. Diabetes 1995; 44: 863–870.

Vaulont S, Vasseur-Cognet M, Kahn A. Glucose regulation of gene transcription. J Biol Chem 2000; 275: 31555–31558.

Viollet B, Foretz M, Guigas B, Horman S, Dentin R, Bertrand L, Hue L and Andreelli F. Activation of AMP-activated protein kinase in the liver: a new strategy for the management of metabolic hepatic disorders. J Physiol 2006; 574: 41-53.

Virkamaki A, Ueki K and Kahn CR. Protein-protein interaction in insulin signaling and the molecular mechanisms of insulin resistance. J Clin Investig 1999; 103: 931–943.

White MF. The IRS-signalling system: a network of docking proteins that mediate insulin action. Mol Cell Biochem 1998; 182: 3–11.

Witters LA and Kemp BE. Insulin activation of acetyl-CoA carboxylase accompanied by inhibition of the 5-AMP activated protein kinase. J Biol Chem 1992; 267: 2864–2867.

Wong RH and Sul HS. Insulin signaling in fatty acid and fat synthesis: a transcriptional perspective. Curr Opin Pharmacol 2010; 10(6): 684-691.

Woods A, Johnstone SR, Dickerson K, Leiper FC, Fryer LG, Neumann D, Schlattner U, Wallimann T, Carison M and Carling D. LKB1 is the upstream kinase in the AMP-activated protein kinase cascade. Curr Biol 2003; 13: 2004–2008.

Xie Z, Dong Y, Zhang M, Cui MZ, Cohen RA, Riek U, Neumann D, Schlattner U and Zou MH. Activation of Protein Kinase CZETA by Peroxynitrite Regulates LKB1-dependent AMP-activated Protein Kinase in Cultured Endothelial Cells. The Journal of Biological Chemistry 2006; 281 (10): 6366–6375.

Zeyda M and Stulning TM. Obesity, inflammation, and insulin resistance - a mini review. Gerontology 2009; 55(4): 379-386.

Zhou G, Myers R, Li Y, Chen Y, Shen X, Fenyk-Melody J, Wu M, Ventre J, Doebber T, Fujii N, Musi N, Hirshman MF, Goodyear LJ and Moller DE. Role of AMP-activated protein kinase in mechanism of metformin action. J Clin Invest 2001; 108: 1167–1174.

Prep1 Controls Insulin Glucoregulatory Function in Liver by Transcriptional Targeting of *SHP1* Tyrosine Phosphatase

Francesco Oriente,[1] Salvatore Iovino,[1] Serena Cabaro,[1] Angela Cassese,[1] Elena Longobardi,[2,3] Claudia Miele,[1] Paola Ungaro,[1] Pietro Formisano,[1] Francesco Blasi,[2,3] and Francesco Beguinot[1]

OBJECTIVE—We investigated the function of the *Prep1* gene in insulin-dependent glucose homeostasis in liver.

RESEARCH DESIGN AND METHODS—Prep1 action on insulin glucoregulatory function has been analyzed in liver of *Prep1*-hypomorphic mice (*Prep1*$^{i/i}$), which express 2–3% of *Prep1* mRNA.

RESULTS—Based on euglycemic hyperinsulinemic clamp studies and measurement of glycogen content, livers from *Prep1*$^{i/i}$ mice feature increased sensitivity to insulin. Tyrosine phosphorylation of both insulin receptor (IR) and insulin receptor substrate (IRS)1/2 was significantly enhanced in *Prep1*$^{i/i}$ livers accompanied by a specific downregulation of the SYP and SHP1 tyrosine phosphatases. *Prep1* overexpression in HepG2 liver cells upregulated *SYP* and *SHP1* and inhibited insulin-induced IR and IRS1/2 phosphorylation and was accompanied by reduced glycogen content. Consistently, overexpression of the Prep1 partner *Pbx1*, but not of *p160MBP*, mimicked Prep1 effects on tyrosine phosphorylations, glycogen content, and on SYP and SHP1 expression. In *Prep1* overexpressing cells, antisense silencing of *SHP1*, but not that of *SYP*, rescued insulin-dependent IR phosphorylation and glycogen accumulation. Both Prep1 and Pbx1 bind SHP1 promoter at a site located between nucleotides −2,113 and −1,778. This fragment features enhancer activity and induces luciferase function by 7-, 6-, and 30-fold, respectively, in response to Prep1, Pbx1, or both.

CONCLUSIONS—SHP1, a known silencer of insulin signal, is a transcriptional target of Prep1. In liver, transcriptional activation of *SHP1* gene by Prep1 attenuates insulin signal transduction and reduces glucose storage. ***Diabetes*** **60:138–147, 2011**

Prep1 is an homeodomain transcription factor of the three-amino acid loop extension (TALE) superclass of proteins (1) that dimerizes with Pbx1, enhancing target specificity and modulating transcription regulatory function (2–8). Prep1 is essential for embryonic development. Indeed, *Prep1* null embryos die before gastrulation (L.C. Fernandez-Diaz and F.B., unpublished observations), whereas *Prep1*- hypomorphic mutant mouse (*Prep1*$^{i/i}$) embryos, which express 2 to 3% of *Prep1* mRNA and up to 10% of the protein, show a leaky embryonic-lethal phenotype and defects in angiogenesis, hematopoiesis, and eye development. Part of the *Prep1*$^{i/i}$ phenotype depends on reduction of the Pbx protein level (9–11).

In addition to Pbx, Prep1 also interacts with p160MBP in competition with Pbx (12), preventing its proteosomal degradation and enhancing its regulatory effect on PGC-1α and hence on its regulation on glucose metabolism (13). The few surviving *Prep1*$^{i/i}$ and the heterozygous *Prep1*$^{i/+}$ mice show decreased insulin and glucagon production, prolonged insulin response, and protection from insulin-deficient diabetes. This phenotype is due to a complex tissue-specific mechanism. At the skeletal muscle level, the enhanced insulin sensitivity was due to a decrease in p160MBP, resulting in activation of PGC-1α, overexpression of GLUT4, and increased glucose uptake (13). On the other hand, the level of Pbx1 was not changed, which drastically increases the Pbx/p160 ratio. Different mechanism must operate in liver since Pbx1 and p160MBP are expressed at different levels compared with skeletal muscle.

Liver gluconeogenesis depends on the enzymes G6Pase and PEPCK, the expression of which requires PGC-1α as well as other transcription factors, including Foxo1 (14–17). For example, in liver, glucagon induces G6Pase and PEPCK and activates gluconeogenesis via PGC-1α (14). This agrees with the *Prep1*$^{i/i}$ phenotype that includes smaller pancreas and reduced glucagon-circulating levels (13). Whether and how *Prep1* affects glucose metabolism in liver is unknown at the present, but must be clarified to elucidate how Prep1 regulates insulin-dependent glucose metabolism at the whole-body level. Indeed, PGC-1α upregulation in *Prep1*-deficient mice is expected to produce sustained gluconeogenesis. In contrast, these animals feature normal glucose tolerance and protection from diabetes.

In liver, insulin-dependent glucoregulatory function is controlled by a number of different mechanisms. Among these, the function of several protein tyrosine phosphatases has been reported to play a major role. PTP1B, SYP, and SHP1, for example, are known to negatively modulate insulin action on liver glucose metabolism through tyrosine dephosphorylation of the insulin receptor and/or IRS (18–20). At variance, the ubiquitously expressed cytosolic SHP2 phosphatase was described to positively modulate insulin signaling (21,22). Thus, the balance of these individual phosphatases represents an important determi-

From the [1]Dipartimento di Biologia e Patologia Cellulare e Molecolare and Istituto di Endocrinologia ed Oncologia Sperimentale del Consiglio Nazionale delle Ricerche, Università degli Studi di Napoli Federico II, Naples, Italy; the [2]Istituto FIRC di Oncologia Molecolare (Fondazione Italiana per la Ricerca sul Cancro Institute of Molecular Oncology), Milano, Italy; and the [3]Università Vita Salute San Raffaele, Milano, Italy.

Corresponding author: Francesco Beguinot, beguino@unina.it.

Received 23 June 2010 and accepted 14 September 2010. Published ahead of print at http://diabetes.diabetesjournals.org on 23 September 2010. DOI: 10.2337/db10-0860.

F.O. and S.I. contributed equally to this study.

© 2011 by the American Diabetes Association. Readers may use this article as long as the work is properly cited, the use is educational and not for profit, and the work is not altered. See http://creativecommons.org/licenses/by-nc-nd/3.0/ for details.

The costs of publication of this article were defrayed in part by the payment of page charges. This article must therefore be hereby marked "advertisement" in accordance with 18 U.S.C. Section 1734 solely to indicate this fact.

nant of normal liver glucoregulation. How this balance is maintained at the physiologic and molecular levels has been only partially elucidated.

In the present work, we have focused on Prep1 action on hepatic glucose metabolism. We show that in liver, Prep1 restrains insulin action by activating transcription of the *SHP1* tyrosine phosphatase gene and inhibiting insulin receptor and IRS signaling.

RESEARCH DESIGN AND METHODS

Materials. Media, sera, antibiotics for cell culture, and the lipofectamine reagent were from Invitrogen (Grand Island, NY). The anti-Prep1 polyclonal antibody and *pBOS-Prep1*, *pSG5-Pbx1*, *PSG5-Prep1*$_{HR1}$, *pRUFneo-p160* vectors have been described previously (12,13). The PGC-1α, actin, IR, Pbx1, Syp, SHP1, PTP1B, G6Pase, and PEPCK antibodies were from Santa Cruz Biotechnology (Santa Cruz, CA). The pY, IRS1, and IRS2 antibodies were from Upstate Biotechnolgy (Lake Placid, NY). The p160 antibody was from Zymed Laboratories (San Francisco, CA). Protein electrophoresis reagents were from Bio-Rad (Richmond, VA), Western blotting and enhanced chemiluminescence (ECL) reagents from Amersham Biosciences (Arlington Heights, IL). All other chemicals were from Sigma (St. Louis, MO).

Studies in mice. High-fat diet treatment of C57BL/6J mice was performed as described by Vigliotta et al. (23). *Prep1*-targeted mice were generated by gene trapping (Lexikon Genetics, The Woodlands, TX). Their general phenotype has been previously described (10,11). Weight of Prep1$^{i/+}$ mice was slightly lower than that of their nonhypomorphic littermates (13). All animal handling conformed to regulations of the Ethics Committee on Animal Use of H.S. Raffaele (Institutional Animal Care and Use Committee, permission number 207). Genotyping strategy has been previously described (13).

Hepatic tissue samples were collected rapidly after mice were killed with a pentobarbitone overdose. Tissues were snap frozen in liquid nitrogen and stored at −80°C for subsequent Western blotting as previously described (13).

Cell culture procedures and transfection. The HepG2 hepatocarcinoma cells and NMuLi mouse liver cells were cultured at 37°C in Dulbecco' s modified Eagle' s medium (DMEM) supplemented with 10% FCS, 2% L-glutamine, 10,000 units/ml penicillin, and 10,000 μg/ml streptomycin. Transient transfection of *Prep1*, *Prep1*$_{HR1}$, *p160* and *Pbx1* plasmids or *Syp* (5′-CTCCGCGATGTCATGTTCCT-3′) and *SHP1* (5′- GAGGTCTCGGTGAAAC CACCT CACCATCCT-3′) phosphorothioate antisense oligonucleotides or scrambled control oligonucleotides *Syp* (5′- TCGCCACGTCGCTCATTGTT-3′) and *SHP1* (5′-GTAGAGTTCCGTGAGACACCTCTCCACCAC-3′) were performed by the Lipofectamine method according to the manufacturer's instruction. In stable transfection studies, individual G418-resistant clones were selected by the limiting dilution technique (G418 effective dose, 0.8 mg/ml). The expression of Prep1 by the individual clones was quantitated by Western blotting. In both transient and stable transfection, the efficiency was consistently between 65 and 75%.

Determination of glycogen content and triglycerides levels. Glycogen was isolated from liver tissue or HepG2 cells homogenized in 0.1% SDS, saturated with Na_2SO_4 for 30′ at 37°C, followed by ethanol (EtOH) precipitation. Glycogen content was determined as previously described (24,25).

The triglyceride content was extracted from frozen liver tissues and determined as described previously (25).

Euglycemic-hyperinsulinemic clamps. Six-month-old male mice were catheterized via the right internal jugular vein under isoflorane anesthesia. After loss of pedal and corneal reflexes was assured, a catheter (platinum-cured silicone tubing, 0.020 internal diameter × 0.037 outer diameter; Harvard Apparatus, Holliston, MA) was inserted into the right internal jugular and advanced to the level of the superior vena cava. The catheter was filled with saline, tunneled, and left in a subcutaneous pocket at the back of the neck. A 6-0 silk suture was attached to the free end of the catheter and exteriorized in such a fashion as to allow retrieval of the catheter on the day of the experiment. Mice were allowed to recover on a heating pad. After 5 days of recovery, mice were subjected to clamp studies. The infusion studies lasted a total of 90 min. At $t = 0$ min, mice began receiving a constant infusion of HPLC-purified [^{3}H]glucose (0.1 μCi/min; Perkin-Elemer), and insulin (3.5 mU/min/kg body weight; Humulin, Eli Lilly). A solution of glucose (20%) was infused at a variable rate as required to maintain euglycemia (140–150 mg/dl). Thereafter, plasma samples were collected to determine glucose levels (at t = 0, 30, 50, 60, 70, 80, and 90 min) as well as [^{3}H]glucose specific activity (at t = 0, 30, 50, 60, 70, 80, and 90 min). Plasma glucose was measured by the glucose oxidase method (Glucose Analyzer, Analox GM-7 microstat).

Under steady-state conditions for plasma glucose concentration, the R_d equals the rate of glucose appearance (R_a). R_a was determined from the ratio of the infusion rate for [^{3}H]glucose (dpm) and the specific activity of plasma [^{3}H]glucose (dpm) under steady-state conditions. The rate of glucose production was therefore obtained from the difference between R_a and the rate of glucose infusion.

Western blot analysis and immunoprecipitation procedures. Tissue samples were homogenized in a Polytron (Brinkman Instruments, NY) in 20 ml Tissue Protein Extraction Reagent /g of tissue according to the manufacturer's instructions (Pierce, IL). Immunoprecipitation and Western blot analysis have been performed as previously described (26).

Real-time RT-PCR analysis. Total cellular RNA was isolated from liver tissue and HepG2 cells by using the RNeasy kit (QIAGEN Sciences, Germany), according to the manufacturer 's instructions. We reverse-transcribed 1 μg of tissue or cell RNA using Superscript II Reverse Transcriptase (Invitrogen, CA). PCR reactions were analyzed using SYBR Green mix (Invitrogen, CA). Reactions were performed using Platinum SYBR Green qPCR Super-UDG using an iCycler IQ multicolor Real Time PCR Detection System (Biorad, CA). All reactions were performed in triplicate and β-actin was used as an internal standard. Primer sequences used were as follows. G6Pase R 5′-GTACCTCAG GAAGCTGCCA-3′, G6Pase F: 5′-TTTGCTATTTTACGTAAATCACCCT-3′, PEPCK R 5′-AATGTCATC ACCCACACA TTC- 3′, PEPCK F: 5′-ATG TATGTCATC CCA TTC AGC- 3′,PGC-1α R 5′-AGGGTCATCGTTTGTGGTCAG-3′, PGC-1α F 5′CAGCGGTCTTAGCAC TCA G-3′, hSyp R 5′-GCTCTCAAAAGCCCTGTGTC-3′, hSyp F 5′ GCTGGGACAAGCTGAAAGTC-3′, hSHP1 R 5′-GTCTCCAAACCAC CCACTGT-3′, hSHP1 F 5′-GACGTTTCTTGTGCGTGAGA-3′, hPTP1B R5′-GCTCTCAAAAGCCCTGTGTC-3′, hPTP1B F 5′-GCTGGGACAAGCTGAAAGTC-3′, mSyp R 5′-TGCCCAGCGTCTCCACCATG-3′, mSyp F 5′-AGCAACGA CGGCAAGTCCAAAG-3′, mSHP1 R 5′ TCCTCCGACTCCTGCTTCTTG 3′, mSHP1 F 5′ GACCTGGTGGAGCACTTCAAG 3′, mPTP1B R 5′ CTCTATGCAACCCAAG GAACTG 3′, mPTP1B F 5′ CTTCAGGTGGTGGAGACAGG 3′, β-actin F 5′-GCGTGACATCAAAGAGAAG-3′ and β-actin R 5′-ACTGTGTTGGCATAGAGG-3′.

Chromatin immunoprecipitation and luciferase assays. Chromatin immunoprecipitation (ChIP) and Re-ChIP assays were performed using nMuLi cells as previously described (27). For luciferase assays, the mouse *SHP1* fragment −1,887/+335 (region n. *2*) was amplified by PCR from genomic mouse DNA isolated from the murine liver cell line (NmuLi cells). The following primers were used: F: 5′-*Kpn*I- TCGGTGTGAGATCGGTACAA-3′ and R:5′-*Sac*I- TCCGAGTTGGTGTCTCAGTG-3′ (*SHP1* n°2), (where *Sac*I and *Kpn*I indicate the restriction sites added to the sequence). The amplified fragments were cloned in the Plg3 promoter vector (Promega) by *Sac*I and *Kpn*I. HeLa cells were cotransfected with 2 μg of *SHP1* n°2 promoter vector together with different amounts of *Prep1* and *Pbx1* expression vectors. Total DNA content (up to 4 μg/plate) was normalized to the empty vector devoid of *Prep1* and *Pbx1* coding sequence. Forty-eight hours after transfection, the cells were harvested and lysed as described previously (27). Luciferase activity was measured by a commercial luciferase assay kit (Promega). Values were normalized for β-galactosidase. Statistical significance was evaluated by *t* test analysis.

Statistical procedures. Data were analyzed with Statview software (Abacus Concepts, Piscataway, NJ) by one-factor ANOVA. P values < 0.05 were considered statistically significant (23).

RESULTS

Hepatic glucose metabolism in Prep1-deficient mice. To address the significance of *Prep1* to the insulin-resistant and diabetic liver, we first examined its expression in high-fat diet-treated (HFD) and in diabetic *db/db* mice. Hepatic expression of Prep1 was 37 and 67% higher, respectively, in the HFD and *db/db* compared with the control mice (Fig. 1*A*), suggesting a role of Prep1 in the altered liver glucose metabolism and glucoregolatory function in the murine models. To investigate this issue in greater detail, we compared liver glycogen and triglyceride content in *Prep1* hypomorphic mice (*Prep1*$^{i/+}$; *Prep1*$^{i/i}$) and in their nonhypomorphic littermates (wild type). Glycogen content was significantly increased in the hypomorphic mice and a *Prep1* gene dosage effect was evidenced (Fig. 1*B*; increases were twofold and threefold, respectively, in the *Prep1*$^{i/+}$ and the *Prep1*$^{i/i}$ mice). At variance, liver triglyceride content was reduced in the Prep1-deficient mice (3.3 ± 1.7 and 14 mg/g ± 2.5 tissue, respectively, in the Prep1$^{i/+}$ and the nonhypomorphic mice) (Fig. 1*C*). However, no significant difference was detected in liver weight between *Prep1* hypomorphic and wild-type

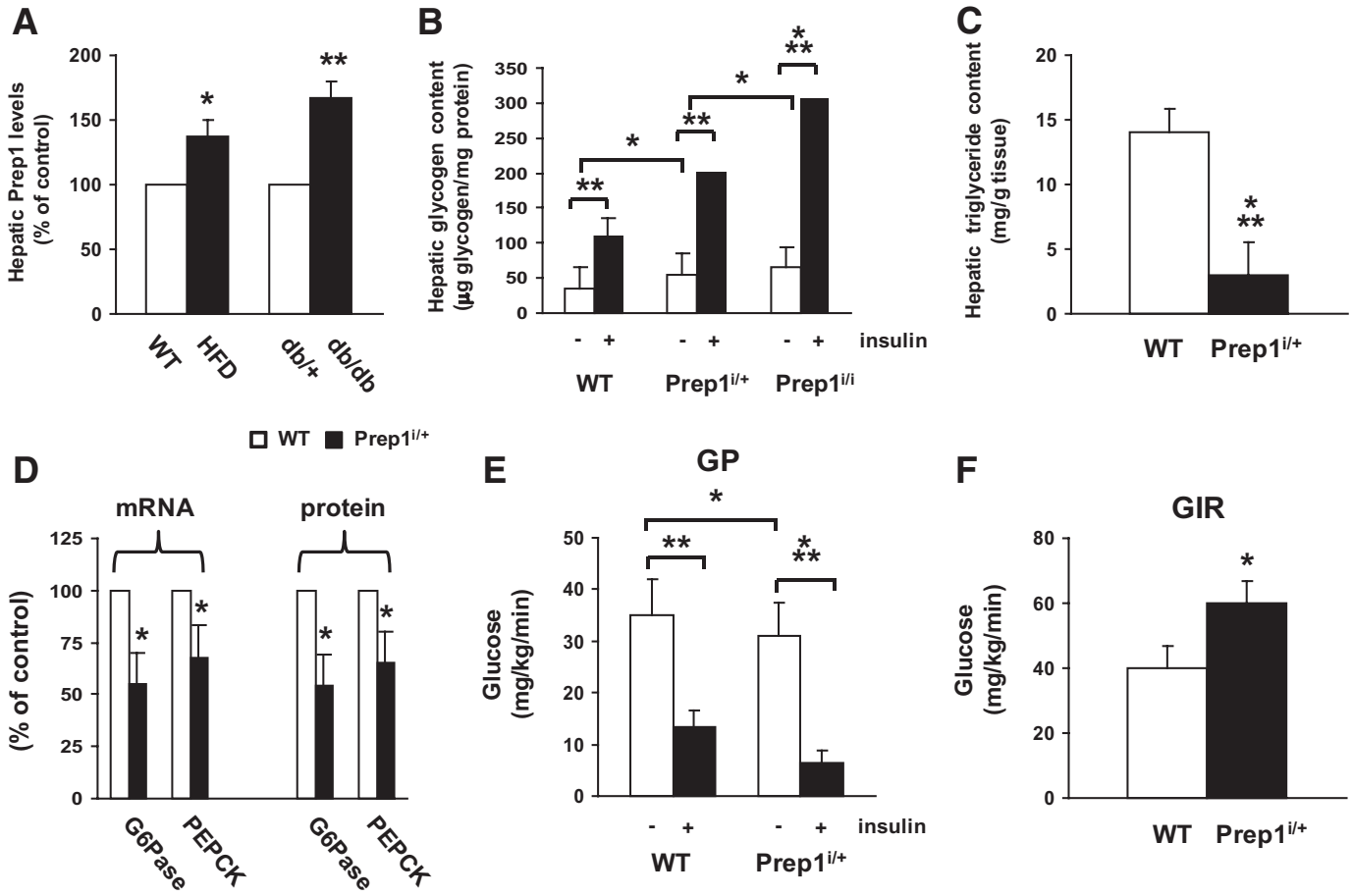

FIG. 1. Hepatic phenotype in HFD, *db/db* and in *Prep1*$^{i/+}$ mice. *A*: Livers from WT, HFD, *db/+*, and *db/db* mice were dissected, solubilized, and Western blotted with anti-Prep1 antibodies. Blots were revealed by ECL and autoradiography and bands quantitated by laser densitometry and normalized for actin. Each bar represents the mean ± SD of duplicate determinations in seven mice per group. *B*: *Prep1* hypomorphic and their nonhypomorphic littermates (WT) were injected with insulin intraperitoneally (0.75 mU/g body weight). After 2 h, livers were isolated and glycogen content was measured as described in RESEARCH DESIGN AND METHODS. Bars represent the means ± SD of determinations in 12 mice per group. *C*: Intrahepatic triglyceride content was measured as described in RESEARCH DESIGN AND METHODS. Bars represent the means ± SD of determinations in nine mice per group. *D*: G6Pase and PEPCK mRNA and protein content was determined by real-time RT-PCR analysis of total RNA isolated from liver of *Prep1*$^{i/+}$ and control mice injected with insulin for 1 h, using *β-actin* as internal control. Bars represent the mean ± SD of four independent experiments, in each of which reactions were performed in triplicate using the pooled total RNAs obtained from six mice per genotype. Glucose production (*E*) and glucose infusion rate (*F*) were assessed by euglycemic hyperinsulinemic clamp. All measurements were performed during the final 40 min of the 90-min clamp procedure, after steady-state conditions for plasma glucose and insulin concentrations, glucose specific activity, and rates of glucose infusion were achieved as described in RESEARCH DESIGN AND METHODS. Asterisks denote statistically significant differences (P* < 0.05; ***P* < 0.01; ****P* < 0.001).**

(WT) animals (data not shown). Expression of the major gluconeogenic enzymes *G6Pase* and *PEPCK* was, respectively, 45 and 30% reduced in these mice compared with controls, both at the mRNA and the protein levels (Fig. 1*D*; $P < 0.01$). We then measured liver sensitivity to insulin and assessed glucose production by euglycemic hyperinsulinemic clamp in conscious *Prep1* hypomorphic mice. In these studies, the rate of insulin infusion was selected to generate a physiologic increase in plasma insulin (to 8 ng/ml) to submaximally stimulate glucose uptake and inhibit glucose production (28). As shown in Fig. 1*E*, basal glucose production (mainly gluconeogenic after 16-h starvation) was slightly but significantly lower in the hypomorphic mice. Insulin suppressed hepatic glucose production to lower levels in *Prep1*$^{i/+}$ mice (8 ± 2.2 mg/kg/min) compared with WT (15 ± 3.1 mg/kg/min), reflecting enhanced hepatic sensitivity to insulin. The increased hepatic sensitivity to insulin in the hypomorphyc mice was further supported by the higher glucose infusion rate (GIR) required to maintain euglycemia during the clamp (60 ± 6 mg/kg/min in the *Prep1*$^{i/+}$ vs. 40 mg/kg/min ± 6 in the WT) (Fig. 1*F*).

The increased insulin sensitivity in muscle from *Prep1* hypomorphic mice is largely contributed by reduced p160 stability, followed by higher PGC-1α levels in this tissue (13). At variance with muscle, p160 abundance was very low in liver and did not change in *Prep1* hypomorphic mice (Fig. 2*A*). PGC-1α levels also showed no change in hypomorphic liver (Fig. 2*B*), suggesting that the action of Prep1 on insulin sensitivity may involve different mechanisms in liver and skeletal muscle. Also, at variance with muscle (13), Pbx1 was abundantly expressed in liver from WT mice but extremely reduced in those from their *Prep1*-deficient littermates (Fig. 2*C*).

Prep1 effect on the insulin signaling pathway in mouse liver. To further analyze Prep1 action on liver sensitivity to insulin, we first profiled the initial steps of the insulin-signaling cascade, both at the intracellular abundance and at the activation levels. No change was evidenced in either insulin receptor, IRS1 or IRS2 protein

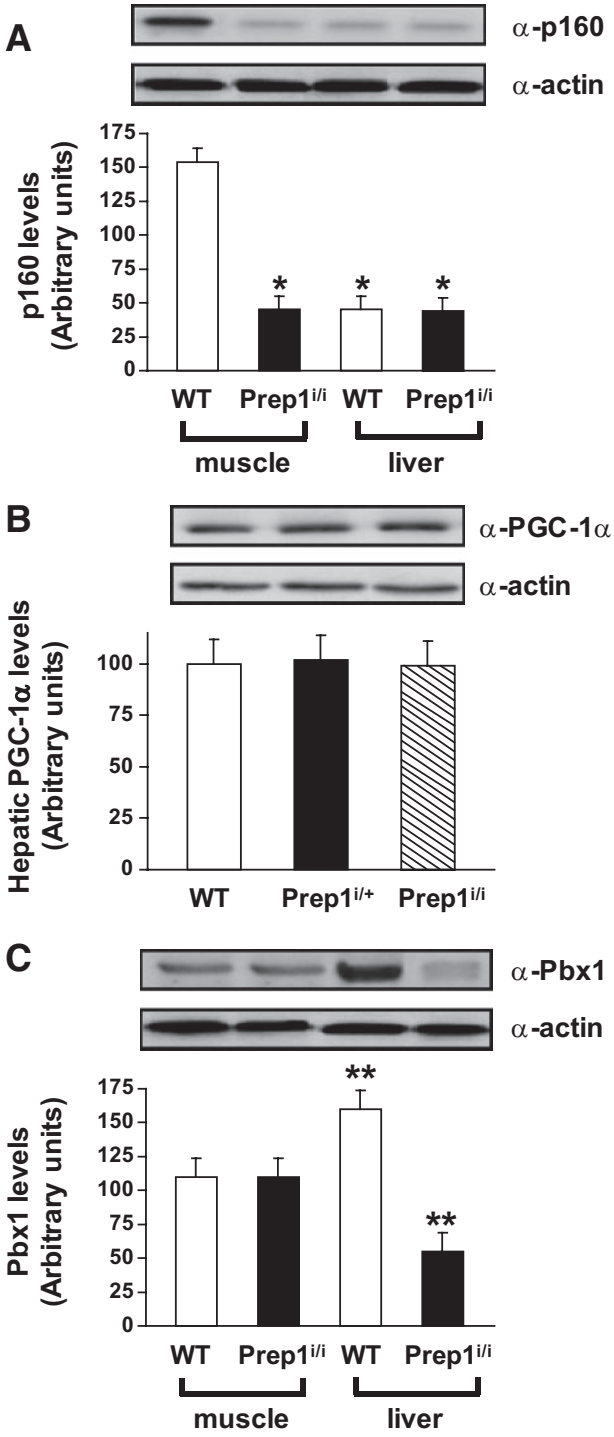

FIG. 2. P160, PGC-1α, and Pbx1 levels in muscle and liver of the WT or *Prep1*-hypomorphic mice. Tisues from *Prep1* hypomorphic and control mice were dissected, solubilized, and 100-μg protein samples analyzed by Western blot with p160 (*A*), PGC-1α (*B*), or Pbx1(*C*) antibodies. Actin antibodies were used for normalization. Blots were revealed by ECL and autoradiographs subjected to densitometric analysis. Each autoradiograph shown on the top of the graphics is representative of four independent experiments. Bars represent the mean ± SD of duplicate determinations in 10 mice per group. Asterisks denote statistically significant differences (P* < 0.05; ***P* < 0.01).**

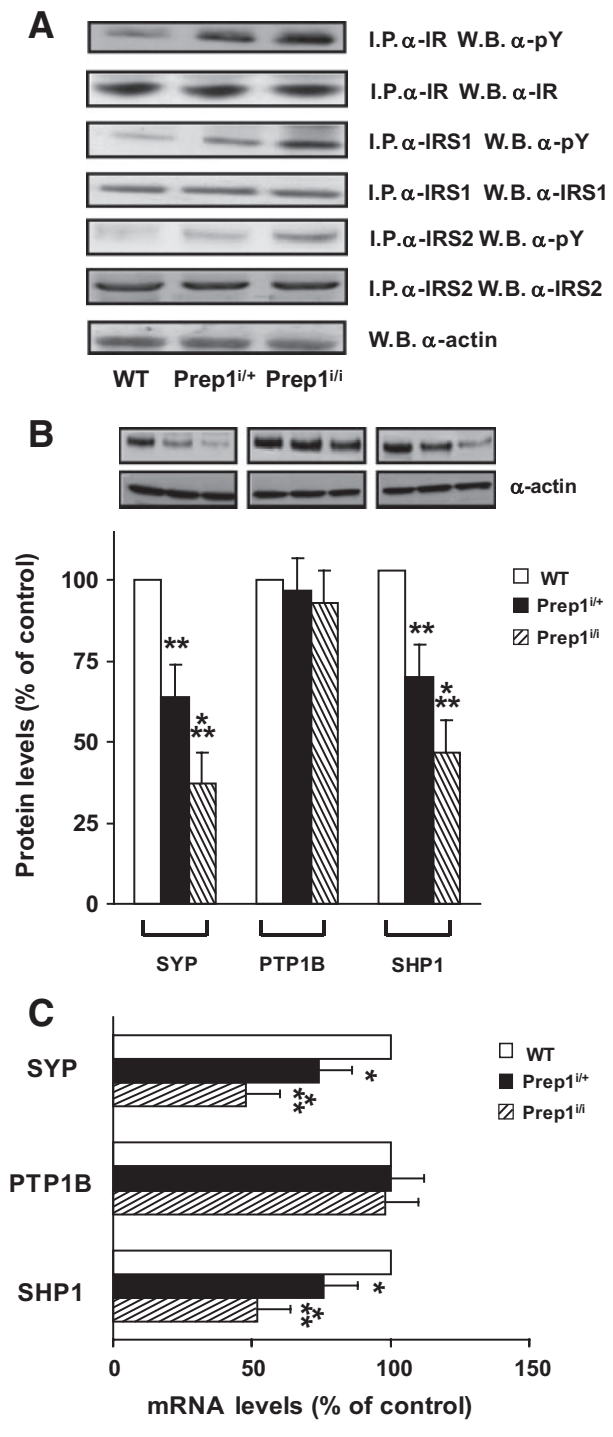

FIG. 3. Insulin signaling in liver of *Prep1*-hypomorphic mice. *A*: Protein lysates (250 μg) from liver of WT and *Prep1*-hypomorphic mice were immunoprecipitated with IR, IRS1 or IRS2 antibodies followed by blotting with pY, IR, IRS1, or IRS2 antibodies. Actin antibodies were used for the normalization. *B*: SYP, PTP1B, and SHP1 protein abundance was measured by Western blot on hepatic tissues from hypomorphic and control mice using specific antibodies. Actin antibodies were used for the normalization. All blots were revealed by ECL and subjected to autoradiography. The autoradiographs shown are representative of three (*A*) and four (*B*) independent experiments. Each bar in panel *B* represents the mean ± SD of duplicate determinations in 10 mice per group. *C*: The abundance of the indicated mRNA was determined by real-time RT-PCR analysis of total RNA isolated from the liver of hypomorphic and control mice, using *β-actin* as internal standard. Bar represents the mean ± SD of four independent experiments, in each of which reactions were performed in triplicate using the pooled total RNAs obtained from six mice per genotype. Asterisks denote statistically significant differences (P* < 0.05; ***P* < 0.01; ****P* < 0.001).**

levels (Fig. 3*A*). However, tyrosine phosphorylation of all of these proteins was significantly and gene dosage-dependently increased in the hypomorphic mice. These changes were accompanied by no change in the amount as well as the phosphorylation of known negative regulators of the

insulin receptor kinase, including PKCα and -δ, ERK1/2, JNK, and GRB10 (data not shown). Interestingly, protein levels of the tyrosine phosphatases SYP and SHP1 were reduced, respectively, by threefold and twofold in the $Prep1^{i/i}$ mouse livers (Fig. 3*B*; $P < 0.001$) and more moderately in the $Prep1^{i/+}$ mice. This reduction seemed at least in part transcriptional as it was observed also at the mRNA level and was specific for the two phosphatases (Fig. 3*C*). Indeed, PTP1B tyrosine phosphatase levels showed no difference in the hypomorphic mice and in their nontransgenic littermates. Activation of the downstream insulin pathway was also observed, with increased phosphorylation of both AKT and Foxo1 (data not shown).

Prep1 regulates insulin action in HepG2 cells. We have transiently transfected a *Prep1* cDNA in the HepG2 hepatoma cells. As shown in Fig. 4*A*, *Prep1* overexpression almost completely prevented insulin-induced tyrosine phosphorylation of the insulin receptor, IRS1 and IRS2. No change was evidenced in the abundance of any of these proteins. However, *Prep1* transfection upregulated *SYP* and *SHP1* expression at both the mRNA and the protein levels, but had no effect on *PTP1B* (Fig. 4*B*).

Prep1 transfection upregulated Pbx1 levels in the HepG2 cells (Fig. 4*A*). Interestingly, transfection of the $Prep1_{HR1}$ mutant cDNA, which is unable to bind Pbx1 (12), had no effect on either the phosphorylation of insulin receptor, IRS1 and IRS2 or the levels of SYP and SHP1 tyrosine phosphatase (Fig. 4*B*). This indicates that the Prep1-Pbx1 dimer controls insulin action in liver cells.

Consistent with this hypothesis, overexpression of a *Pbx1* cDNA in HepG2 cells mimicked Prep1 effects on insulin-stimulated tyrosine phosphorylation of the insulin receptor and IRS-1/2 (Fig. 5*A*), as well as on the level of SYP and SHP1 (Fig. 5*B*). At variance, liver cell overexpression of the other major Prep1 partner, *p160*, elicited no effect on these early steps in the insulin signaling cascade (Fig. 5*C*). Importantly, transfection of the *Prep1* or *Pbx1* cDNAs, but not that of the $Prep1_{HR1}$ mutant, abolished insulin-induced glycogen accumulation in the HepG2 cells (Fig. 5*D*). The failure of $Prep1_{HR1}$ to mimic Prep1 effects indicated that Prep1 action is exerted via dimerization with Pbx1 rather than via p160.

SHP1 mediates the effect of Prep1 on insulin signaling. To explore the significance of SYP and SHP1 tyrosine phosphatases to Prep1 regulation of insulin signaling in liver, we have stable transfected a *Prep1* full-length cDNA in the HepG2 cells. Several clones were obtained, and three of those, expressing increasing levels of Prep1, were selected and further characterized (Fig. 6*A*). The $HepG2_{Prep1c}$ clone overexpressed Prep1 by fivefold and featured a fourfold and threefold increased cellular content of SYP and SHP1, respectively (Fig. 6*B*). SYP and SHP1 levels in the $HepG2_{Prep1a}$ and $HepG2_{Prep1b}$ cells directly paralleled the lower level of Prep1 overexpression in each clone (data not shown). Transient transfection of the $HepG2_{Prep1c}$ cells with phosphorothioate antisense oligonucleotides specific for SYP (SYP-AS) caused a >65% reduction in SYP levels but elicited almost no change in insulin-stimulated phosphorylation of the insulin receptor, suggesting no change in insulin action in these cells (Fig. 6*C*). At variance, treatment with *SHP1* antisense oligonucleotides (SHP1-AS) silenced SHP1 by only 50% but increased insulin receptor tyrosine phosphorylation by almost threefold (Fig. 6*D*). Indeed, the impaired insulin-dependent accumulation of glycogen observed in liver cells overexpressing Prep1 was unaffected by SYP silencing but was rescued by the SHP1 AS (Fig. 6*E*). Thus, the *SHP1* gene mediates Prep1 control on insulin signaling in the HepG2 hepatoma cells.

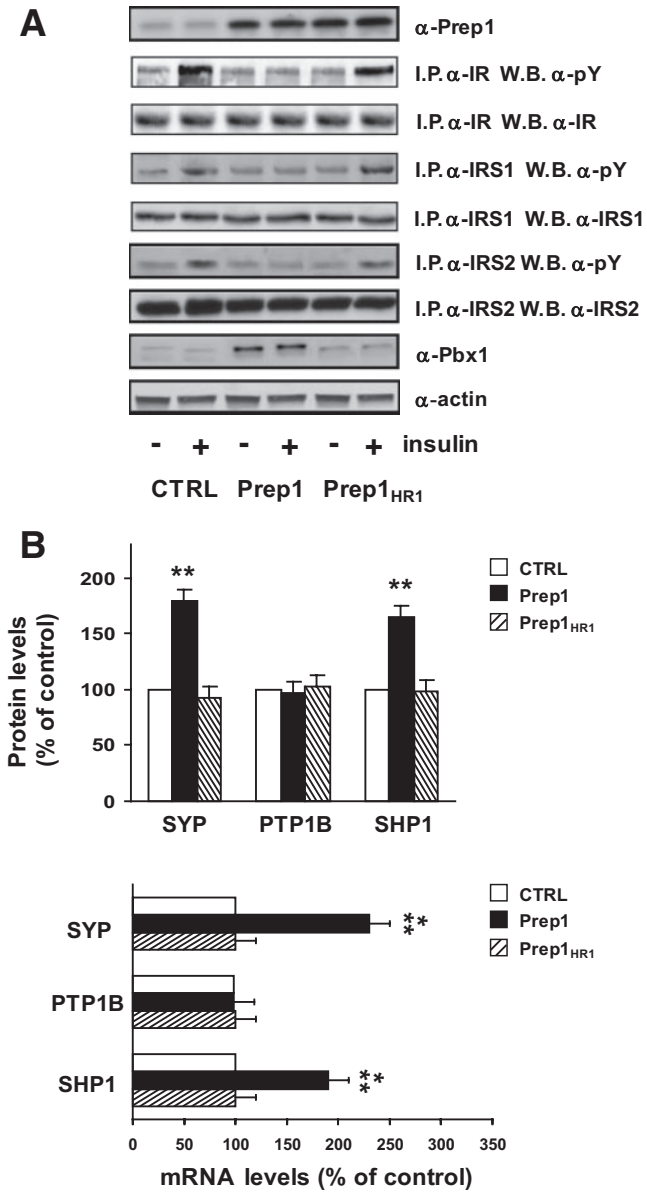

FIG. 4. Effect of the overexpression of *Prep1* and $Prep1_{HR1}$ mutant on insulin signaling in HepG2 cells. *A*: HepG2 cells were transiently transfected with the *Prep1* and $Prep1_{HR1}$ mutant and exposed to 100 nmol/l insulin for 5 min. Cells were then solubilized and lysates were immunoprecipitated with anti IR, IRS1, or IRS2 antibodies followed by blotting with pY, IR, and IRS1 or IRS2 antibodies. Actin antibodies were used for normalization. Bands were revealed by ECL and autoradiography. The autoradiograph shown is representative of five independent experiments. *B*: Lysates from HepG2 cells overexpressing *Prep1* or the $Prep1_{HR1}$ mutant were blotted with *SYP*, *PTP1B*, and *SHP1* antibodies, followed by ECL and densitometry. Each bar represents the mean ± SD of duplicate determinations in four independent experiments. The levels of *SYP*, *PTP1B*, and *SHP1* mRNAs in cells transfected with the *Prep1* and $Prep1_{HR1}$ mutant cDNAs was quantitated by real-time RT-PCR analysis, using *β actin* as internal standard. Bars represent the mean ± SD of four independent experiments. Asterisks denote statistically significant differences ($P < 0.01$; ***$P < 0.001$).**

Prep1 regulation of SHP1 gene transcription. We therefore examined the further possibility that Prep1 directly regulates *SHP1* gene function. Bioinformatic analysis revealed the presence of several potential binding

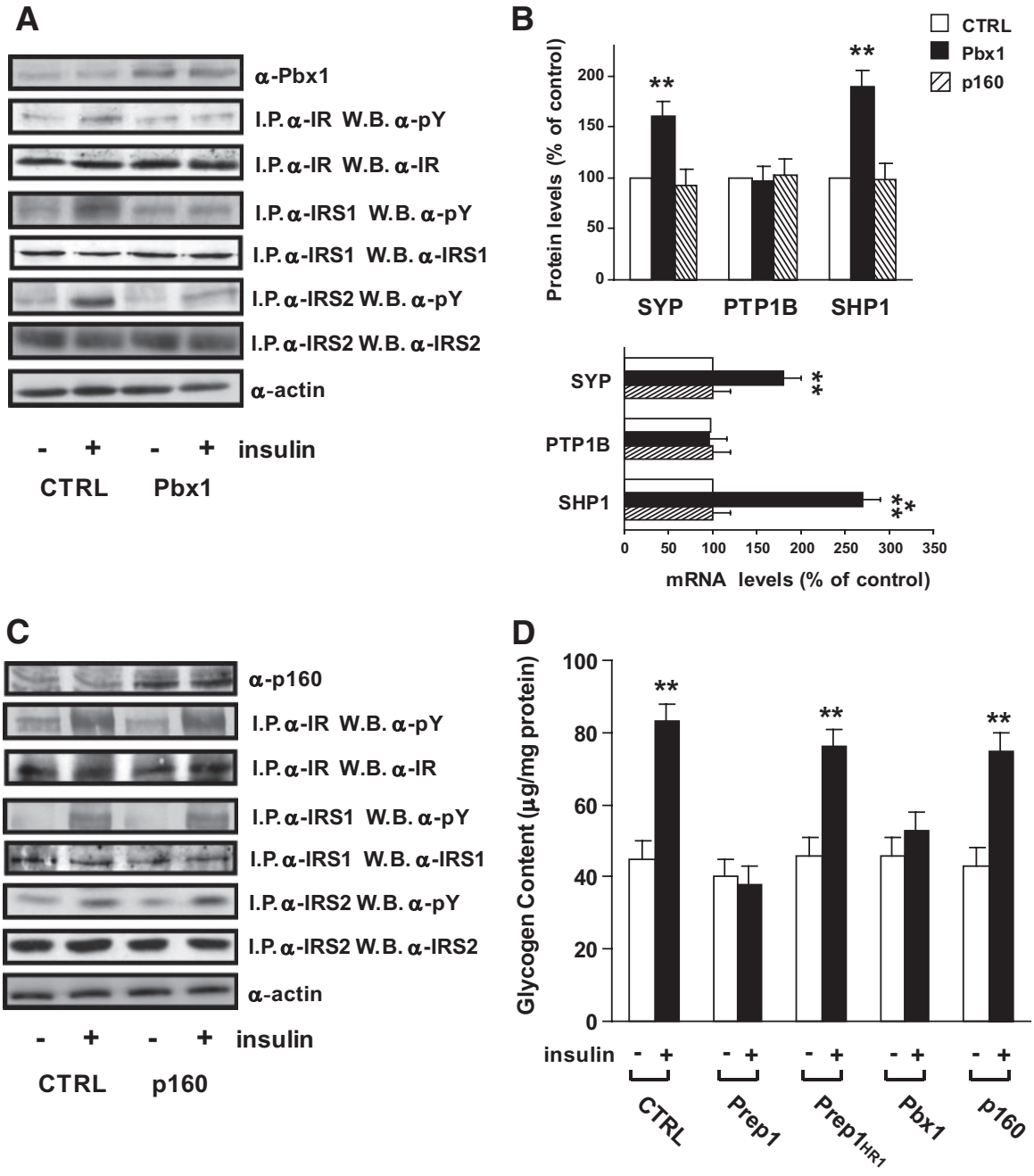

FIG. 5. Effect of *Pbx1* and *p160* overexpression on insulin signaling in HepG2 cells. HepG2 cells transiently overexpressing *Pbx1* (*A*) or *p160* (*C*) were treated with 100 nmol/l insulin for 5 min, lysed, immunoprecipitated with anti IR, IRS1, or IRS2 antibodies, and analyzed by Western blot with pY, IR, IRS1, or IRS2 antibodies. Identical aliquots of the lysates were also blotted with *Pbx1* (*A*) or *p160* (*C*) or actin antibodies (*A* and *C*). Bands were revealed by ECL and autoradiography. The autoradiograph shown is representative of five independent experiments. *B*: HepG2 cells were transiently transfected with *Pbx1 and p160*, and the lysates were blotted with *SYP*, *PTP1B*, and *SHP1* antibodies. Blots were revealed by ECL and autoradiography, and autoradiographs subjected to densitometry. Bars represent the mean ± SD of duplicate determinations in four independent experiments. The levels of *SYP*, *PTP1B*, and *SHP1* mRNAs in cells transfected with *p160* and *Pbx1* cDNAs were quantitated by real-time RT-PCR analysis, using *β actin* as internal standard. Bars represent the mean ± SD of four independent experiments. *D*: HepG2 cells transfected with the *Prep1*, *Prep1*$_{HR1}$ mutant, *p160*, and *Pbx1* cDNAs or with the empty vector (control [CTRL]) were exposed to 100 nmol/l insulin, and glycogen content was assayed as described in RESEARCH DESIGN AND METHODS. Bars represent mean values ± SD of determinations in four independent experiments, each in duplicate. Asterisks denote statistically significant differences (*P* < 0.01; ****P* < 0.001).**

sites for both Prep1 and Pbx1 in the 4,000 base pair region upstream the *SHP1* transcription initiation site. By ChIP, two of these sites bound Prep1 (Fig. 7*A*; positions nucleotide [nt] −2,489 to −2,139, nt −2,113 to −1,778), but re-ChIP assays revealed that Pbx1 was simultaneously present only at position nt −2,113 to −1,778. To investigate whether this last region features enhancer activity, we subsequently cloned this fragment in the *pgl3* basic construct upstream the luciferase gene (*pgl3*$_{LUC}$). The construct was then cotransfected in HeLa cells together with the *Prep1*, *Pbx1* cDNAs or both and luciferase activity was measured (Fig. 7*B*). Prep1 and Pbx1 increased the *SHP1* reporter activity, respectively, by 7.1-fold and 6-fold. Simultaneous cotransfection of the two plasmids

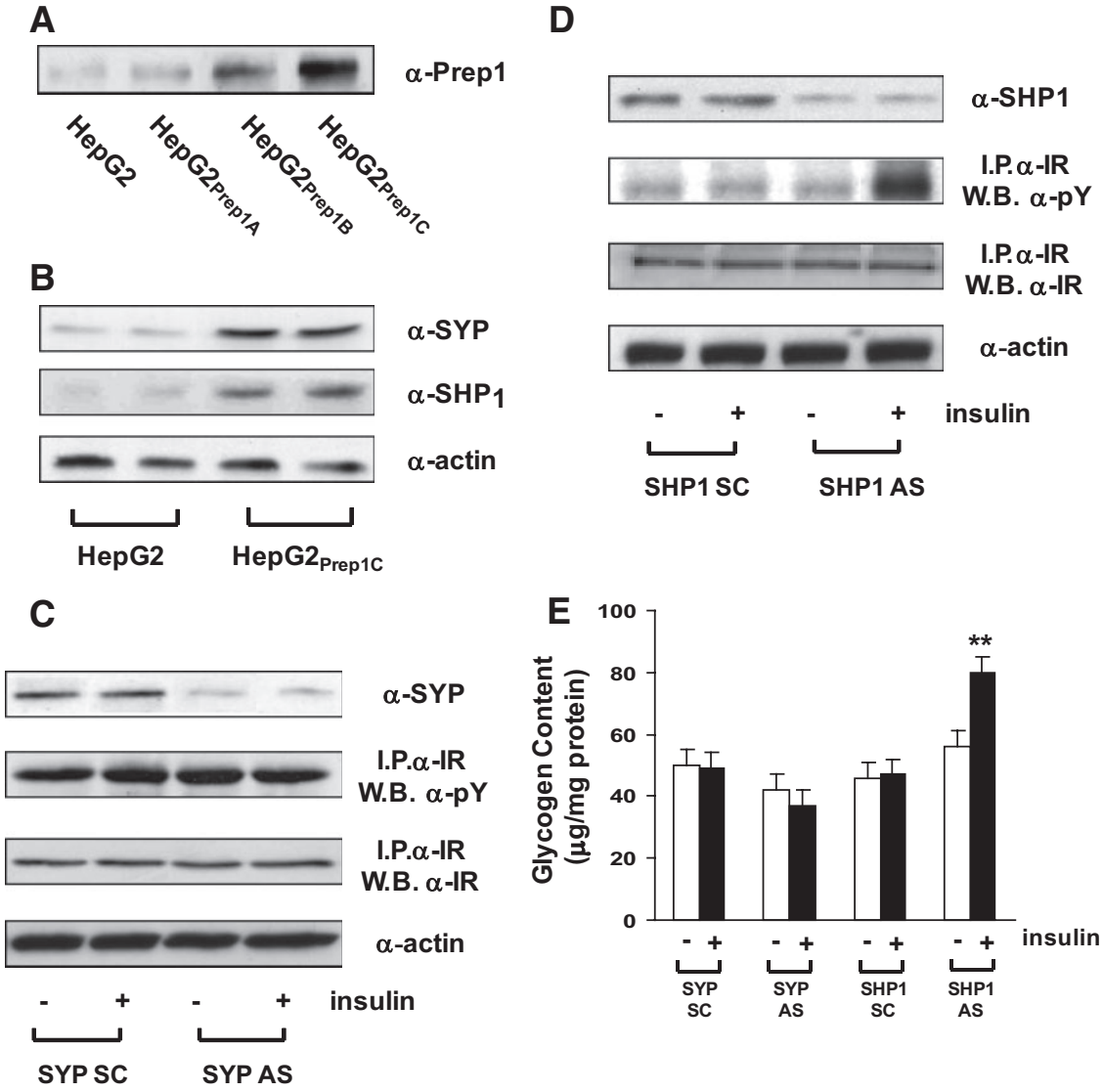

FIG. 6. Effect of *SYP* and *SHP1* antisense oligonucleotides on insulin signaling in HepG2 cells stable transfected with *Prep1*. *A*: HepG2 cells were stable transfected with a *Prep1* cDNA, as described under RESEARCH DESIGN AND METHODS. Clones of cells expressing varying levels of *Prep1* ($HepG2_{Prep1A}$, $HepG2_{Prep1B}$, $HepG2_{Prep1C}$) and the untransfected cells (HepG2) were analyzed by immunoblotting with Prep1 antibodies and autoradiography. *B*: Lysates from HepG2or $HepG2_{Prep1c}$ cells were analyzed by immunoblotting with *SYP*, *SHP1* or actin antibodies followed by ECL and autoradiography. *C* and *D*: HepG2or $HepG2_{Prep1c}$ cells were transfected with *SYP* (SYP-AS) (*C*) or *SHP1* (SHP1-AS) (*D*) specific phosphorothioate antisense oligonucleotides, stimulated with 100 nmol/l insulin for 5 min and immunoprecipitated with insulin receptor antibodies followed by blotting with either pY or IR antibodies. For control, identical aliquots of the lysates were also blotted with *SYP*, *SHP1*, or actin antibodies. Bands were revealed by ECL and autoradiography as reported under RESEARCH DESIGN AND METHODS. The autoradiographs shown are representative of four independent experiments. *E*: The $HepG2_{Prep1c}$ cells were transfected with SYP-AS and the SHP1-AS and further stimulated with 100 nmol/l insulin for 5 min. Glycogen content was then assayed as described under RESEARCH DESIGN AND METHODS. Bars represent mean values ± SD of determinations in four independent experiments, each in duplicate. Asterisks denote statistically significant differences ($P < 0.01$).**

caused an almost 30-fold induction, indicating *SHP1* transcriptional regulation by the Prep1/Pbx1 complex.

DISCUSSION

Previous studies have identified *Prep1* as a physiologic regulator of insulin-mediated glucose metabolism in skeletal muscle (13). In *Prep1*-deficient mice, muscle sensitivity to insulin action on glucose disposal is significantly increased, due to downregulation of the major Prep1 partner p160 and induction of the *GLUT4* gene activator PGC-1 α (13). In the present paper, we show that in high-fat diet-treated or *db/db* mice, hepatic Prep1 levels are increased, suggesting a role of Prep1 in controlling insulin sensitivity and glucose metabolism in this organ as well. Indeed, Prep1-deficient mice showed increased hepatic glycogen content and decreased glucose output and triglyceride levels. Hypoinsulinemia, which represents a prominent feature of the *Prep1*-deficient mice (13), is likely essential to enable these animals to maintain plasma glucose levels only slightly below those of their nonhypomorphyc littermates. The mechanisms responsible for Prep1 action in liver differ from those in the skeletal muscle, however. First, at variance with muscle, Prep1 major functional partner in liver appears to be Pbx1 rather than p160. We have shown that in this organ, Prep1 expression determines Pbx1 levels as *Prep1*-hypomorphic mice exhibit a very significant reduction of liver Pbx1. Importantly, Pbx1 mimics Prep1 action on glycogen con-

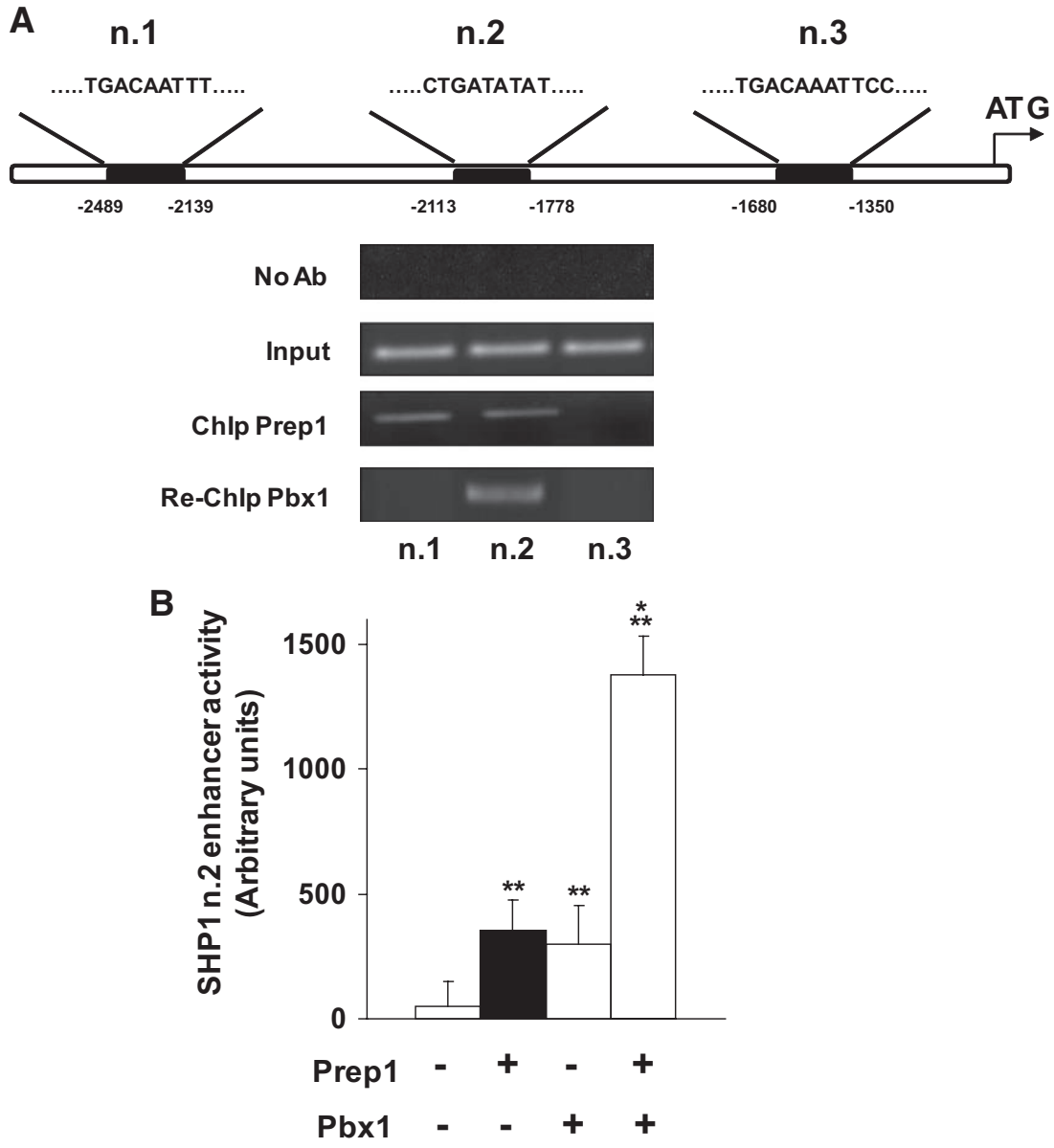

FIG. 7. ***Prep1/Pbx1*** **binding to the** ***SHP1*** **DNA sequences and regulation of** ***SHP1*** **reporter gene activity.** ***A*****: Schematic representation of 5′ sequences upstream the putative** ***SHP1*** **transcription start site including the potential binding sites for** ***Prep1*** **and** ***Pbx1*****. Soluble chromatin was prepared from NMuLi mouse liver cells and immunoprecipitated with Prep1 antibodies. Total (input) and immunoprecipitated DNAs were amplified using primer pairs covering the indicated** ***SHP1*** **fragments. Re-ChIP assay with Pbx1 antibodies was performed as described under RESEARCH DESIGN AND METHODS.** ***B*****: HeLa cells were transfected with 2 μg of the** ***SHP1*****-enhancer luciferase construct alone or in combination with** ***Prep1*****,** ***Pbx1*****, or both the cDNA plasmids. Luciferase activity was assayed and normalized as described in RESEARCH DESIGN AND METHODS. Bars represent mean values ± SD of determinations in four independent experiments. Asterisks denote statistically significant differences (*****P*** **< 0.01; ******P*** **< 0.001).**

tent in hepatocytes, whereas p160, which is expressed at very low levels in this cell type and is not regulated by Prep1, does not. Second, Prep1 does not induce repression of PGC-1α levels in the liver cells. Indeed, the repression of PGC-1α occurring in skeletal muscle is achieved by Prep1 increase in p160 half-life which directly represses PGC-1α (13). Foxo1 nuclear localization is a major event determining PGC-1α induction of the key gluconeogenetic genes G6Pase and PEPCK (17). In *Prep1*-hypomorphic mice, Akt as well as Foxo1 phosphorylation is increased, indicating induced nuclear export (data not shown). We suggest that the reduced nuclear abundance of Foxo1 may, at least in part, explain how the upregulated insulin signaling observed in $Prep1^{i/i}$ mice downregulates G6Pase and PEPCK gene transcription in the presence of unaltered PGC-1α levels.

Analysis of the initial steps in insulin signaling in the *Prep1*-deficient mouse liver revealed increased tyrosine phosphorylation of both insulin receptor and the major IRSs present in these cells. Interestingly, although no change in the intracellular levels of these proteins was detected, the levels of both the SYP and SHP1 tyrosine phosphatases were found significantly decreased in *Prep1*-hypomorphic mouse liver and underwent opposite changes in cultured liver cells transiently transfected with a *Prep1* cDNA. Previously published data from gene knockout and transgenic overexpression models have identified an important role of phosphotyrosine phospha-

tases in the regulation of insulin sensitivity and glucose homeostasis in vivo (19,20,22). The PTP1B phosphotyrosine phosphatase has received particular attention as genetic and biochemical findings indicate a key inhibitory role for PTP1B in modulating insulin signaling (29,30). However, PTP1B levels were unaffected both in liver tissue from *Prep1*-deficient mice and in cells overexpressing *Prep1*, indicating specificity in Prep1 control of phosphotyrosine phosphatase. More recent studies in *SHP1*-deficient mice have shown an important role for SHP1 in the modulation of insulin sensitivity and glucose metabolism at the whole-body as well as liver levels (31). In this study, the functional relevance of Prep1 control of SHP1 versus SYP expression to hepatic sensitivity to insulin was assessed in further experiments in HepG2 liver cells stable transfected with *Prep1*. These cells feature a very significant reduction of insulin effect on glycogen accumulation. However, antisense silencing of *SHP1*, though not of *SYP*, rescued insulin effect in these cells, thus establishing SHP1 as the functionally relevant target of Prep1 in the liver. Previous in vitro and in vivo studies of SHP1 function have identified the insulin receptor as the primary target of SHP1 action in the upstream insulin signaling cascade (31,32). Based on this information, we propose that enhanced insulin action in the liver of *Prep1*-deficient mice results from reduced SHP1-insulin receptor binding and attenuated dephosphorylation with secondary activation of the IRS system.

SHP1 downregulation in liver tissue from the *Prep1*-hypomorphic mice occurred both at the protein and at the mRNA levels, raising the possibility that Prep1 acts, at least in part, by regulating *SHP1* gene expression. Indeed, we show that the regulatory region of *SHP1* gene contains several Prep1 binding sites in the 4,000 base-pair region upstream *SHP1* transcription initiation site and one Prep1/Pbx1 binding site responding to the ectopic expression of Prep1 and Pbx1 in cotransfection experiments in vitro. In these assays, a fragment containing single Prep1/Pbx1 binding site displays a powerful enhancer function. In addition, ChIp experiments with Prep1 and Pbx1 antibodies showed that these proteins bind the *SHP1* regulatory region, suggesting that *SHP1* gene is a target of the Prep1/Pbx1 complex and not just Prep1. However, since Pbx1 increases the nuclear localization of Prep1 (7,8), it is also possible that the forced expression of Pbx1 causes the nuclear accumulation of Prep1, thereby enhancing its transcriptional effect on SHP1.

At variance with the liver, in muscle cells, the prevalent association of Prep1 with p160, rather than with Pbx1, may account for the lack of significant SHP1 upregulation by Prep1 (data not shown) and the reported lower abundance of SHP1, particularly in the nuclear compartment of muscle cells (33,34). Thus, at least in part, different partners may account for the tissue specificity in Prep1 regulatory functions. Variation in Prep1 action in the major insulin-responsive tissues are likely relevant to the phenotype of *Prep1*-hypomorphic and are paralleled by the phenotype of *SHP1*-deficient mice. Both of these mice are markedly glucose tolerant and insulin sensitive, at both muscle and hepatic levels (31,13). In both mouse models, SHP1 downregulation causes improved insulin-dependent suppression of hepatic glucose output. However, the enhanced peripheral (muscle) sensitivity to insulin in the *SHP1*-deficient mice is further contributed by p160 repression in the *Prep1*-hypomorphic mouse muscles (13).

In conclusion, we have identified the SHP1 tyrosine phosphatase, a known negative regulator of insulin signaling, as a novel transcriptional target of Prep1. In the liver, Prep1 silencing enhances insulin signaling, thereby increasing glucose storage and reducing glucose output. This effect might be further amplified by the reduction in glucagon levels which also occurs in *Prep1* hypomorphic mice (13). Indeed, these mice feature a slower recovery from insulin-induced hypoglycemia when compared with their nonhypomorphic littermates, and they appear to continue to accumulate glycogen (13). The findings reported in the present paper might have clinical relevance as preliminary evidence in our laboratory indicates that *Prep1* gene is overexpressed in euglycemic offspring of type 2 diabetic individuals. These subjects have a very high risk of diabetes (35) and are known to be insulin resistant, suggesting that Prep1 overexpression may provide an early contribution to diabetes progression in these individuals. Whether and how genetic variability at the *Prep1* locus affects glucose tolerance in humans is an important issue that deserves to be investigated in detail.

ACKNOWLEDGMENTS

This work was supported by the European Foundation for the Study of Diabetes, the European Community's PREPOBEDIA (201681), grants from the Associazione Italiana per la Ricerca sul Cancro (AIRC), and from the Ministero dell'Università e della Ricerca Scientifica (PRIN and Fondo pergli Investimenti della Ricerca di Base: RBIP0689BS). The financial support of Telethon, Italy, to F.Be. and F.Bl. is also gratefully acknowledged.

No potential conflicts of interest relevant to this article were reported.

F.O. and S.I. generated data, discussion, and manuscript writing. S.C., A.C., and E.L. researched data, performed experimental work, and contributed to discussion. C.M., P.U., P.F., and F.Bl. contributed to critical discussion and experimental planning. F.Be. directed and planned research.

The authors thank Dr. Silvana Obici, Dr. Paulo Martins and Michael Haas (Metabolic Diseases Institute, Division of Endocrinology, Department of Internal Medicine, University of Cincinnati, Cincinnati, OH) for their advice regarding euglycemic hyperinsulinemic clamps.

REFERENCES

1. Moens CB, Selleri L. Hox cofactors in vertebrate development. Dev Biol 2006;291:193–206
2. Berthelsen J, Zappavigna V, Ferretti E, Mavilio F, Blasi F. The novel homeoprotein Prep1 modulates Pbx-Hox protein cooperativity. EMBO J 1998;17:1434–1445
3. Calvo KR, Knoepfler P, McGrath S, Kamps MP. An inhibitory switch derepressed by pbx, hox, and Meis/Prep1 partners regulates DNA-binding by pbx1 and E2a-pbx1 and is dispensable for myeloid immortalization by E2a-pbx1. Oncogene 1999;18:8033–8043
4. Knoepfler PS, Calvo KR, Chen H, Antonarakis SE, Kamps MP. Meis1 and pKnox1 bind DNA cooperatively with Pbx1 utilizing an interaction surface disrupted in oncoprotein E2a-Pbx1. Proc Natl Acad Sci U S A 1997;94:14553–14558
5. Pai CY, Kuo TS, Jaw TJ, Kurant E, Chen CT, Bessarab DA, Salzberg A, Sun YH. The Homothorax homeoprotein activates the nuclear localization of another homeoprotein, extradenticle, and suppresses eye development in Drosophila. Genes Dev 1998;12:435–446
6. Rieckhof GE, Casares F, Ryoo HD, Abu-Shaar M, Mann RS. Nuclear translocation of extradenticle requires homothorax, which encodes an extradenticle-related homeodomain protein. Cell 1997;91:171–183
7. Berthelsen J, Kilstrup-Nielsen C, Blasi F, Mavilio F, Zappavigna V. The subcellular localization of PBX1 and EXD proteins depends on nuclear

import and export signals and is modulated by association with PREP1 and HTH. Genes Dev 1999;13:946–953
8. Jaw TJ, You LR, Knoepfler PS, Yao LC, Pai CY, Tang CY, Chang LP, Berthelsen J, Blasi F, Kamps MP, Sun YH. Direct interaction of two homeoproteins, homothorax and extradenticle, is essential for EXD nuclear localization and function. Mech Dev 2000;91:279–291
9. Deflorian G, Tiso N, Ferretti E, Meyer D, Blasi F, Bortolussi M, Argenton F. Prep1.1 has essential genetic functions in hindbrain development and cranial neural crest cell differentiation. Development 2004;131:613–627
10. Ferretti E, Villaescusa JC, Di Rosa P, Fernandez-Diaz LC, Longobardi E, Mazzieri R, Miccio A, Micali N, Selleri L, Ferrari G, Blasi F. Hypomorphic mutation of the TALE gene Prep1 (pKnox1) causes a major reduction of Pbx and Meis proteins and a pleiotropic embryonic phenotype. Mol Cell Biol 2006;26:5650–5062
11. Penkov D, Di Rosa P, Fernandez Diaz L, Basso V, Ferretti E, Grassi F, Mondino A, Blasi F. Involvement of Prep1 in the αβ T-cell receptor T-lymphocytic potential of hematopoietic precursors. Mol Cell Biol 2005; 25:10768–10781
12. Díaz VM, Mori S, Longobardi E, Menendez G, Ferrai C, Keough RA, Bachi A, Blasi F. p160 Myb-binding protein interacts with Prep1 and inhibits its transcriptional activity. Mol Cell Biol 2007;27:7981–7990
13. Oriente F, Fernandez Diaz LC, Miele C, Iovino S, Mori S, Diaz VM, Troncone G, Cassese A, Formisano P, Blasi F, Beguinot F. Prep1 deficiency induces protection from diabetes and increased insulin sensitivity through a p160-mediated mechanism. Mol Cell Biol 2008;28: 5634–5645
14. Barthel A, Schmoll D. Novel concepts in insulin regulation of hepatic gluconeogenesis. Am J Physiol Endocrinol Metab 2003;285:E685–E692
15. Herzig S, Long F, Jhala US, Hedrick S, Quinn R, Bauer A, Rudolph D, Schutz G, Yoon C, Puigserver P, Spiegelman B, Montminy M. CREB regulates hepatic gluconeogenesis through the coactivator PGC-1. Nature 2001;413:179–183
16. Yoon JC, Puigserver P, Chen G, Donovan J, Wu Z, Rhee J, Adelmant G, Stafford J, Kahn CR, Granner DK, Newgard CB, Spiegelman BM. Control of hepatic gluconeogenesis through the transcriptional coactivator PGC-1. Nature 2001;413:131–138
17. Puigserver P, Rhee J, Donovan J, Walkey CJ, Yoon JC, Oriente F, Kitamura Y, Altomonte J, Dong H, Accili D, Spiegelman BM. Insulin-regulated hepatic gluconeogenesis through FOXO1-PGC 1 α interaction. Nature 2003;423:550–555
18. Zabolotny JM, Haj FG, Kim YB, Kim HJ, Shulman GI, Kim JK, Neel BG, Kahn BB. Transgenic overexpression of protein-tyrosine phosphatase 1B in muscle causes insulin resistance, but overexpression with leukocyte antigen-related phosphatase does not additively impair insulin action. J Biol Chem 2004;279:24844–24851
19. Elchebly M, Payette P, Michaliszyn E, Cromlish W, Collins S, Loy AL, Normandin D, Cheng A, Himms-Hagen J, Chan CC, Ramachandran C, Gresser MJ, Tremblay ML, Kennedy BP. Increased insulin sensitivity and obesity resistance in mice lacking the protein tyrosine phosphatase-1B gene. Science 1999;283:1544–1548
20. Klaman LD, Boss O, Peroni OD, Kim JK, Martino JL, Zabolotny JM, Moghal N, Lubkin M, Kim YB, Sharpe AH, Stricker-Krongrad A, Shulman GI, Neel BG, Kahn BB. Increased energy expenditure, decreased adiposity, and tissue-specific insulin sensitivity in protein-tyrosine phosphatase 1B-deficient mice. Mol Cell Biol 2000;20:5479–5489
21. Yamauchi K, Milarski KL, Saltiel AR, Pessin JE. Protein-tyrosine-phosphatase SHPTP2 is a required positive effector for insulin downstream signaling. Proc Natl Acad Sci U S A 1995;92:664–668
22. Maegawa H, Hasegawa M, Sugai S, Obata T, Ugi S, Morino K, Egawa K, Fujita T, Sakamoto T, Nishio Y, Kojima H, Haneda M, Yasuda H, Kikkawa R, Kashiwagi A. Expression of a dominant negative SHP-2 in transgenic mice induces insulin resistance. J Biol Chem 1999;274: 30236–30243
23. Vigliotta G, Miele C, Santopietro S, Portella G, Perfetti A, Maitan MA, Cassese A, Oriente F, Trencia A, Fiory F, Romano C, Tiveron C, Tatangelo L, Troncone G, Formisano P, Beguinot F. Overexpression of the ped/pea-15 gene causes diabetes by impairing glucose-stimulated insulin secretion in addition to insulin action. Mol Cell Biol 2004;24:5005–5015
24. Wang Y, Torres-Gonzalez M, Tripathy S, Botolin D, Christian B, Jump DB. Elevated hepatic fatty acid elongase-5 activity affects multiple pathways controlling hepatic lipid and carbohydrate composition. J Lipid Res 2008;49:1538–1552
25. Singh V, Grötzinger C, Nowak KW, Zacharias S, Göncz E, Pless G, Sauer IM, Eichhorn I, Pfeiffer-Guglielmi B, Hamprecht B, Wiedenmann B, Plöckinger U, Strowski MZ. Somatostatin receptor subtype-2-deficient mice with diet-induced obesity have hyperglycemia, nonfasting hyperglucagonemia, and decreased hepatic glycogen deposition. Endocrinology 2007;148:3887–3899
26. Miele C, Caruso M, Calleja V, Auricchio R, Oriente F, Formisano P, Condorelli G, Cafieri A, Sawka-Verhelle D, Van Obberghen E, Beguinot F. Differential role of insulin receptor substrate (IRS)-1 and IRS-2 in L6 skeletal muscle cells expressing the Arg1152 –> Gln insulin receptor. J Biol Chem 1999;274:3094–3102
27. Ungaro P, Teperino R, Mirra P, Cassese A, Fiory F, Perruolo G, Miele C, Laakso M, Formisano P, Beguinot F. Molecular cloning and characterization of the human PED/PEA-15 gene promoter reveal antagonistic regulation by hepatocyte nuclear factor 4α and chicken ovalbumin upstream promoter transcription factor II. J Biol Chem 2008;283:30970–30979
28. Buettner C, Patel R, Muse ED, Bhanot S, Monia BP, McKay R, Obici S, Rossetti L. Severe impairment in liver insulin signaling fails to alter hepatic insulin action in conscious mice. J Clin Invest 2005;115:1306–1313
29. Goldstein BJ. Protein-tyrosine phosphatases: emerging targets for therapeutic intervention in type 2 diabetes and related states of insulin resistance. J Clin Endocrinol Metab 2002;87:2474–2480
30. Asante-Appiah E, Kennedy BP. Protein tyrosine phosphatases: the quest for negative regulators of insulin action. Am J Physiol Endocrinol Metab 2003;284:E663–E670
31. Dubois MJ, Bergeron S, Kim HJ, Dombrowski L, Perreault M, Fournès B, Faure R, Olivier M, Beauchemin N, Shulman GI, Siminovitch KA, Kim JK, Marette A. The SHP-1 protein tyrosine phosphatase negatively modulates glucose homeostasis. Nat Med 2006;12:549–556
32. Bousquet C, Delesque N, Lopez F, Saint-Laurent N, Estève JP, Bedecs K, Buscail L, Vaysse N, Susini C. sst2 somatostatin receptor mediates negative regulation of insulin receptor signaling through the tyrosine phosphatase SHP-1. J Biol Chem 1998;273:7099–7106
33. Tenev T, Böhmer SA, Kaufmann R, Frese S, Bittorf T, Beckers T, Böhmer FD. Perinuclear localization of the protein-tyrosine phosphatase SHP-1 and inhibition of epidermal growth factor-stimulated STAT1/3 activation in A431 cells. Eur J Cell Biol 2000;79:261–271
34. Duchesne C, Charland S, Asselin C, Nahmias C, Rivard N. Negative regulation of β-catenin signaling by tyrosine phosphatase SHP-1 in intestinal epithelial cells. J Biol Chem 2003;278:14274–14283
35. Laakso M, Zilinskaite J, Hansen T, Boesgaard TW, Vänttinen M, Stancáková A, Jansson PA, Pellmé F, Holst JJ, Kuulasmaa T, Hribal ML, Sesti G, Stefan N, Fritsche A, Häring H, Pedersen O, Smith U; EUGENE2 Consortium. Insulin sensitivity, insulin release and glucagon-like peptide-1 levels in persons with impaired fasting glucose and/or impaired glucose tolerance in the EUGENE2 study. Diabetologia 2008;51:502–511

PED/PEA-15 induces autophagy and mediates TGF-beta1 effect on muscle cell differentiation.

Salvatore Iovino[1], Francesco Oriente[1], Ginevra Botta[1], Serena Cabaro[1], Valentina Iovane[2], Orlando Paciello[2], Davide Viggiano[3], Giuseppe Perruolo[1], Pietro Formisano[1], Francesco Beguinot[1].

[1]Department of Cellular and Molecular Biology and Pathology & Institute of Sperimental Oncology and Endocrinology, University of Naples Federico II, via Sergio Pansini, 5, 80131 Naples, Italy.

[2]Department of Pathology and Animal Health, University of Naples Federico II, via Delpino, 1, 80137 Naples, Italy.

[3]Department of Health Sciences, University of Molise, Campobasso, 86100, Italy.

Running title: **PED/PEA-15 and skeletal muscle differentiation.**

Keywords: Skeletal muscle differentiation, TGF-beta1, PED/PEA-15, autophagy.

Corresponding author: Francesco Beguinot, MD, PhD, Department of Cellular and Molecular Biology and Pathology, "Federico II" University of Naples, Via Pansini 5, 80131 Naples, Italy
Phone: +39 081 7463248; Fax: +39 0817463235; email: beguino@unina.it

Word count (Abstract): 199
Word count (Main text): 2577
Number of figures: 9

ABSTRACT

TGF-beta1 has been shown to induce autophagy in certain cells but whether and how this action is exerted in muscle and whether this activity relates to TGF-beta1 control of muscle cell differentiation remains unknown. Here we show that expression of the autophagy-promoting protein PED/PEA-15 progressively declines during L6 and C2C12 skeletal muscle cell differentiation. *PED/PEA-15* underwent rapid induction upon TGF-beta1 exposure of L6 and C2C12 myoblasts, accompanied by impaired differentiation into mature myotubes. TGF-beta1 also induced autophagy in the L6 and C2C12 cells through a PP2A/FoxO1-mediated mechanism. Both the TGF-beta1 effect on differentiation and that on autophagy were blocked by specific *PED/PEA-15* ShRNAs. Myoblasts stably overexpressing PED/PEA-15 did not differentiate and showed markedly enhanced autophagy. In these same cells, the autophagy inhibitor 3-Methyladenine rescued TGF-beta1 effect on both autophagy and myogenesis, indicating that PED/PEA-15 mediates TGF-beta1 effects in muscle. Muscles from transgenic mice overexpressing *PED/PEA-15* featured a significant number of atrophic fibers, accompanied by increased LC3II to LC3I ratio and reduced PP2A/FoxO1 phosphorylation. Interestingly these mice showed significantly impaired locomotor activity compared to their non-transgenic littermates. TGF-beta1 causes transcriptional upregulation of the autophagy-promoting gene *PED/PEA-15*, which in turn is capable to induce atrophic responses in skeletal muscle *in vivo*.

INTRODUCTION

The superfamily of Transforming Growth Factor-beta (TGF-beta) cytokines are ubiquitously expressed and induce a wide variety of effects ultimately depending on the cell context and including regulation of cell growth, proliferation, differentiation, adhesion, migration and apoptosis (1-6). Also, different members of the TGF-beta superfamily, including the archetypal TGF-beta family member TGF-beta1, have been found to inhibit myogenic differentiation in primary cultures and in myoblast cell lines from different species (7-9). These findings have evoked considerable translational interest, as inhibitors of the TGF-beta signalling cascade are currently being targetted to reduce muscle wasting accompanying both acute metabolic derangements and chronic disorders such as cancer, congestive heart failure, sarcopenia, acquired immunodeficiency and long-lasting and poorly compensated diabetes mellitus (10).

In all of these catabolic conditions, protein breakdown is enhanced and exceeds protein synthesis, resulting in loss of muscle mass and myofiber atrophy. There is substantial evidence indicating that autophagic flux is increased during muscle atrophy due to up or down-regulation of different sets of genes designated atrogenes (11,12). These include genes encoding proteins that are degraded when autophagosomes fuse with lysosomes, such as the microtubule-associated protein 1 light chain 3 (LC3I). The latter is converted to LC3II during autophagy, so that the LC3II to LC3I ratio is often taken as representative of autophagy induction. However, whether autophagy itself causes muscle fiber degeneration remains a debated issue (13).

While TGF-beta1 has recently been shown to represent an important regulator of autophagy in liver and mammary cells (14), autophagy in the skeletal muscle is peculiar as compared to that occurring in other metabolically relevant tissues. During fasting, most tissues show a transient activation of autophagy. In contrast, skeletal muscle shows a persistent generation of autophagosomes that

continues for days (11), suggesting that different mechanisms control autophagosome formation during short or long periods of induced autophagy. Whether and how TGF-beta1 features autophagy promoting activity in muscle cells and whether this activity may lead to impaired myogenesis is unknown.

Phosphoprotein Enriched in Diabetes/Phosphoprotein Enriched in Astrocytes (PED/PEA-15) is a 15 KDa molecule which binds to different signalling proteins thereby regulating their function and several survival and metabolic transduction pathways (15,16). PED/PEA-15 cellular levels are controlled by both transcriptional and post-translational mechanisms (16) which have been shown to be dysregulated in human disorders including type 2 diabetes. Many type 2 diabetic individuals feature exagerated expression of *PED/PEA-15* (17,18), leading to impaired insulin action and secretion and, possibly, contributing to diabetes long-term complications (19). Quite recently, evidence has been reported indicating that PED/PEA-15 promotes autophagy in glioma cells through a JNK-dependent mechanism (20), rendering the cells resistant to starvation and other adverse stimuli. In the present work, we show that PED/PEA-15 autophagy-promoting action is necessary for enabling complete TGF-beta1 control of myogenesis.

RESULTS

Effect of PED/PEA-15 on L6 cell differentiation - Low serum exposure causes L6 and C2C12 skeletal muscle cells to spontaneously differentiate in culture with the generation of multinucleate myotubes (7-9, 21). As previously reported (7-9), the L6 and C2C12 myotube formation is accompanied by upregulation of a number of genes including *MyoD1*, *myogenin* and *GLUT4*. Unexpectedly however, these same gene profile studies revealed that expression of the autophagy regulator *PED/PEA-15* underwent progressive reduction both during L6 and C2C12 cell

differentiation (**Fig.1A, left panel**). Similar changes occurred in the case of PED/PEA-15 protein levels (**right panel**), raising the possibility that this multifunctional molecule exerts a previously unidentified physiological role in myogenesis. To test this hypothesis further, we have transfected L6 or C2C12 myoblasts with a *PED/PEA-15* cDNA, increasing PED/PEA-15 levels by approximately 10-fold (**Fig.1B, top panel**). We then compared differentiation in these cells and in cells transfected with the empty vector. As shown in **Fig.1B,C,** *PED/PEA-15* overexpression impaired myotube formation both in L6 and C2C12 and reduced activation of the myogenesis markers *MyoD1, myogenin and GLUT4* by > 2-fold in these cell types. At variance, the abundance of *GLUT1* mRNA was 3-fold higher in *PED/PEA-15*-transfected as compared to the control cells.

Role of PED/PEA-15 in TGF-beta1 action - To explore the role of *PED/PEA-15* in muscle differentiation in greater detail, we have further examined its expression in L6 and C2C12 myoblasts upon addition of TGF-beta1 into their culture medium. Indeed, TGF-beta1 exerts a physiological role in controlling muscle development and constrains myogenesis in different cultured skeletal muscle cells (7-9). Interestingly, TGF-beta1 exposure enhanced *PED/PEA-15* expression by almost 5-fold upon 6h exposure (**Fig.2A**) and exhibited a consistent time- and dose-dependent effect on PED/PEA-15 protein levels as well (data not shown). The effect of TGF-beta1 on *PED/PEA-15* expression was significantly reduced in L6 (or C2C12, data not shown) cells by the SB431542 inhibitor of the TGF-beta1 receptor, in parallel with SMAD3 phosphorylation (**Figs.2B,C**). Significant inhibition of TGF-beta1 effect was also achieved using a specific phosphorothioate antisense of SMAD3 (SMAD3 AS), indicating that TGF-beta1 stimulates PED/PEA-15 expression in a TGF-beta1R/SMAD3-dependent manner.

Based on *MyoD1*, *Myogenin* and *GLUT4* mRNA levels, TGF-beta1 treatment impaired L6 myoblasts differentiation (**Fig.3A-C**). This effect was largely prevented by two specific ShRNAs ($ShPED_1$ and $ShPED_2$) which silence *PED/PEA-15* expression by >70% (**Fig.3A-D**). The effect of TGF-beta1 on myotube generation was similarly affected by the *PED/PEA-15* ShRNA (**Suppl.**

Fig.1). Phosphorylation of PED/PEA-15 was also required for TGF-beta1-mediated myoblasts differentiation. In fact, in presence of the PED_{S116A} mutant, TGF-beta1 failed to reduce *MyoD1*, *Myogenin* and *GLUT4* mRNA levels (Fig.4A-D). Thus, in the L6 skeletal muscle cells, the complete regulatory role of TGF-beta1 on myogenesis requires the impact of TGF-beta1 signalling on PED/PEA-15. Same results were obtained in C2C12 (data not shown).

Promotion of autophagy by TGF-beta1 in L6 cells - Current evidence indicates that fine tuning of autophagy plays a major role in enabling differentiation (11-13). This observation led us to hypothesize that the recently recognized autophagy-promoting function of PED/PEA-15 (20) is necessary for the myogenesis constrain imposed by TGF-beta1, as TGF-beta1 has also been very recently shown to induce autophagy in non-muscle cells (14). FACS analysis of acridine orange-stained cells revealed that differentiating L6 (or C2C12, data not shown) cells treated with TGF-beta1 for 6 days accumulated acidic vescicular organelles (AVOs, a prominent feature of autophagy) to a significantly greater extent than control cells (**Fig.5A**). In parallel, TGF-beta1 treatment significantly increased both LC3I to LC3II conversion and Beclin 1 cell abundance, two known markers of autophagy activation (**Fig.5B**). In addition, exposure of L6 or C2C12 differentiating cells to the autophagy inhibitor 3-Methyladenine led to rescue of the myotube differentiation markers in the presence of TGF-beta1 (**Fig.5C**), indicating that promotion of autophagy by TGF-beta1 is relevant to the differentiation constrain. Previous studies revealed that the forkhead transcription factor FoxO1 regulates the expression of several autophagy-related genes, including Beclin1 and LC3 and induces muscle wasting (22-25). Consistently, exposure of L6 or C2C12 differentiating cells to TGF-beta1 led to dephosphorylation of both FoxO1 and of its upstream regulator, the PP2A serine/threonine phosphatase (**Fig.5D**)

PED/PEA-15 promotion of autophagy mediates TGF-beta1 effect on differentiation in L6 cells - The overexpression of PED/PEA-15 (10-fold above the endogenous levels) was sufficient to

determine a 10-fold increase in AVO accumulation, enhanced LC3I to LC3II conversion and augmentation in Beclin1 abundance (**Fig.6A,B**). As it is the case for myogenesis, $ShPED_1$ (or $ShPED_2$, data not shown) vector silencing of endogenous *PED/PEA-15* impaired TGF-beta1 effects on both AVO accumulation and the autophagy markers (**Fig.6C,D**). Moreover, in L6 myoblasts, expression of exogenous PED/PEA-15 reduced PP2A and FoxO1 phosphorylation while *PED/PEA-15* silencing significantly attenuated TGF-beta1 effect on their phosphorylation (**Fig.6B,D**). At variance, transfection of the PED_{S116A} mutant did not elicit any effect on TGF-beta1-mediated autophagy as well as FoxO1 and PP2A dephosphorylation (data not shown).

Importantly, 3-Methyladenine treatment of L6 differentiating cells stably overexpressing *PED/PEA-15* reduced autophagy to levels similar to those detected in the untransfected cells and rescued myotube biochemical and morphological differentiation (**Fig.7A-C**). Same results were obtained in C2C12 (data not shown). Thus, the autophagy-promoting function of PED/PEA-15 appeared to mediate the induction of autophagy and the impaired myogenesis which follows TGF-beta1 exposure.

In vivo consequences of skeletal muscle overexpression of *PED/PEA-15* - To address the significance of these findings to skeletal muscle *in vivo*, we performed histological analysis of tibialis anterior and quadriceps muscles from *PED/PEA-15* transgenic mice. These animals have been previously described (19,26) and feature about 10-fold overexpression of the PED/PEA-15 gene in their muscles. As shown in **Fig.8A-C**, Hematoxylin-Eosin and Engel trichrome stained sections revealed a 10% increase in atrophic fibers between *PED/PEA-15* transgenic mice and WT. (**panel A**). Rimmed vacuoles (**panel B**) and vacuoles with red inclusions (**panel C**) were also significantly increased in the *PED/PEA-15* transgenic muscles. Staining with specific antibodies revealed significantly higher expression of LC3 and Beclin1 in muscles form transgenic compared to those of control mice (**Fig.8D,E**). Indeed, muscles from the *PED/PEA-15* transgenic mice

revealed a > 4-fold increase in the LC3II to LC3I ratio with similarly-sized reduction in phospho-PP2A and phospho-FoxO1 levels (**Fig.9A**). MyoD1 and Myogenin mRNA levels were also significantly reduced in muscles from the PED/PEA-15 transgenics (**Fig.9B**). Whether these biochemical changes were paralleled by *in vivo* functional abnormalities was further analyzed by determining transgenic mouse traveled distance in an open field. Interestingly, this test revealed a significant decrease in locomotor activity in the *PED/PEA-15* transgenic mice (**Fig.9C**), suggesting a causal relationship between the muscle phenotype of these transgenic mice and the control of muscle development by *PED/PEA-15*.

DISCUSSION

Skeletal muscle ontogeny and postnatal physiology are regulated by the TGF-beta family of cytokines in different animal systems from mice to humans. Significant advancement has also been made in the elucidation of the detailed mechanisms involved in this regulation (1-6). However, many aspects of the TGF-beta signalling events leading to its action on skeletal muscle mass remain unsettled. In the present work, we have identified the multifunctional protein PED/PEA-15 as a key molecule transducing TGF-beta 1 signals and enabling TGF-beta1 repression of the myogenesis program.

We now report that, in the L6 and in C2C12 skeletal muscle cells the expression of PED/PEA-15 gene progressively declines during myogenesis. In addition, exogenous *PED/PEA-15* overexpression inhibits myotubes generation and differentiation leading us to hypothesize that PED/PEA-15 is implicated in mechanisms controlling myogenesis. Indeed, we have further found that exposure to TGF-beta 1 restrains differentiation and, simultaneously, enhances *PED/PEA-15* gene transcription significantly increasing abundance of PED/PEA-15 protein into the cell. This effect appears to be achieved *via* the TGF-beta1R/SMAD3 pathway activation, as inhibition or

silencing of these key molecules significantly impaired PED/PEA-15 upregulation by TGF-beta1. Similar effects have been noted also in primary myoblasts from WT and TgPED mice (data not shown). Different Smad Response Elements were identified in the *PED/PEA-15* promoter region whose occupancy increased following L6 cell exposure to TGF-beta1 (data not shown), suggesting regulation of *PED/PEA-15* gene by TGF-beta1 signalling. Importantly, we show that ShRNAs silencing of endogenous *PED/PEA-15* and abrogation of *PED/PEA-15* phosphorylation at seryl 116 largely prevented TGF-beta1 action on muscle cell differentiation, indicating that PED/PEA-15 exerts a major role in mediating the myogenesis control exerted by TGF-beta1. The (TGF-beta1-mediated) phosphorylation status of PED/PEA-15 also may play a central role in this process because non-phosphorylated PED/PEA-15 lacks the capability to induce myogenic gene expression. Despite intensive investigation, how TGF-beta1 inhibits myogenesis has been only partially elucidated. Smad3 is the key mediator (27,28), as it physically interacts with both MyoD and MEF2C (29). The presence of PED/PEA-15 in this network was unanticipated and led us to explore its significance to TGF-beta1 action in greater detail. Autophagy is a dynamic process in which intracellular membrane structures, the autophagosomes, sequester proteins and organelles for degradation (30). Autophagy is implicated in homeostasis and cell-size regulation in multiple organs both during normal development and under stress conditions (31,32). Recently, the role of autophagy in muscle differentiation has attracted much attention (11-13). However, it remains unclear whether autophagy is detrimental and part of the mechanisms that induce muscle degeneration, or whether it is a compensatory mechanism for cell survival. Both TGF-beta1 and PED/PEA-15 have been reported to activate autophagy in several tissues, though not in skeletal muscle (14,20). In the present report, we describe that both of these molecules exert an autophagy-promoting action in the L6 skeletal muscle cells. Importantly, we obtained evidence that PED/PEA-15 promotion of autophagy mediates the effect of TGF-beta1 on differentiation in the L6 cells. Indeed, while silencing of the endogenous *PED/PEA-15* blocked TGF-beta1-induced autophagy, inhibition with 3-Methyladenine in L6 cells overexpressing *PED/PEA-15* reduced autophagy to

levels comparable to the untransfected cells and rescued myogenesis. All together, these findings led us to conclude that the autophagy-promoting function of PED/PEA-15 mediates both the autophagy induction and the impaired myogenesis caused by TGF-beta1. These effects have been obtained also in primary myoblasts from WT and TgPED mice (data not shown).

Very recent evidence indicates a direct role of the forkhead transcription factors (FoxOs) in regulating the cellular mechanisms responsible for autophagy activation and impairment of myoblasts differentiation. Foxo1 ablation in C2C12 cells or in mice increases the levels of MyoD while forced expression of FoxO1 upregulates autophagic and atrophic responses in muscle cells (12, 22-25, 33). Indeed, FoxOs have been shown to promote the expression of different autophagy-related genes. These include *BECLIN1, ATG8, Gabarapl1, ATG12, ATG4B and VSP34* (21-24). FoxO1, in turn, is highly regulated at the post-transcriptional level. Dephosphorylation at Ser256 by the Ser/Thr phosphatase PP2A activates FoxO1, inducing its nuclear translocation (34,35). Interestingly, PP2A has been shown to undergo activation in response to TGF-beta1 in different cell types (36). Here we show that, in the L6 cells, full activation of the PP2A/FoxO1 signalling by TGF-beta1 requires PED/PEA-15. Indeed, i. forcing *PED/PEA-15* expression is sufficient to dephosphorylate PP2A and FoxO1, thus driving the nuclear translocation of FoxO1; and ii., *PED/PEA-15* silencing significantly attenuates the effect of TGF-beta1 on the PP2A/FoxO1-transduced signal (34-36). How PED/PEA-15 impacts on PP2A has not been completely demonstrated yet. However, data from our own and other laboratories indicate that PED/PEA-15 induces PKC-delta in different cell types, including the L6 cells. PKC-delta, in turn, enhances PP2A activity (37,38), indicating that it might induce PP2A in the L6 cell, as well.

These findings may have *in vivo* relevance as PP2A and FoxO1 activation accompanied by higher levels of autophagy markers and acidic vescicular organelles were also detected in skeletal muscle tissue from transgenic mice overexpressing *PED/PEA-15*. These changes were paralleled by

detectable muscle atrophy and decreased locomotor activity in these animals. Indeed, there is now evidence that the FoxO family of transcription factors plays a major transcriptional role in the muscle atrophy accompanying a number of disorders, including Type 2 diabetes. In the Type 2 diabetic individual, resistance to insulin in the PI3K/AKT signalling cascade is believed to represent a major mechanism responsible for muscle atrophy and sarcopenia, as impaired AKT function releases the brake on FoXO1 activity (34,35). However, increased TGF-beta1 levels have also been reported in Type 2 diabetes (19). Here we show that TGF-beta1 upregulates *PED/PEA-15* and may contribute to the increased *PED/PEA-15* expression described in many individuals with type 2 diabetes (17,18). This increased expression has no effect on PI3K/AKT signalling. Thus, TGF-beta1 induction of *PED/PEA-15*, may represent a previously unrecognized mechanism leading to FoxO1 activation, impaired myoblasts differentiation, muscle atrophy and decreased muscle mass which accompany long-lasting diabetes. This hypothesis is currently under active investigation in our laboratory.

In conclusion, in the present report, we have identified PED/PEA-15 as novel molecule in the TGF-beta1 signaling network of the muscle cell. In this cell types, transcriptional up-regulation of the *PED/PEA-15* gene by TGF-beta1 induces autophagic responses, atrophy and might contribute to the decreased muscle mass accompanying long-lasting Type 2 diabetes.

MATERIAL AND METHODS

Materials. Media, sera, antibiotics for cell culture and the lipofectamine reagent were from Invitrogen (Grand Island, NY). The PED/PEA-15 polyclonal antibody and pcDNAII-PED/PEA-15 vector have been previously described (19). The actin, pSMAD3, SMAD3, PP2A, pPP2A, and Beclin1 antibodies were from Santa Cruz Biotechnology, Inc. (Santa Cruz, CA); the FoxO1 and pFoxO1 antibodies were from Upstate Biotechnolgy (Lake Placid, NY); LC3 antibodies were from

Cell Signaling Technology, Inc (Beverly, MA). TGF-beta1 citokine was from PeproTech, Inc. (Rocky Hill, NJ). The phosphorothioate oligonucleotides antisense sequences were as follows: SMAD3 AS: 5′-GCAGGATGGACGACAT-3′; SMAD3 S: 5′-GGAGTCAGACTGACGA-3′. Protein electrophoresis reagents were purchased from Bio-Rad (Richmond, VA), Western blotting and ECL reagents from Amersham Biosciences (Arlington Heights, IL). *PED/PEA-15* ShRNA vectors and all other chemicals were from Sigma (St. Louis, MO).

Cell culture procedures and transfection. The L6 muscle and C2C12 cells were grown in Dulbecco's modified Eagle's medium (DMEM) supplemented with 10% fetal bovine serum, 10,000 U/ml penicillin, 10 mg/ml streptomycin, and 2% l-glutamine in a humidified CO_2 incubator and differentiated as described in (39). Stable transfection of the *PED/PEA-15* cDNA and transient transfection of antisense oligonucleotides or PED/PEA-15 S116A mutant (PED_{S116A}) were performed by the lipofectamine method according to the manufacturer's instructions (Invitrogen). For these studies, 70 to 80% confluent cells were washed twice with Optimem (Invitrogen) and incubated for 8 h with 5 μg of plasmid construct, ShRNA vectors or antisense oligonucleotides (200nM) and 45 to 60 μl of lipofectamine reagent. The medium was then replaced with DMEM with 10% (vol./vol.) fetal bovine serum and cells further incubated for 15 h before being assayed. In transient transfection studies, the medium was then replaced with DMEM with 10% fetal bovine serum and cells were further incubated for 15 h before being assayed. For experiments with stably transfected cells, individual G418-resistant clones were selected by the limiting dilution technique (G418 effective dose, 0.8 mg/ml). The expression of *PED/PEA-15* by the individual clones was quantitated by Western blotting. In all transfection studies, the efficiency was consistently between 65 and 75%. Transfection efficiency of antisense oligonucleotides was estimated as 45±10% by co-transfection with green fluorescent protein.

TGF-beta1 treatment in differentiating L6 and C2C12 cells. When cells reached ~90% of confluence (day 0), the medium was replaced with the differentiation-promoting medium (DMEM 2% fetal bovine serum), and the cells stimulated with TGF-beta1 (5ng/ml) for 6 or 9 days (cytokine

added on days 1, 3, 5 and 1, 3, 5, 7). Control cells were maintained in differentiation medium. The cells were then harvested and lysates were analyzed by western blotting, real time PCR, FACS analysis on days 6 and 9.

Mouse generation and phenotyping. The transgenic mice overexpressing *PED/PEA-15* have been previously described (25). These mice were fertile. Their body weight is comparable to that of their wild-type littermates (25). All procedures described below were approved by the Institutional Animal Care and Utilisation Committee. Animals were kept in a 12-h dark–light cycle and had free access to standard diet. Mice chosen for experimentation were randomly selected from each box of mice housed in groups of three to four.

Open-field exploration. Free exploration in a square arena (walls made of transparent plexiglas 50 x 50 com, 40 cm high) was allowed as previously described (40). Mice were enabled to explore for 5 minutes the open-field apparatus, placed in an experimental room with several large-scale environmental visual cues and homogeneous illumination. Exploratory behavior was recorded with a high definition digital camera and on-line viedeotracking was implemented using custom software written in Matlab environment. Total travelled distance was taken as an index of locomotor activity.

Muscle dissection and immunohistochemical examination. Skeletal muscle specimens (tibialis anterior or quadriceps) from *PED/PEA-15* transgenic or control mice were processed according to (41). Briefly, dissected muscles were frozen in isopentane pre-cooled in liquid nitrogen and stored at -80°C until being further analyzed. Sections (8 μm) were stained with Haematoxylin and Eosin (HE), Engel trichrome, or cytochrome C oxidase (COX).

For immunohistochemical examination, frozen sections (6 μm) were fixed in acetone at 4 °C for 5 min, then blocked for endogenous peroxidase in 0.3% H_2O_2 in methanol for 20 min. Muscle sections were further incubated with mouse monoclonal antibodies against LC3 (dilution 1:50) and BECN1 (dilution 1:50) overnight at 4°C. Slides were washed three times with PBS, incubated with biotinylated anti-rabbit and labeled streptavidin biotin (LSAB kit; DakoCytomation, Denmark) for 30 min, followed by incubation with streptavidin conjugated to horseradish peroxidase (LSAB Kit;

DakoCytomation, Denmark). Color development was assessed following 5 minutes of diaminobenzidine treatment (DakoCytomation, Denmark) treatment. Sections were counterstained with Mayer's haematoxylin. In the corresponding negative control section, the primary antibody was either omitted or replaced with normal mouse serum.

Tissue and cell lysates and western blot analysis. Tissue samples were homogenised in a Polytron (Brinkman Instruments, Westbury, NY, USA) in 20 ml T-PER reagent (Pierce,Rockford, IL, USA) per gram of tissue according to the manufacturer's instructions. After centrifugation at 5000×g for 5 min, the supernatant fractions were collected. Cells were solubilised in lysis buffer (50 mmol/L HEPES, pH 7.5, 150 mmol/L NaCl, 10 mmol/L EDTA, 10 mmol/L $Na_4P_2O_7$, 2 mmol/L Na_3VO_4, 100 mmol/L NaF, 10% (vol./vol.) glycerol, 1% (vol./vol.) Triton X-100, 1 mmol/L PMSF, 10 mg/ml aprotinin) for 1 h at 4°C and lysates were centrifuged at 5,000×g for 20 min. Total homogenates were separated by SDS-PAGE and transferred to 0.45 μm Immobilon-P membranes as previously described (20). Upon incubation with primary and secondary antibodies, immunoreactive bands were detected by ECL according to the manufacturer's instructions.

Real-time RT-PCR analysis. Total cellular RNA was isolated from muscles of wild-type and *PED/PEA-15* transgenic mice using a commercial kit (RNeasy; Qiagen, Hilden, Germany) and according to the manufacturer's instructions. Tissue or cell RNA (1 μg) was reverse-transcribed using Superscript III Reverse Transcriptase (Invitrogen). PCR reactions were analysed using SYBR Green mix (Invitrogen). Reactions were performed using Platinum SYBR Green qPCR Super-UDG and a multicolour real-time PCR detection system (Cycler IQ; Bio-Rad). All reactions were performed in triplicate and β-actin was used as an internal standard. Primer sequences were as follows: TGF-beta1 (forward) 5′-ATACGCCTGAGTGGCTGTCT-3′, (reverse) 5′-TGGGACTGATCCCATTGATT-3′; β-actin (forward) 5′-GCGTGACATCAAAGAGAAG-3, (reverse) 5′-ACTGTGTTGGCATAGAGG-3′, MyoD1 (forward) 5'-TCGACTCACCAGACCTGCGCT-3', (reverse) 5'-CTTGCAGGCCCACAGCAAGC; myogenin: (forward) 5'-ACTCCCTTACGTCCATCGTG-3', (reverse) 5'- CAGGACAGCCCCACTTAAAA-

3’, Glut4: (forward) 5’- CAGAAGGTGATTGAACAGAG-3’, (reverse) 5'- AATGATGCCAATGAGAAAGG-3’; Glut1: (forward) 5’- GGGAATGTCCTCATCTTGGA-3’, (reverse) 5’- TGAGGCTCTGTGTGGTTCTG-3’.

Quantification of Acidic Vesicular Organelles with acridine orange. Autophagy in the L6 cells was assessed as previously described (42). Briefly, Acidic Vescicular Organellles (AVOs) were quantified by acridine orange staining. For these studies cells were treated as necessary for each individual experiment and then gently detached with 0.05% trypsin–EDTA followed by 1.0 μ g/mL acridine orange staining for 15 minutes at room temperature. Stained cells were then analyzed on a FACS cytometer (Dako Cytomation, U.S.A.) and the Summit V4.3 software (Dako) (42).

Statistical methods. Data were analysed with Statview software (Abacus Concepts, Piscataway, NJ, USA) by one-factor analysis of variance. p values of less than 0.05 were considered statistically significant (19).

ACKNOWLEDGEMENTS

This work was supported by the European Foundation for the Study of Diabetes (EFSD), the European Community’s PREPOBEDIA (201681), grants from the Associazione Italiana per la Ricerca sul Cancro (AIRC), and from the Ministero dell’Università e della Ricerca Scientifica (MERIT initiative, FIRB program: RBNE08NKH7). The financial contribution of Telethon Italy is gratefully acknowledged.

S.I. and F.O. generated data, discussion, and wrote the manuscript. G.B. researched data, performed experimental work, and contributed to discussion. S.C., V.I., D.V. and G.P., researched data, O.P. contributed to critical discussion and researched data, P.F. and F.B. directed and planned research and wrote the manuscript.

S.I. and F.O. equally contributed to the study.

REFERENCES

1. Ten Dijke P, Hill CS. New insights into TGF-beta-Smad signalling. Trends Biochem Sci 2004; 29: 265–273.
2. Massague J, Blain SW, Lo RS. TGFbeta signaling in growth control, cancer, and heritable disorders. Cell 2000; 103: 295-309.
3. Dai C, Liu Y. Hepatocyte growth factor antagonizes the profibrotic action of TGF-β1 in mesangial cells by stabilizing Smad transcriptional corepressor TGIF. J Am Soc Nephrol 2004; 15:1402–1412.
4. Letterio, JJ, Roberts AB. Regulation of immune responses by TGF-beta. Annu Rev Immunol 1998; 16:137-61.
5. Ha H, Yu MR, Lee HB. High glucose-induced PKC activation mediates TGF-beta 1 and fibronectin synthesis by peritoneal mesothelial cells. Kidney Int 2001; 59:463–470.
6. Toda S, Matsumura S, Fujitani N, Nishimura T, Yonemitsu N, Sugihara H. Transforming growth factor-beta1 induces a mesenchyme-like cell shape without epithelial polarization in thyrocytes and inhibits thyroid folliculogenesis in collagen gel culture. Endocrinology 1997; 138: 5561-75.
7. Massague J, Cheifetz S, Endo T, Nadal-Ginard B. Type beta transforming growth factor is an inhibitor of myogenic differentiation. Proc Natl Acad Sci 1986; 83: 8206–8210.
8. Kollias HD, McDermott JC, Transforming growth factor-beta and myostatin signaling in skeletal muscle. J Appl Physiol 2008; 104: 579–587.
9. Schabort EJ, Van Der Merwe M, Loos B, Moore FP, Niesler CU. TGF-beta's delay skeletal muscle progenitor cell differentiation in an isoform-independent manner. Exp Cell Res 2009; 315: 373-84.
10. Glass DJ. Skeletal muscle hypertrophy and atrophy signaling pathways. Int J Biochem Cell Biol 2005; 37: 1974–1984
11. Sandri M. Autophagy in skeletal muscle. FEBS 2010; 584: 1411-6.
12. Zhao J, Brault JJ, Schild A, Cao P, Sandri M, Schiaffino S, et al. FoxO3 coordinately activates protein degradation by the autophagic/lysosomal and proteasomal pathways in atrophying muscle cells. Cell Metab 2007; 6: 472–483.
13. Masiero E, Agatea L, Mammucari C, Blaauw B, Loro E, Komatsu M, et al. Autophagy is required to maintain muscle mass. Cell Metab 2009; 10: 507-15.
14. Suzuki HI, Kiyono K, Miyazono K. Regulation of autophagy by transforming growth factor-beta (TGFbeta) signaling. Autophagy 2010; 14: 6.

15. Araujo H, Danziger N, Cordier J, Glowinski J, Chneiweiss H. Characterization of PEA-15 a major substrate for protein kinase C in astrocytes. J Biol Chem 1993; 268: 5911–5920.
16. Fiory F, Formisano P, Perruolo G, Beguinot F. Frontiers: PED/PEA-15, a multifunctional protein controlling cell survival and glucose metabolism. Am J Physiol Endocrinol Metab 2009; 297: 592-601.
17. Condorelli G, Vigliotta G, Iavarone C, Caruso M, Tocchetti CG, Andreozzi F, et al. PED/PEA-15 gene controls glucose transport and is overexpressed in type 2 diabetes mellitus. EMBO J 1998; 7: 3858–3866.
18. Valentino R, Lupoli G, Raciti GA Oriente F, Farinaro E, Della Valle E, et al. The PEA15 gene is overexpressed and related to insulin resistance in healthy first degree relatives of patients with type 2 diabetes. Diabetologia 2006; 49: 3058–3066.
19. Oriente F, Iovino S, Cassese A, Romano C, Miele C, Troncone G, et al. Overproduction of phosphoprotein enriched in diabetes (PED) induces mesangial expansion and upregulates protein kinase C-beta activity and TGF-beta1 expression. Diabetologia 2009; 52: 2642-52.
20. Böck BC, Tagscherer KE, Fassl A, Krämer A, Oehme I, Zentgraf HW, et al. The PEA-15 protein regulates autophagy via activation of JNK. J Biol Chem 2010; 285:21644-54.
21. Pisani DF, Cabane C, Derijard B, Dechesne CA. The topoisomerase 1-interacting protein BTBD1 is essential for muscle cell differentiation. Cell Death Differ. 2004; 11: 1157-65.
22. Salih DA, Brunet A. FoxO transcription factors in the maintenance of cellular homeostasis during aging. Curr Opin Cell Biol 2008; 20:126-36.
23. Sengupta A, Molkentin JD, Yutzey KE. FoxO transcription factors promote autophagy in cardiomyocytes. J Biol Chem 2009; 284: 28319-31.
24. Sandri M, Sandri C, Gilbert A, Skurk C, Calabria E, Picard A, et al. Foxo transcription factors induce the atrophy-related ubiquitin ligase atrogin-1 and cause skeletal muscle atrophy. Cell 2004; 117: 399-412.
25. Kamei Y, Miura S, Suzuki M, Kai Y, Mizukami J, Taniguchi T, et al. Skeletal muscle FOXO1 (FKHR) transgenic mice have less skeletal muscle mass, down-regulated Type I (slow twitch/red muscle) fiber genes, and impaired glycemic control. J Biol Chem 2004; 279: 41114-23.
26. Vigliotta G, Miele C, Santopietro S, Portella G, Perfetti A, Maitan MA, et al. Overexpression of the ped/pea-15 gene causes diabetes by impairing glucose-stimulated insulin secretion in addition to insulin action. Mol Cell Biol 2004; 24: 5005-15.

27. Trendelenburg AU, Meyer A, Rohner D, Boyle J, Hatakeyama S, Glass DJ. Myostatin reduces Akt/TORC1/p70S6K signaling, inhibiting myoblast differentiation and myotube size. Am J Physiol Cell Physiol 2009; 296: 1258-70.
28. Sartori R, Milan G, Patron M, Mammucari C, Blaauw B, Abraham R, et al. Smad2 and 3 transcription factors control muscle mass in adulthood. Am J Physiol Cell Physiol 2009; 296: 1248-57.
29. Kollias HD, McDermott JC. Transforming growth factor-b and myostatin signaling in skeletal muscle. J Appl Physiol 2007: 104:579-587.
30. Meléndez A, Neufeld TP. The cell biology of autophagy in metazoans: a developing story. Development 2008; 135: 2347-60.
31. Shintani T, Klionsky DJ. Autophagy in health and disease: a double-edged sword. Science 2004; 306: 990-5.
32. Vellai T, Bicsák B, Tóth ML, Takács-Vellai K, Kovács AL. Regulation of cell growth by autophagy. Autophagy 2008; 4: 507-509.
33. Liu CM, Yang Z, Liu CW, Wang R, Tien P, Dale R et al. Effect of RNA oligonucleotide targeting Foxo-1 on muscle growth in normal and cancer cachexia mice. Cancer Gene Ther. 2007; 14: 945-52.
34. Yan L, Lavin VA, Moser LR, Cui Q, Kanies C, Yang E. PP2A regulates the pro-apoptotic activity of FOXO1. J Biol Chem 2008; 283: 7411-20.
35. Brunet A, Bonni A, Zigmond MJ, Lin MZ, Juo P, Hu LS, et al. Akt promotes cell survival by phosphorylating and inhibiting a Forkhead transcription factor, Cell 1999; 96: 857–868.
36. Petritsch C, Beug H, Balmain A, Oft M. TGF-beta inhibits p70 S6 kinase via protein phosphatase 2A to induce G(1) arrest. Genes Dev 2000; 14: 3093-101.
37. Renault-Mihara F, Beuvon F, Iturrioz X, Canton B, De Bouard S, Léonard N, et al. Phosphoprotein enriched in astrocytes-15 kDa expression inhibits astrocyte migration by a protein kinase C delta-dependent mechanism. Mol Biol Cell 2006; 17: 5141-52.
38. Zhang D, Kanthasamy A, Yang Y, Anantharam V, Kanthasamy A. Protein kinase C delta negatively regulates tyrosine hydroxylase activity and dopamine synthesis by enhancing protein phosphatase-2A activity in dopaminergic neurons. J Neurosci 2007; 27: 5349-62.
39. Caruso M, Miele C, Formisano P, Condorelli G, Bifulco G, Oliva A, et al. In skeletal muscle, glucose storage and oxidation are differentially impaired by the IR1152 mutant receptor. J Biol Chem 1997; 272: 7290-7.
40. Mignogna P, Viggiano D, Brain distribution of genes related to changes in locomotor activity. Physiol Behav 2010; 19: 618-626.

41. Paciello O, Papparella S. Histochemical and immunohistological approach to comparative neuromuscular diseases. Folia Histochem Cytobiol 2009; 47: 143-152.
42. Skehan P, Storeng R, Scudiero D, Monks A, McMahon J, Vistica D, et al. New colorimetric cytotoxicity assay for anticancer-drug screening. J Natl Cancer Inst 1990; 82: 1107-12.

FIGURE LEGENDS

Fig. 1 – Effect of PED/PEA-15 on L6 cell and C2C12 differentiation. A. L6 and C2C12 cells were plated and differentiation was induced as described under Materials and Methods. Upon the indicated times in culture, the cells were lysed and protein samples were analysed by Western Blotting using PED/PEA-15 antibodies and beta-actin for control. Blots were revealed by ECL and autoradiography. Alternatively (left panel), total RNA was obtained from the cells and *PED/PEA-15* mRNA was assessed by real-time RT-PCR using beta-actin as internal control. Each bar represents the mean ± SD of 4 independent experiments, each of which was performed in triplicate. B. In L6 and C2C12 cells transfected with a cDNA encoding PED/PEA-15 (pcDNAIII-PED) or the empty vector (pcDNAIII), differentiation was induced as described under Materials and Methods. C. Differentiated myotubes were then lysed and lysates blotted with PED/PEA-15 antibodies (top panel). Alternatively, total RNA was obtained from the cells and *MyoD1*, *Myogenin*, *GLUT4*, *Glut1* and *TGF-beta1* mRNAs were quantitated by real-time RT-PCR (bottom panel). Values are expressed as % of those in cells transfected with the empty vector. Each bar represents the mean ± SD of four independent experiments in triplicate. Asterisks denote statistically significant differences (*$p < 0.05$; **$p < 0.01$). Brightfield images of the L6 and C2C12 cells (100 x magnification) transfected with either the PED/PEA-15 cDNA or with the empty vector upon 6 days in culture. The microphotographs shown are representative of five other independent sets of observations.

Fig.2 – Effect of TGF-beta 1 on PED/PEA-15 expression in L6 and C2C12 cells. A. Skeletal muscle cells were stimulated with 5 ng/mL TGF-beta1 for the indicated times. Total RNA was then isolated from the cells and the levels of *PED/PEA-15* mRNA were assessed by real-time RT-PCR using beta-actin as internal control. Alternatively, the cells were treated with 0.1 μM of the TGF-beta1 receptor inhibitor SB431542 or transiently transfected with 200 nM SMAD3

phosphorothioate antisense (SMAD3 AS) followed by stimulation with 5 ng/ml TGF-beta1, as described under Materials and Methods. The cells were then harvested for assessment of *PED/PEA-15* mRNA levels (B) or Western blotted with specific PED/PEA-15, phospho-SMAD3 (pSMAD3) and SMAD3 antibodies (C). Blots were revealed by ECL and autoradiography using beta-actin as a loading control. The autoradiograps shown are representative of four independent experiments. Bars represent the mean ± SD of four independent experiments. Asterisks denote statistically significant differences (* $p < 0.05$; ** $p < 0.01$, *** $p < 0.001$).

Fig.3 – The role of PED/PEA-15 in TGF-beta1-impaired myogenesis in L6 cells. L6 myoblasts were transfected either with a scrambled or a *PED/PEA-15* ShRNAs and maintained in culture enabling them to differentiate for the indicated times and in the presence or the absence of 5 ng/mL TGF-beta1. Total RNA preparations were then obtained from the cells and the levels of *MyoD1* (A), *Myogenin* (B), *Glut4* (C) and *PED/PEA-15* mRNA (D) were quantitated by real-time RT-PCR analysis, using beta-actin as internal standard. Each bar represents the mean ± SD of four independent experiments in which each reaction was performed in triplicate. Asterisks denote statistically significant differences (# $p<0.01$ for differences between Sc at day 6 or 9 and Sc at day 0, * $p < 0.05$; ** $p < 0.01$, *** $p < 0.001$).

Fig.4 – The role of PED/PEA-15 phosphorylation in TGF-beta1-impaired myogenesis in L6 cells. L6 cells transfected with the empty (*pcDNAIII*) or the PED/PEA-15 (*pcDNAIII-PED*) vector or the PED/PEA-15 S116A mutant (PED_{S116A}) were maintained in culture enabling them to differentiate for the indicated times and in the presence or the absence of 5 ng/mL TGF-beta1. Total RNA preparations were then obtained from the cells and the levels of *MyoD1* (A), *Myogenin* (B), *Glut4* (C) and *PED/PEA-15* mRNA (D) were quantitated by real-time RT-PCR analysis, using beta-actin as internal standard. Each bar represents the mean ± SD of four independent experiments in which each reaction was performed in triplicate. Asterisks denote statistically significant

differences (# $p<0.01$ for differences between Sc at day 6 and Sc at day 0, **$p < 0.01$, ***$p < 0.001$).

Fig.5 – TGF-beta1 effect on autophagy in L6 and C2C12 cells. A. Differentiating L6 cells were treated with 5 ng/mL TGF-beta1 as described under Materials and Methods. After 6 days in culture, the cells were stained with acridine orange and AVO accumulation was determined by flow cytometric analysis. Calculated percentages represent the red-positive cells in the upper quadrants (R10 and R11). FITC Lin, green color intensity; PE Texas Red Area, red color intensity. Those shown are representative of four independent experiments. Alternatively (B,D), L6 and C2C12 cells were lysed as described under Materials and Methods and Western blotted using PED/PEA-15, Beclin1, LC3 I, LC3 II, phospho-Tyr307-PP2A, phospho-Ser256-FoxO1 or FoxO1 antibodies. Blots were revealed by ECL and autoradiographs, using beta-actin as loading control. The autoradiographs shown are representative of three independent experiments. C. L6 and C2C12 cells were plated and exposed for 72h to 5 ng/mL TGF-beta1 in the absence or the presence of 1 mM 3-Methyladenine (3MA). Upon 6 days of differentiation, total RNA was isolated and the levels of *MyoD1*, *Myogenin* and *Glut4* mRNA were quantitated by real-time RT-PCR analysis, with each reaction performed in triplicate. Bars represent the mean ± SD of four independent experiments.

Fig.6 – PED/PEA-15 autophagy promoting activity mediates TGF-beta1 action on L6 cell differentiation. L6 cells stably overexpressing PED/PEA-15 (pcDNAIII-PED) or transfected with the empty vector (pcDNAIII) were plated and enabled to differentiate as described under Materials and Methods. AVO accumulation was determined as outlined in Fig.4 (A). The one shown is representative of 4 independent experiments. B. Alternatively, the cells were lysed and 100 microgram protein samples were analyzed by Western blotting using the indicated antibodies. Blots were revealed by ECL and autoradiography, using beta-actin as loading control. The autoradiograph shown is representative of three independent experiments. C. Differentiated myotubes were

transiently transfected with either the ShPED/PEA-15 RNA (Sh PED/PEA-15) or a scrambled RNA (Sc) and then exposed to 5 ng/mL TGF-beta1. AVO accumulation was assessed as outlined in Fig.4. The one shown is representative of three independent experiments. D. Alternatively, the cells were lysed and protein samples were analyzed by Western blotting using the indicated antibodies. Blots were revealed by ECL and autoradiography, using beta-actin as loading control. The autoradiograph shown is representative of four independent experiments.

Fig.7 – 3-Methyladenine rescues differentiation in PED/PEA-15 overexpressing L6 cells. L6 myoblasts stably overexpressing *PED/PEA-15* were plated and differentiated in culture as described under Materials and Methods. 72 hour prior to the experiment, the cells were exposed to 1 mM 3-Methyladenine (3MA). AVO accumulation was then assessed as outlined under Fig.4 (A). The figures shown are representative of four independent experiments. Alternatively, total RNA was obtained by the cells followed by quantitation of *MyoD1*, *Myogenin*, *GLUT4* and *GLUT1* mRNA levels by RT-PCR, using beta-actin as internal standard (B). Data are presented as % of the levels measured in control cells. Bars represent the mean ± SD of four independent experiments in which each reaction was performed in triplicate. Asterisks denote statistically significant differences (**p < 0.01, ***p < 0.001). C. Brightfield images (100 x) of L6 cells stably transfected with either the PcDNAIII-PED vector or the empty PcDNAIII vector in the absence or the presence of 3-Methyadenine. The microphotographs shown are representative of three additional experiments.

Fig.8 – Histological and immunohistochemical analysis of skeletal muscles from *PED/PEA-15* transgenic mice. Sections from skeletal muscles (tibialis anterior) from 6- month old transgenic mice and non transgenic littermates (control; WT) were stained with either Hematoxylin-Eosin (H/E; A,B) or Engel-Trichrome (C) or immunostained with LC3 or Beclin1 (BECN1) antibodies (D,E). The arrows in the microphotographs (40 x) indicate atrophic muscle fibers with basophilic cytoplasm (A), small rimmed vacuoles (B), vacuoles with red inclusions (C), decoration with LC3

(D) and Beclin1 (BECN1; E) antibodies. The microphotographs shown are representative of findings observations in 6 transgenic and 8 non-transgenic animals.

Fig.9 – Functional consequences of PED/PEA-15 overexpression in skeletal muscle of transgenic mice. A.Tibialis anterior muscles from PED/PEA-15 transgenic mice and from their non transgenic littermates (WT) were dissected, solubilized and 100 microgram protein samples were analyzed by Western blottin using LC3-I, LC3-II, phospho-tyr307-PP2A (P-PP2A), PP2A, phospho-ser256-FoxO1 (p-FoxO1) and FoxO1 antibodies. Beta actin was used as loading control. Blots were revealed by ECL and autoradiography. The autoradiograph shown is representative of studies performed with n=8 mice/group. Alternatively (B), the muscle were used for obtaining total RNA preparation. *MyoD1* and *Myogenin* mRNA was subsequently assessed by realtime RT-PCR analysis, using beta-actin as internal standard. Bars represent the mean ± SD of four independent experiments each performed in triplicate C. Travel distance was compared in transgenic and non transgenic littermates (16 animals/group) enabled to explore the open-field appartus for 5 min. as described under Materials and Methods. Bars represent the mean ± SD of four independent studies each involving 4 mice/group. Asterisks denote statistically significant differences (*$p < 0.05$; ***$p < 0.001$).

Supplemental Figure 1 – PED/PEA-15 mediates TGF-beta1 action on L6 cell differentiation. L6 cells were transfected either with a PED/PEA-15 ShRNA or a scramble RNA, exposed to 5 ng/mL TGF-beta1 and cultured for the indicated times. The microphotographs shown are brightfield images (100 x magnification) representative of four independent sets of observations.

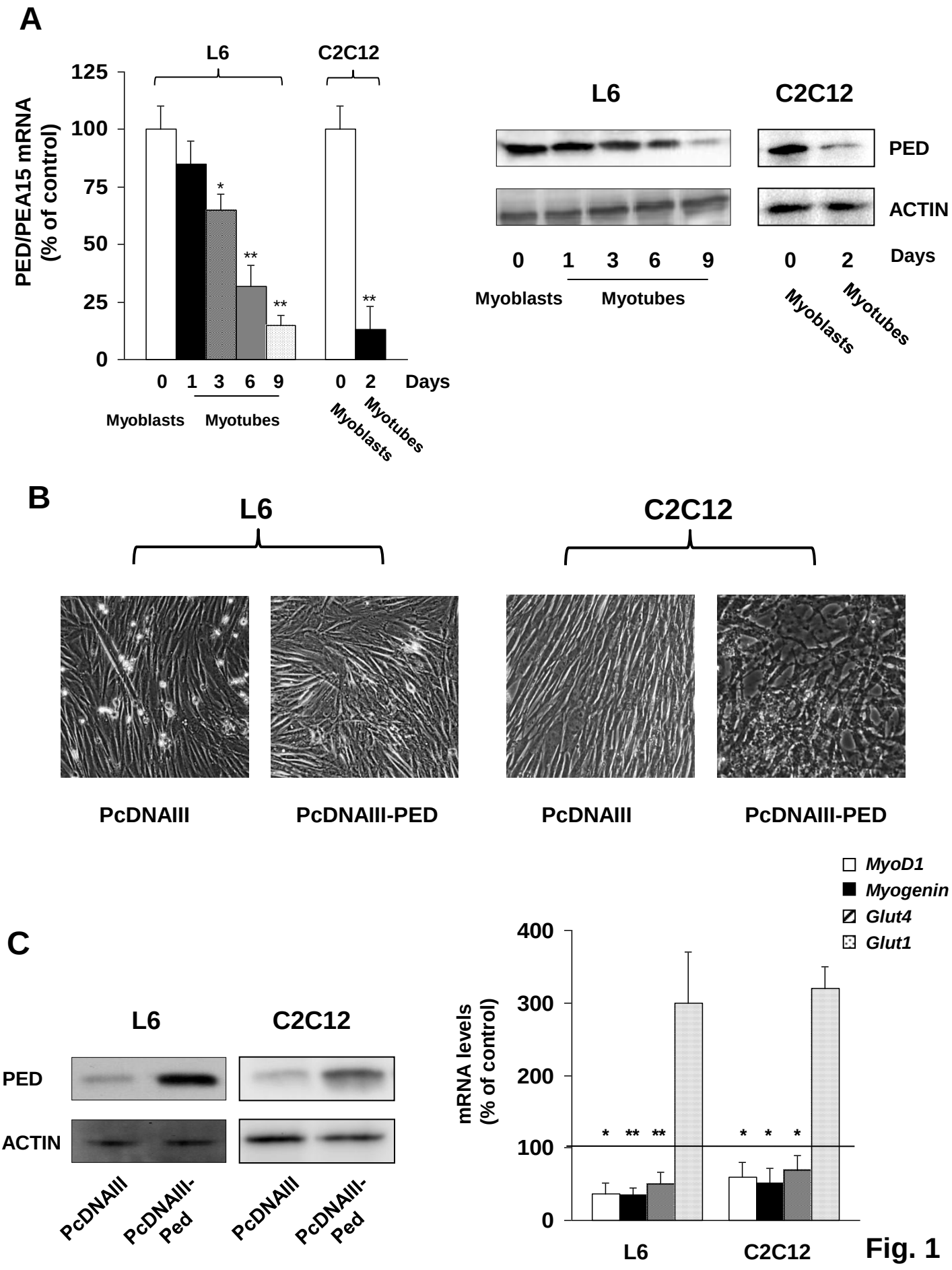
A
L6
C2C12
PED/PEA15 mRNA (% of control)
125
100
75
50
25
0
*
**
**
**
0 1 3 6 9
0 2
Days
Myoblasts
Myotubes
Myoblasts
Myotubes
L6
C2C12
PED
ACTIN
0 1 3 6 9
0 2
Days
Myoblasts
Myotubes
Myoblasts
Myotubes
B
L6
C2C12
PcDNAIII
PcDNAIII-PED
PcDNAIII
PcDNAIII-PED
C
L6
C2C12
PED
ACTIN
PcDNAIII
PcDNAIII-Ped
PcDNAIII
PcDNAIII-Ped
MyoD1
Myogenin
Glut4
Glut1
mRNA levels (% of control)
400
300
200
100
0
* ** **
* * *
L6
C2C12

Fig. 1

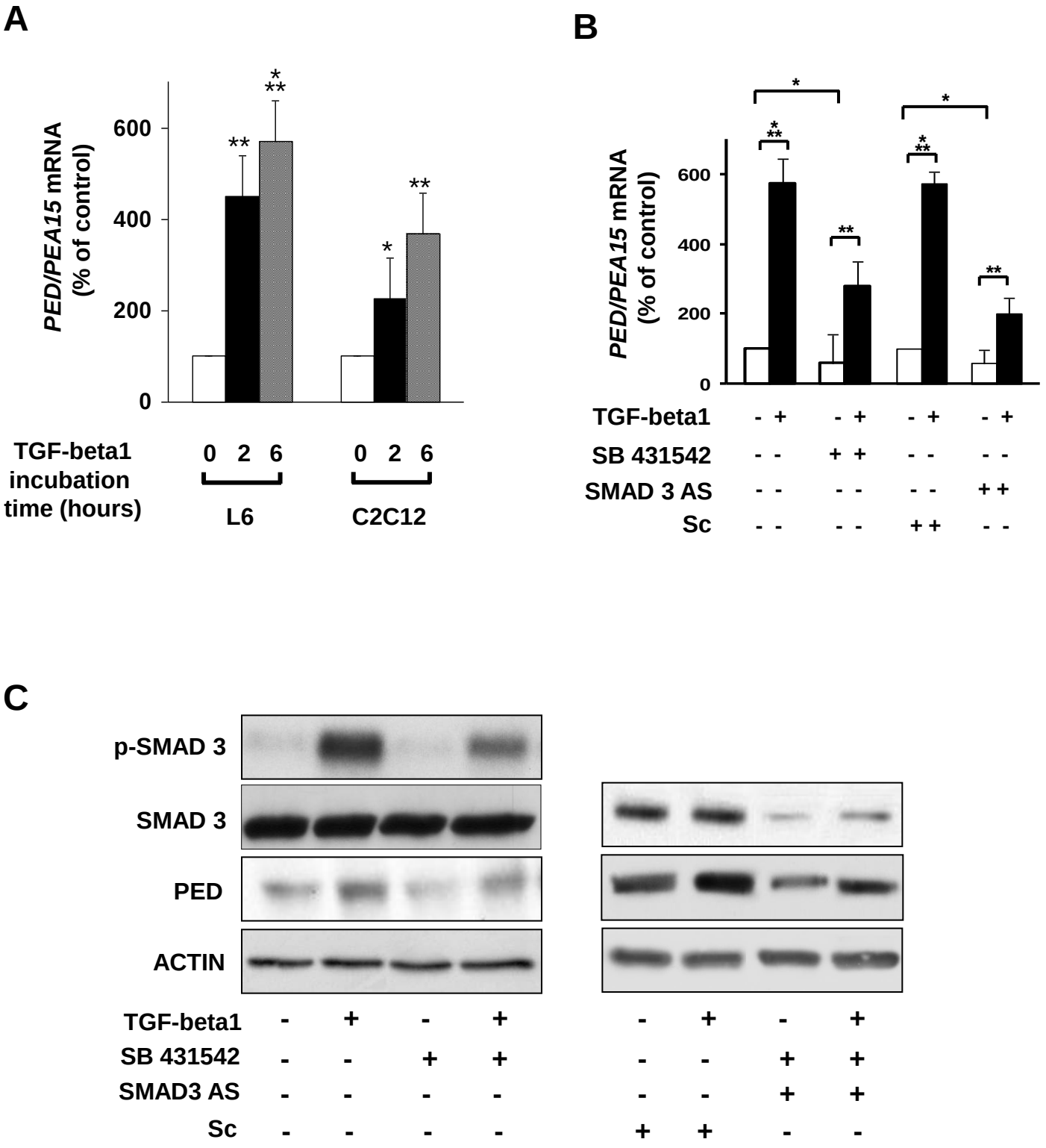
A
PED/PEA15 mRNA (% of control)
600
400
200
0
TGF-beta1 incubation time (hours)
0 2 6
0 2 6
L6
C2C12
B
PED/PEA15 mRNA (% of control)
600
400
200
0
TGF-beta1 - + - + - + - +
SB 431542 - - + + - - - -
SMAD 3 AS - - - - - - + +
Sc - - - - + + - -
C
p-SMAD 3
SMAD 3
PED
ACTIN
TGF-beta1 - + - + - + - +
SB 431542 - - + + - - + +
SMAD3 AS - - - - - - + +
Sc - - - - + + - -

Fig. 2

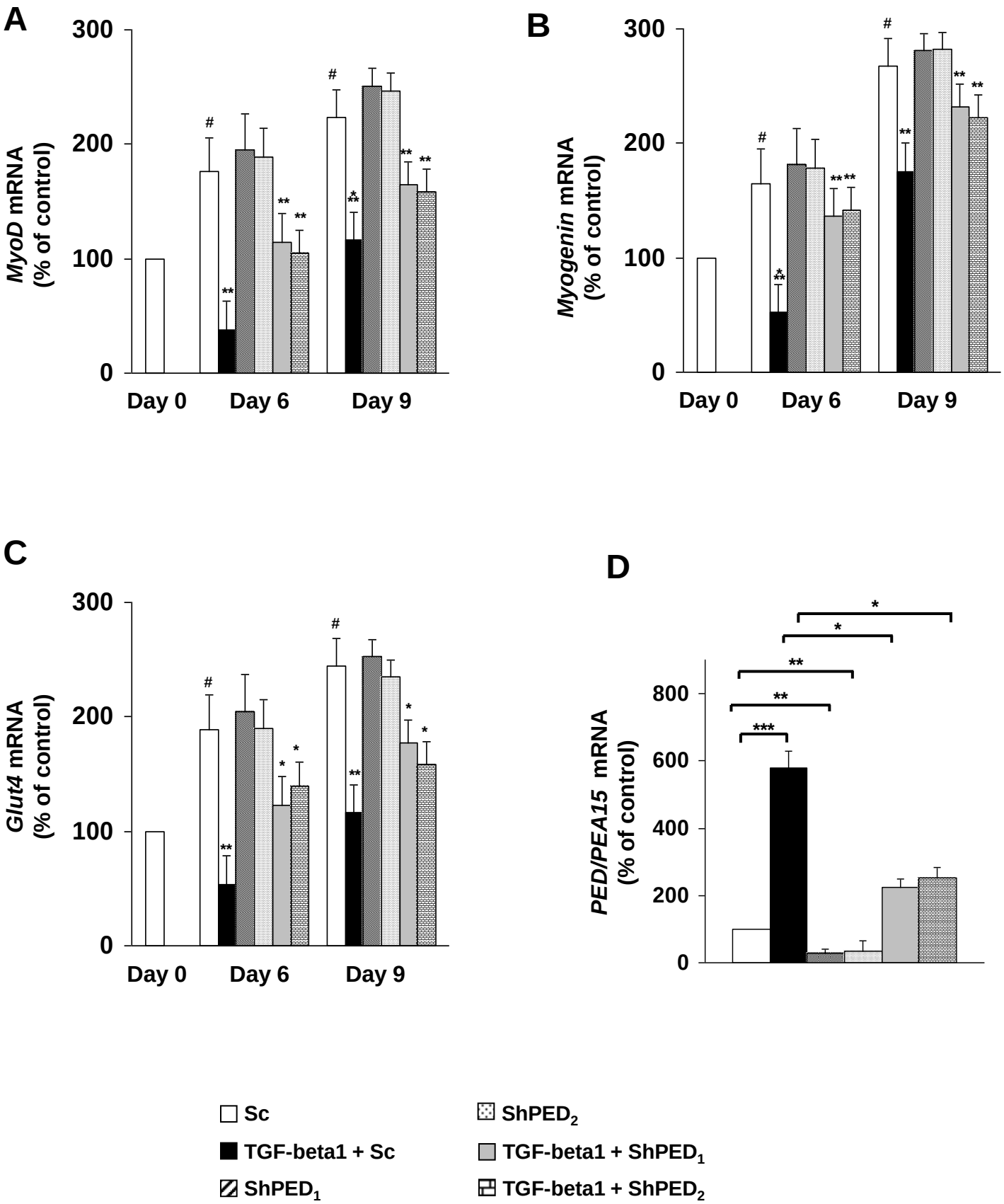
A
B
C
D
MyoD mRNA (% of control)
Myogenin mRNA (% of control)
Glut4 mRNA (% of control)
PED/PEA15 mRNA (% of control)
300
200
100
0
800
600
400
200
Day 0
Day 6
Day 9
Sc
TGF-beta1 + Sc
ShPED1
ShPED2
TGF-beta1 + ShPED1
TGF-beta1 + ShPED2

Fig. 3

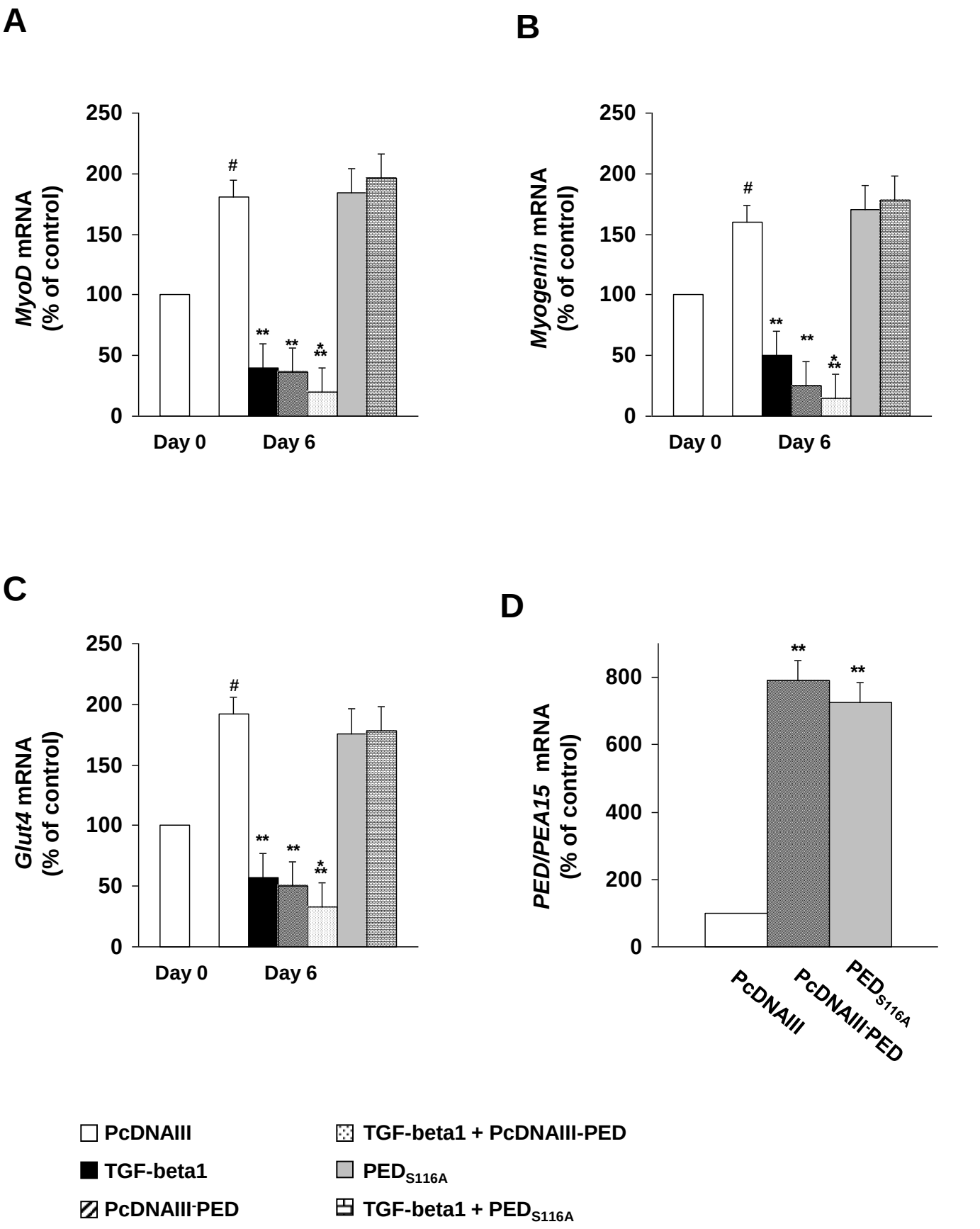
A
B
C
D
MyoD mRNA (% of control)
Myogenin mRNA (% of control)
Glut4 mRNA (% of control)
PED/PEA15 mRNA (% of control)
Day 0
Day 6
PcDNAIII
PcDNAIII-PED
PED S116A
PcDNAIII
TGF-beta1
PcDNAIII-PED
TGF-beta1 + PcDNAIII-PED
PED S116A
TGF-beta1 + PED S116A

Fig. 4

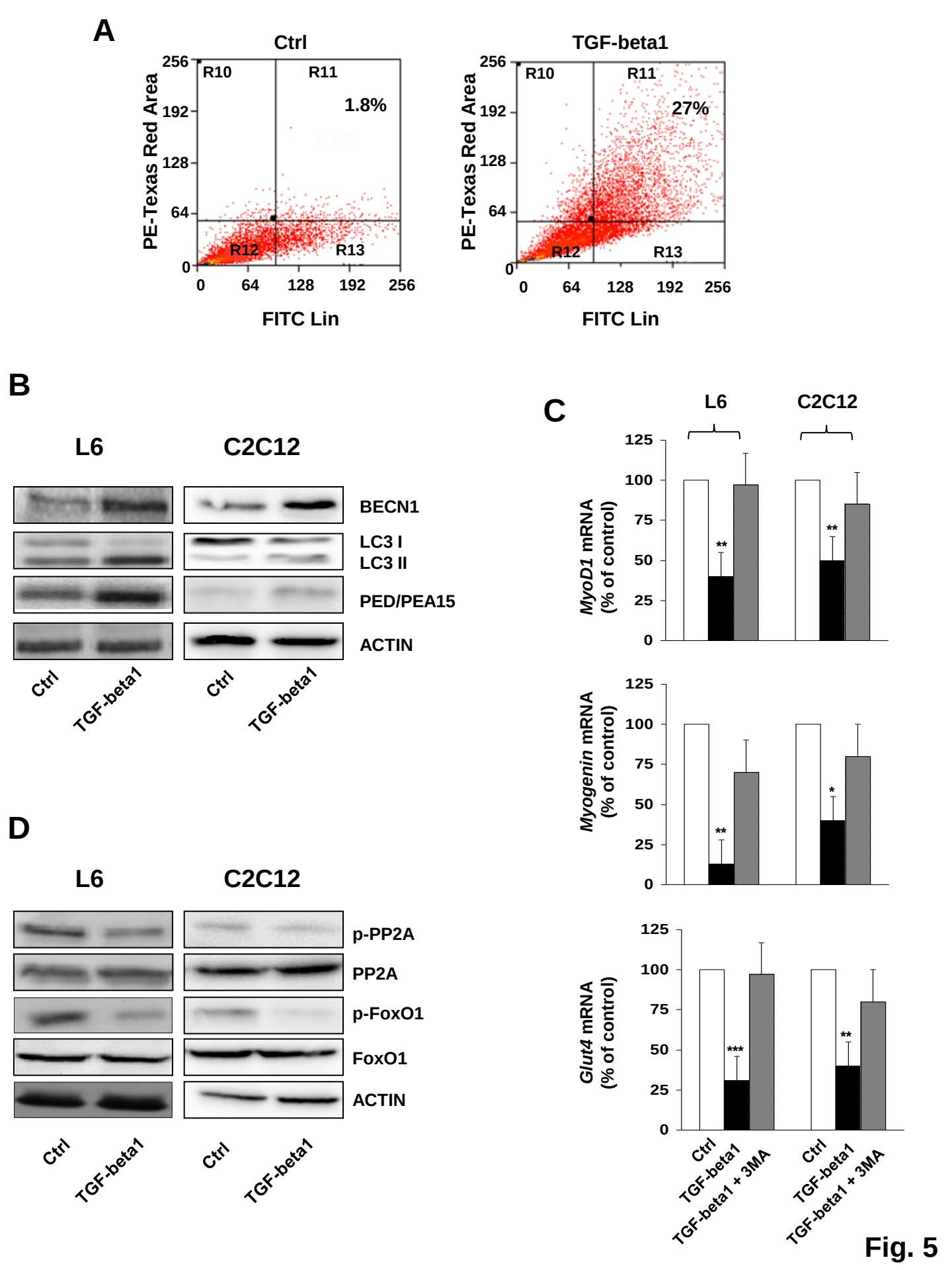
A
Ctrl
TGF-beta1
PE-Texas Red Area
FITC Lin
R10
R11
R12
R13
1.8%
27%
256
192
128
64
0
B
L6
C2C12
BECN1
LC3 I
LC3 II
PED/PEA15
ACTIN
Ctrl
TGF-beta1
C
L6
C2C12
MyoD1 mRNA (% of control)
Myogenin mRNA (% of control)
Glut4 mRNA (% of control)
125
100
75
50
25
0
**
*
***
Ctrl
TGF-beta1
TGF-beta1 + 3MA
D
L6
C2C12
p-PP2A
PP2A
p-FoxO1
FoxO1
ACTIN
Ctrl
TGF-beta1

Fig. 5

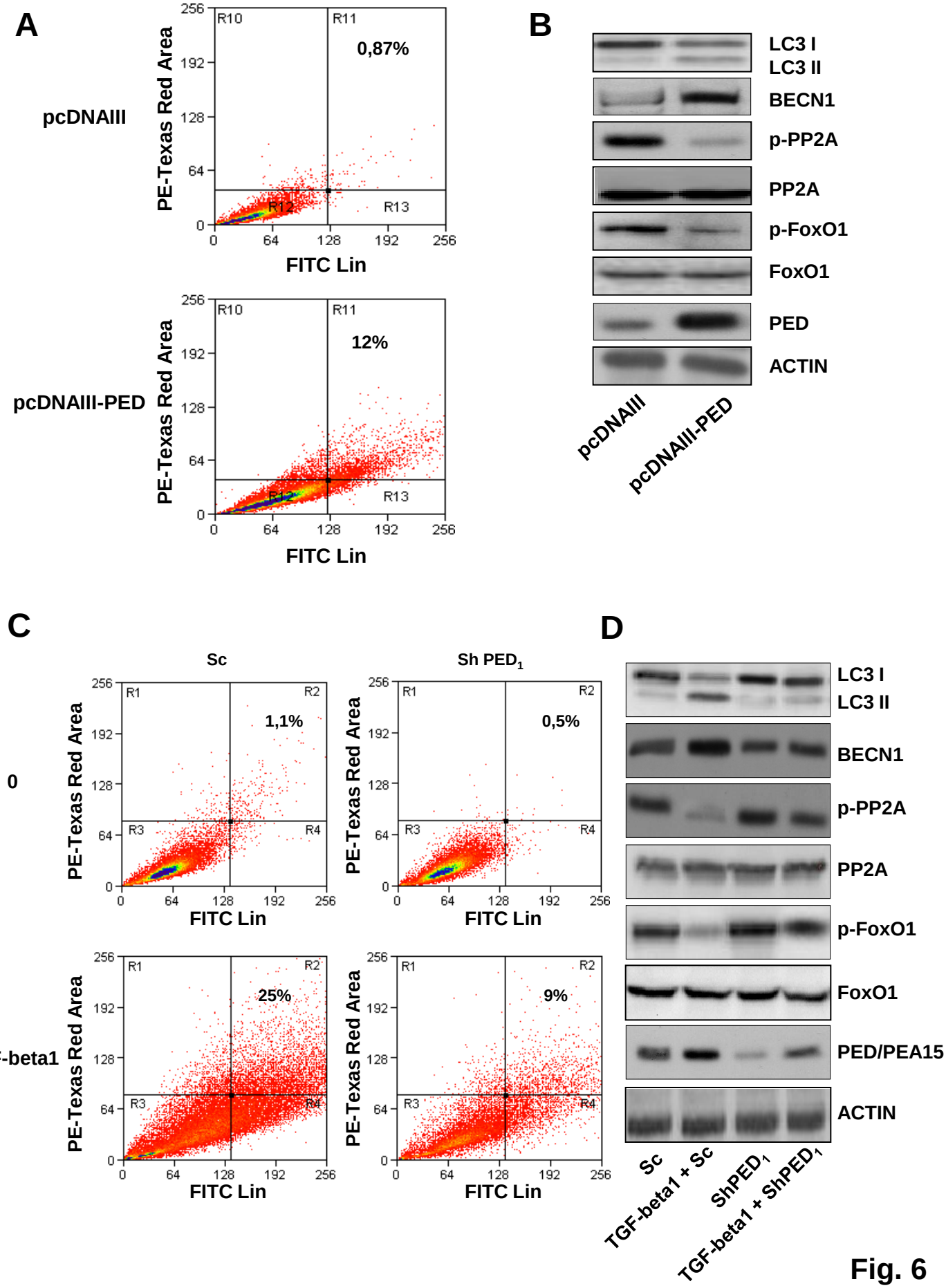
A
pcDNAIII
pcDNAIII-PED
PE-Texas Red Area
FITC Lin
R10
R11
R12
R13
0,87%
12%
B
LC3 I
LC3 II
BECN1
p-PP2A
PP2A
p-FoxO1
FoxO1
PED
ACTIN
pcDNAIII
pcDNAIII-PED
C
Sc
Sh PED1
0
TGF-beta1
R1
R2
R3
R4
1,1%
0,5%
25%
9%
D
LC3 I
LC3 II
BECN1
p-PP2A
PP2A
p-FoxO1
FoxO1
PED/PEA15
ACTIN
Sc
TGF-beta1 + Sc
ShPED1
TGF-beta1 + ShPED1

Fig. 6

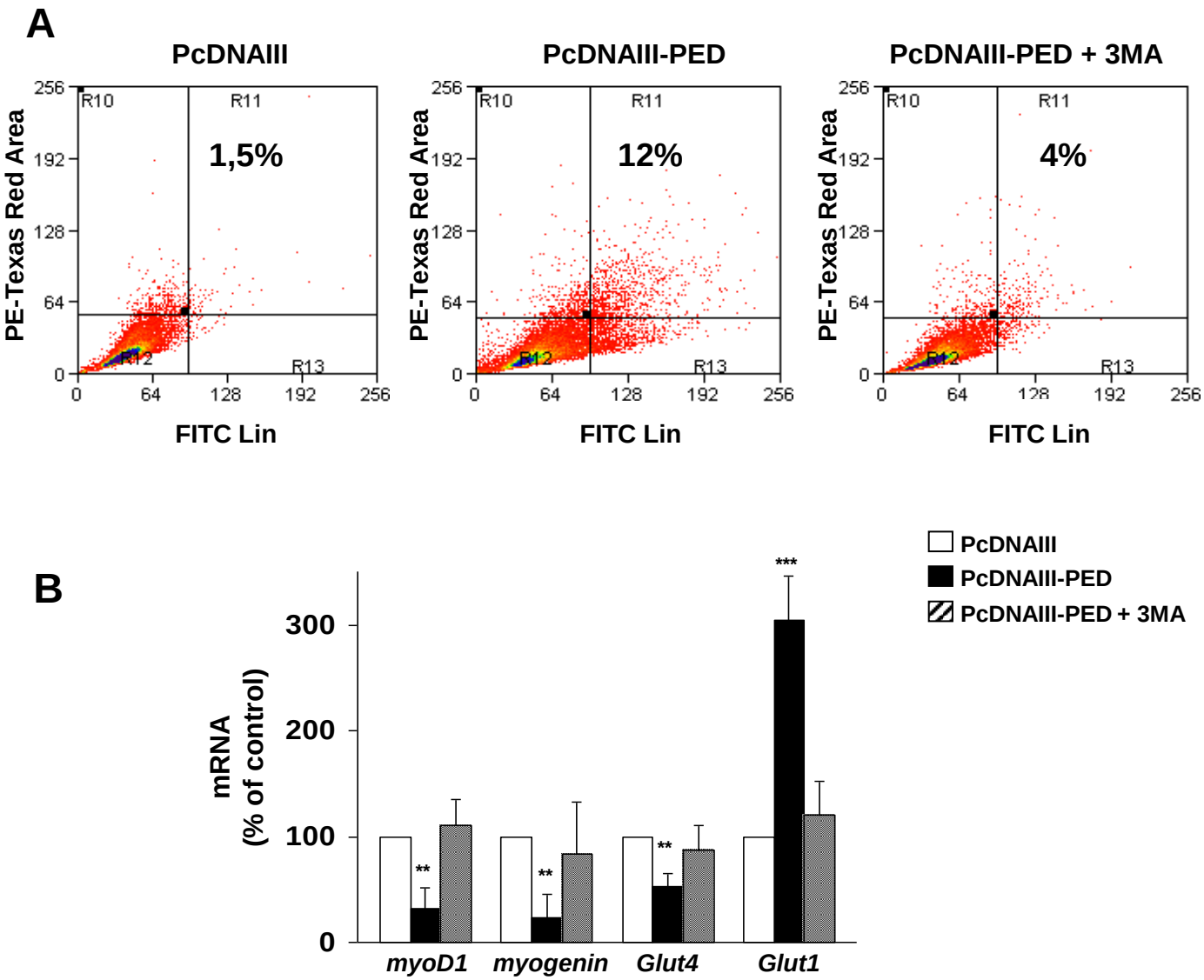
A
PcDNAIII
PcDNAIII-PED
PcDNAIII-PED + 3MA
PE-Texas Red Area
FITC Lin
R10
R11
R12
R13
1,5%
12%
4%
0
64
128
192
256
B
PcDNAIII
PcDNAIII-PED
PcDNAIII-PED + 3MA
mRNA
(% of control)
300
200
100
0
**
***
myoD1
myogenin
Glut4
Glut1
C
PcDNAIII
PcDNAIII-PED
PcDNAIII-PED +
3MA

Fig. 7

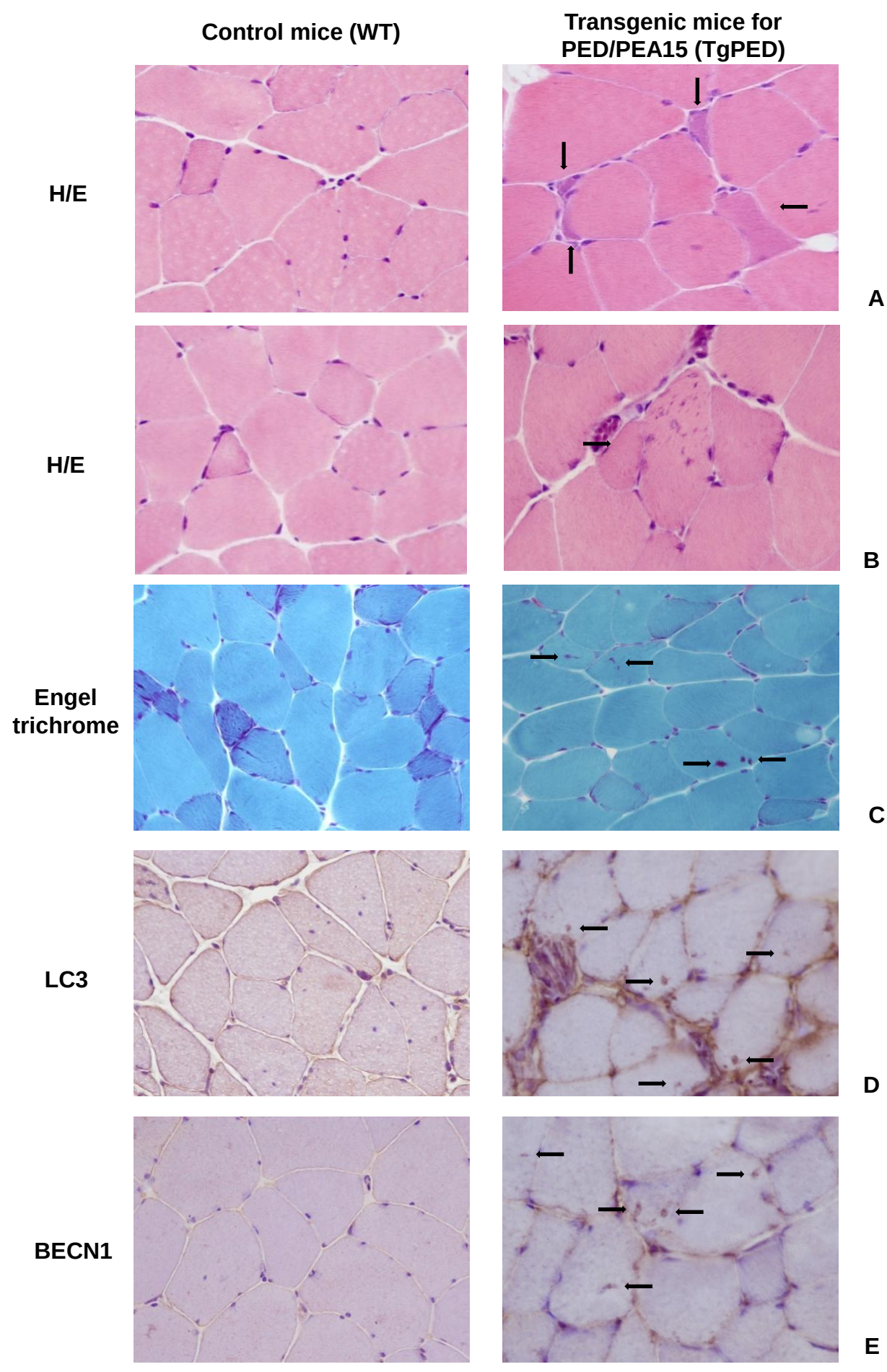
Control mice (WT)
Transgenic mice for PED/PEA15 (TgPED)
H/E
A
H/E
B
Engel trichrome
C
LC3
D
BECN1
E

Fig. 8

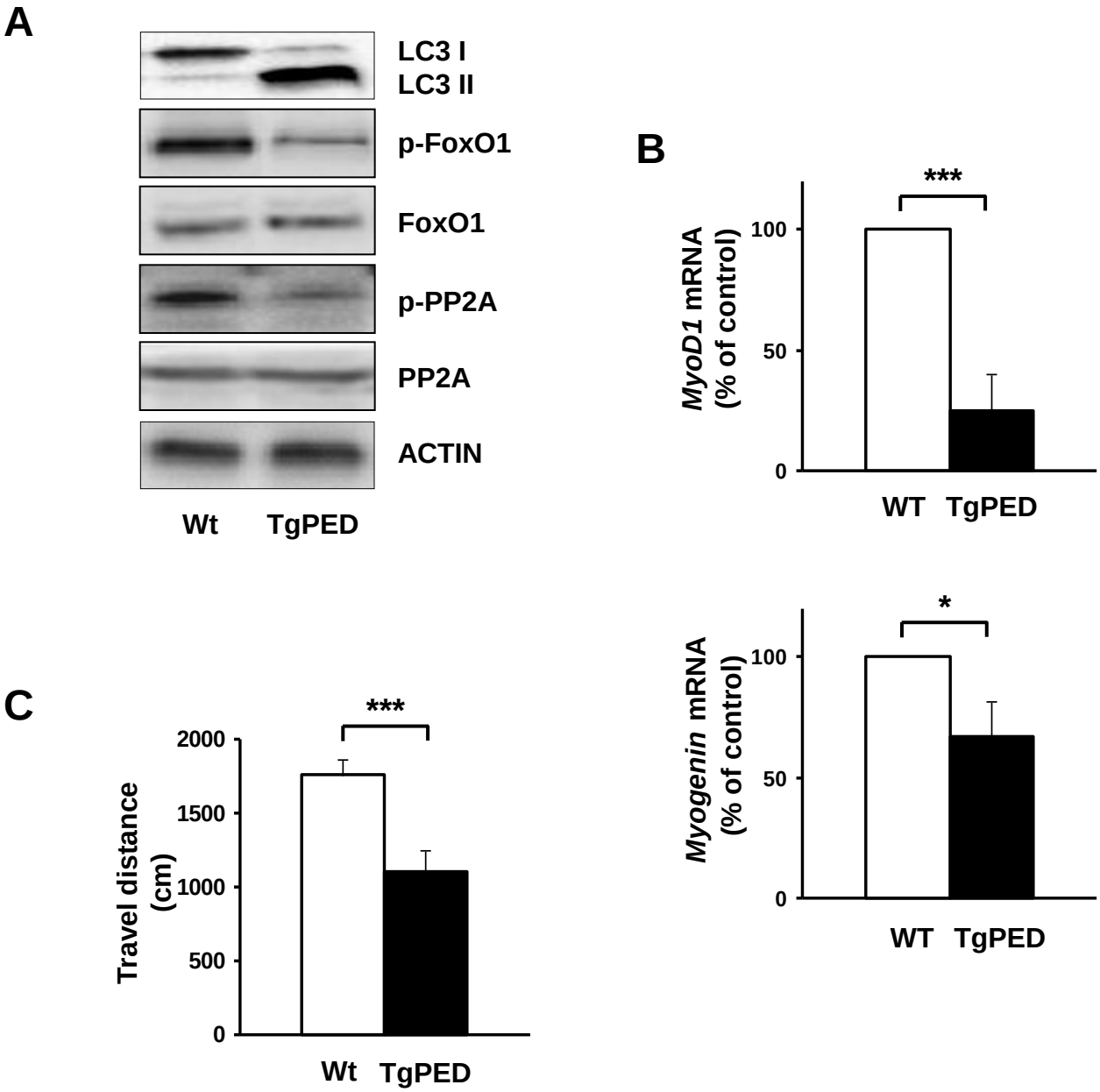
A
LC3 I
LC3 II
p-FoxO1
FoxO1
p-PP2A
PP2A
ACTIN
Wt
TgPED
B
***
MyoD1 mRNA
(% of control)
100
50
0
WT
TgPED
*
Myogenin mRNA
(% of control)
100
50
0
WT
TgPED
C
***
Travel distance
(cm)
2000
1500
1000
500
0
Wt
TgPED

Fig. 9

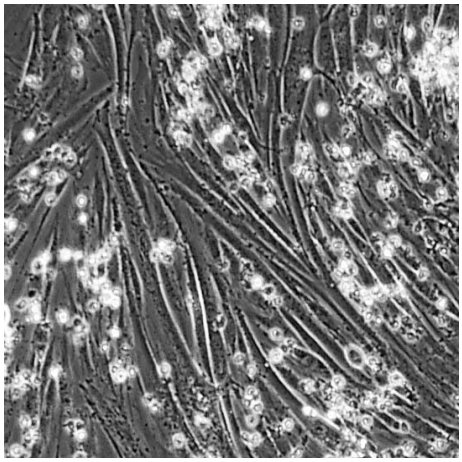

Day 6

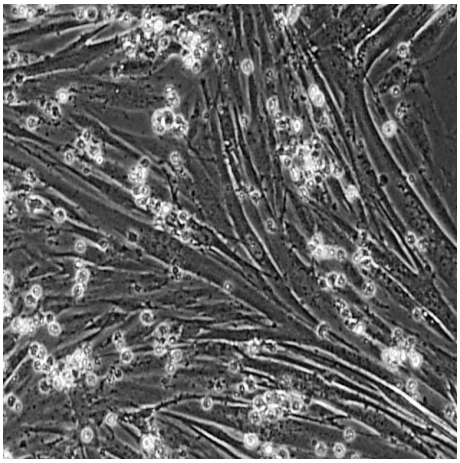

Day 9

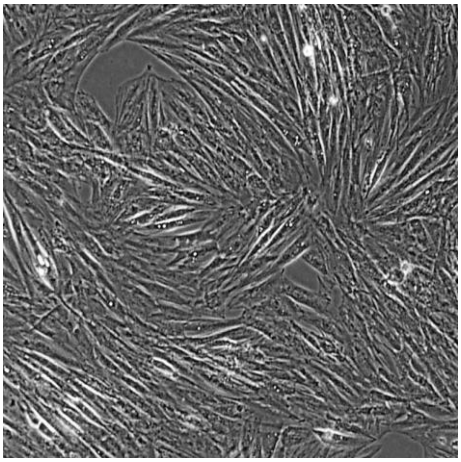

Day 6 TGF-beta1 +Sc

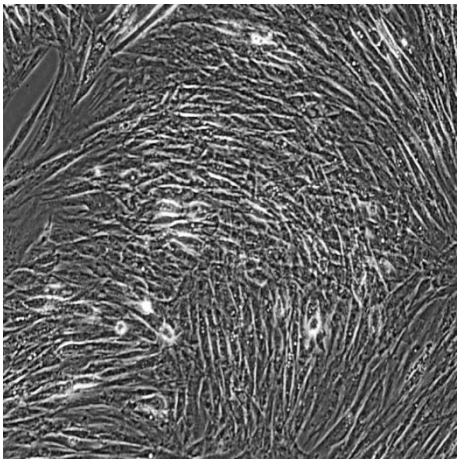

Day 9 TGF-beta1 + Sc

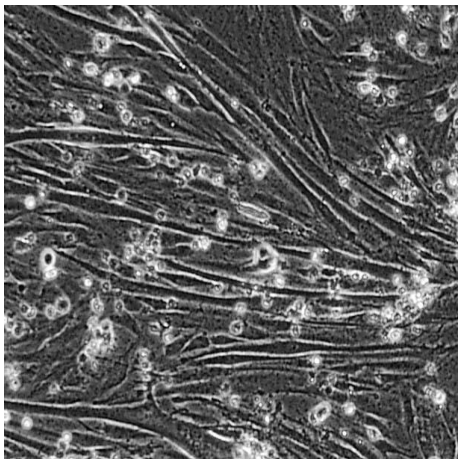

Day 6 TGF-beta1 + ShPED

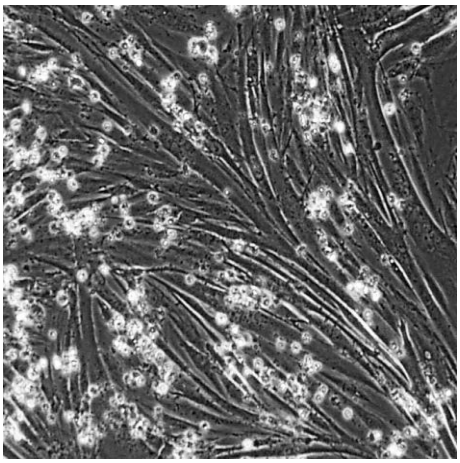

Day 9 TGF-beta1 + ShPED

Supplemental Fig. 1